TECHNICAL REPORT No. 51

CLIMATOLOGY AND SYSTEMATIC ERROR OF RAINFALL FORECASTS AT ECMWF

by

Franco Molteni* and Stefano Tibaldi

*Visiting Scientist on leave from
Geodata
Milan, Italy

October 1985

Abstract

The purpose of this study is to test the reliability of global and regional monthly rainfall fields deduced from operational ECWMF forecasts, and to compare them with the large-scale climatology and observed data over Europe.

Daily forecasts extending to D1 (12-36h), D2 (36-60h), D4 (84-108h) and D7 (156-180h) were used to compute monthly fields for January, April, July and October for the years 1981, 1982 and 1983; mean fields for each of the four months were also computed by averaging the data for the three available years.

Zonally-averaged values for the whole globe, the continents and the oceans, as well as global patterns, were compared with Jaeger's rainfall climatology (1976); also data from Corona (1978) were used to estimate the interannual variability of rainfall totals over the continents. Observed data from about 200 stations over Europe were used for the regional verification.

Even though the forecast fields reproduce almost all the main features of the large scale geographical distribution of rainfall, there are some systematic errors which occur even in D1 forecasts. Global averages of precipitation are always underestimated by the forecasts, the error being between 5% and 15%. This underestimation is concentrated over the oceans, whereas continental rainfall is usually overestimated, especially in the tropics and in midlatitudes during summer.

A short study of the hydrological balance in January and July, 1983 showed that the deficit of oceanic rainfall is related to an even stronger deficit in evaporation, so that a balance between precipitation and evaporation is achieved only when a significant fraction of the global precipitable water has been removed from the model atmosphere; these results are in agreement with the findings of Heckley (1985). Inadequacies in the parameterisation of vertical transports of moisture seem to be the main cause of this systematic error. Other sources of error can be found in the convection scheme, which is too active over the continents and particularly over the mountains, and in the smoothed representation of the orography, which generates a deficit of rainfall on the windward side of the mountains and an excess on the lee side in winter.

The important changes which occurred in the operational model during the three years considered in this study had a clear impact on rainfall forecasts, so that a poor correlation can be found between the interannual variations of monthly rainfall. However, during the periods when no relevant modification occurred, the correspondence between the observed and the forecast variations was much better. If the main sources of the systematic errors could be at least partially eliminated, the short range rainfall forecasts could become a very important source of information for the diagnostics of the global hydrological cycle of the real atmosphere.

C O N T E N T S

1. INTRODUCTION

Despite the continuous improvement in the global network of rainfall observations and in the data analysis algorithms, global or regional estimates of the rainfall which occurred in a particular period are still very difficult to obtain. In practice, reliable estimates of precipitation can be obtained only for densely populated areas, but little or no information is available for vast areas where high precipitation occurs, namely a large part of the mountain chains and the oceans. Because of this lack of information, diagnostic studies of the observed global balance of energy and water still suffer from a large degree of uncertainty, and the evaluation of the skill of general circulation models in reproducing or predicting the hydrological cycle of the earth is possible only over limited areas.

Even the total amount and the climatological distribution of global rainfall are known only approximately. Jaeger (1976, 1983) reviewed a number of studies and produced precipitation maps for most of the globe and computed mean monthly and annual maps of global precipitation with a 5° latitude/longitude resolution using data from previous investigations. Although his maps are probably the most reliable sources of information available about global rainfall climatology, they suffer from a considerable uncertainty in the oceanic areas: Jaeger used Geiger's global map (1965) of mean annual rainfall to deduce the annual totals over each oceanic grid box, and distributed these total values among the twelve months using monthly rainfall frequencies deduced from the U.S. marine climatic atlas for the years 1955-1965. At the end of his computation he found a mean global value of 966 mm for the annual precipitation, whereas some other studies seemed to indicate 1000 mm as a lower limit; therefore he multiplied all the values over the oceans and the polar regions by a factor of 1.062 to obtain a mean annual

global rainfall of 1000 mm. The technique used by Jaeger has been presented as an example; in general, in all the studies based on surface observations, oceanic precipitation has been estimated by either extrapolating the values recorded at coastal or island stations, or by using the frequencies of present weather types recorded on ships as indicators of rainfall amounts (see Tucker, 1961; Dorman and Bourke, 1979, 1981), or by adopting a suitable combination of these two techniques.

Since about 1970, a considerable number of studies have been published in which the rainfall distribution over oceanic areas was deduced from satellite observations. Many different techniques were developed, using data recorded in the visual (see Barrett, 1970; Ramage, 1975; Kilonsky and Ramage, 1976), infrared (see Richards and Arkin, 1981; Arkin, 1983) or microwave (see Wilheit et al., 1977; Rao and Theon, 1977) band of the spectrum. An extensive treatment of this subject is given in the book by Barret and Martin (1981). However, these studies were restricted to limited periods in time (two years for some of them) and the methods used are subject to a number of limitations. First of all, they have been developed for convective precipitation only, and so are not useful in middle (apart from the summer period) and high latitudes. In addition, they often rely on statistical assumptions and are tuned by means of empirical parameters derived by fitting the model to the data observed over island or coastal areas. Although some of these methods seem to be quite general, especially if applied to the estimation of monthly values in large areas, it is difficult to evaluate their validity when they are used outside the area over which they have been tuned. The experience of these investigations seems to indicate that most estimates are only accurate to about a factor of two.

We can conclude that reliable estimations of monthly global rainfall (both of its climatological value and of its actual distribution in a particular year) are not yet available. This fact prevents the global rainfall distribution predicted by numerical models being verified in studies relating to the sensitivity to boundary conditions or the potential skill of extended range forecasts.

We have, therefore, investigated the possibility of using the short range forecasts of rainfall produced by the operational model of ECMWF to produce global estimates of actual monthly rainfall. Our study has tried to answer the following questions:

- Is the global rainfall climatology deduced from short range forecasts in agreement with available climatological estimates?
- What is the amplitude and the geographical distribution of the systematic error of the model forecasts?
- What differences can be found between climatologies computed from forecasts with different verification times?
- Is the ECMWF model able to simulate the interannual variability of the rainfall distribution?
- What is the probability of getting a reliable estimate of the monthly rainfall over an area for which a dense set of observations is available?

After a summary of previous studies on ECMWF rainfall forecasts (Sect.2), the methods used in our research are explained in Sect.3. Sect.4 to Sect.7 present and discuss the results of the study, while Sect.8 summarises our answers to the questions posed above and points out the need for further investigations.

2. PREVIOUS VERIFICATIONS OF ECMWF RAINFALL FORECASTS

Among the many investigations concerning the verification of ECMWF operational products, some have been totally or partially devoted to rainfall forecasts. Verification of rainfall predicted over Europe can be found in Åkesson (1981), Åkesson et al. (1982) and Johannessen (1982), while Heckley (1981) investigated the skill of ECMWF rainfall forecasts in the tropics. A brief summary of their results will be given here.

Åkesson (1981) performed verifications of area-averaged daily forecasts versus area-averaged observations for 5 European areas (each one consisting of 6 grid points of the operational model, 3 in longitude x 2 in latitude) during the months of October and November 1980. Also the verification of local values was made for two stations in two of the five selected areas; a bilinear interpolation from the nearest grid points was used to compute the corresponding forecast values. Åkesson showed that for the area-averaged values, the skill of the model was good at day 1 (00-24h) and day 2 (24-48h), with a correlation coefficient greater than .6 between observed and predicted values, but declined in the following days and reached very low levels at day 5. The errors increased with increasing observed amounts; there was a systematic underestimation of heavy rainfall, whereas small or medium amounts were often predicted when little or no rainfall was observed. In general, these two effects combined to give a small negative bias at day 1 and a negligible bias at day 2. On the following days there was a positive bias (18% at day 3, 15% at day 4 and 9% at day 5 when averaged over the 5 areas), but the magnitude of the bias showed considerable variation among the regions. Åkesson also showed that, as expected, the verification scores were much lower where station reports were used instead of area-averaged observations, while little differences were found when verifying forecasts at single points against averaged observations.

Similar results were obtained by Åkesson et al. (1982) in a study devoted to the verification of forecasts of surface parameters at 17 European stations in December 1980 and January 1981. They examined rainfall totals in twelve-hour periods from H12 (00-12 hours) to H168, and found that only H24 and H36 forecasts scored slightly better than persistence (these results were much worse than those presented in the previous study because no averaging was performed on the observations). Even though the difference was very small, H24 had a better skill score than H12 when chance was used as a reference; this can be explained by the fact that during the spin-up time of the model there are some inconsistencies between the humidity and vertical velocity fields. Also in this study the underestimation of high rainfall and the excessive occurrence of low and moderate precipitation were found, with almost no bias in the total monthly values for these stations during the first 24 hours and a positive mean error which slowly increased in the following days.

The main results obtained in these studies were confirmed by the more extensive study undertaken by Johannessen (1982), who compared grid point forecasts over the European area with observations averaged over a grid box from January 1980 to April 1981. Johannessen pointed out that the ratio of large scale rain to convective rain did not show significant variations during the forecast cycle, with a mean value obviously depending on the month of the year.

This study also allowed the evaluation of the effect of the orography on the forecast errors; it showed a general underestimation of rainfall on the windward side of mountain chains and an overestimation on the lee side. When the verification was performed only in non-mountainous regions with a high density of stations, the systematic error was greatly reduced in the first

five day of the forecast. Unfortunately, Johannessen only performed this comparison for April 1982, the first month in which a new operational orography was introduced into the model, and he noticed that this did not lead to improvements in the systematic error in the mountain areas. However, it became clear that the great positive bias in the mountain areas in that month was due to the fact that the horizontal diffusion of moisture and temperature computed on sigma surfaces did not work well with a steeper orography since it led to excessive convection on the mountains (Tibaldi, 1982). When a new horizontal diffusion scheme was introduced, this bias was considerably reduced; thus April 1981 is not a suitable month to use for the investigation of the performance of the ECMWF model in mountainous regions and over plains, even though Johannessen's general conclusions are qualitatively valid.

A verification of ECMWF rainfall forecasts in the tropical area from February to May 1981 was performed by Heckley (1981). Comparing the distribution of monthly totals at different forecast times with Jaeger's climatology, he noted a general underestimation of rainfall (~20%) in the equatorial region and an overestimation of rainfall in the northern hemisphere's mid-latitudes. The geographical distribution of forecast rainfall was increasingly similar to the climatological field as forecast time increased; however, forecasts at day 1 and day 2 showed a better resemblance to the observed anomaly of monthly mean outgoing longwave radiation derived from NOAA satellite data and also had a good agreement with observed monthly totals over South America except over the Andes. Heckley also pointed out the strong correlation between precipitation and velocity potential fields in the lower troposphere, suggesting the use of the latter fields as an aid to the verification of rainfall forecasts over oceanic areas.

More recently, the errors in rainfall forecasts have been discussed in a number of works covering most aspects of the systematic error of ECMWF operational models, such as those by Arpe (1983), Arpe and Klinker (1984) and Heckley (1985). These studies confirm the previous results about the geophysical distribution of rainfall systematic error, but allow a better understanding of its interactions with the errors in atmospheric humidity fields. Heckley's results on this subject will be referred to again in Sect.5, where a study of the hydrological balance in January and July 1983 is presented.

3. DATA USED IN THE STUDY

As already described in the introduction, this study is devoted to the evaluation of the reliability of the distribution of global and regional monthly precipitation obtained from daily short-range rainfall forecasts. For this purpose, daily forecasts of total rainfall (large-scale + convective) verifying in the months of January, April, July and October were selected for the years 1981, 1982, 1983 and for the following forecast times:

- from 12 to 36 hours (D1);
- from 36 to 60 hours (D2);
- from 84 to 108 hours (D4);
- from 156 to 180 hours (D7);.

The data covered the whole globe and were extracted on a 1.875° lat-lon grid. We avoided using the first 12 hours of the forecast because of the problems related to the imbalance of moisture and vertical velocity fields which occurs during the 'spin up' time; these problems are always present in objectively analysed meteorological fields produced by data assimilation cycles where normal mode initialisation is employed, as is done at ECMWF. We have, therefore, defined D1, D2, D4 and D7 as the 24-hour periods for which the central times are 1, 2, 4 and 7 days after the time of the initial analysis.

From these data, the following global fields were computed for each of the 4 selected months and for each forecast time:

- total monthly rainfall;
- monthly rainfall amount due to daily rainfall below 2 mm/day (Class I);
- monthly rainfall amount due to daily rainfall between 2 and 20 mm/day (Class II);
- monthly rainfall amount due to daily rainfall above 20 mm/day (Class III).

For each of the four months of the year, mean fields were then computed and then averaged over the three years available. These mean fields will be shown in Sect.4, and they will be compared with climatological estimates over the whole globe and some selected areas; differences which arise during the forecast cycle will also be discussed. In Sect.5, the balance between precipitation and evaporation will be examined for January and July 1983.

Sections 6 and 7 will be devoted to the verification of rainfall forecasts against direct observations over the European area, namely an area consisting of 725 grid points between 15°W and 37.5°E in longitude, 30°N to 75°N in latitude. For this purpose, all the reports from GTS stations in the European area were extracted and daily amounts were computed by adding the values in the 0600 and 1800 reports. Stations reporting less than 16 daily values in a particular month were excluded from the subsequent computations for that month.

Monthly values for each 1.875° grid box were then computed by averaging all the daily data from stations located inside the box, and multiplying the results by the number of available days in each month; in this way, the contribution of each station to the monthly value was proportional to its number of daily reports. In addition to the monthly totals, the contributions due to the three rainfall classes were computed; the resulting values were assigned to the grid point at the centre of each box. Obviously, it was not possible to define these rainfall values for each of the 725 grid points in the selected area. Therefore it was decided that at least 50 daily reports were needed for the grid point data to be significant; in this way, data from at least two stations were used to define a grid point value. Nearly 200-250 values could be computed for each month.

Finally, mean monthly values for each of the four months were calculated for all the grid points in which data were available in all the three years; the number of such grid points was 184 for January, 203 for July and 204 for April and October. In Sect. 6, these observed fields will be compared with the mean forecasts in the corresponding months, while in Sect. 7 fields in single months will be examined in order to see if the model is able to reproduce the interannual variability of the rainfall data and whether the skill of short-range forecasts improved from 1981 to 1983.

4. GLOBAL CLIMATOLOGY OF RAINFALL FORECASTS

As mentioned in the previous section, only three years of data were available for our computations. Therefore, the mean fields obtained by averaging these data are obviously only a first approximation to a reliable climatology of short term rainfall forecasts. Besides, the changes which occurred in these years in the operational model had an influence on the rainfall distribution, even though it is difficult to give a quantitative estimate of this effect. However, despite these limitations, we think that the average fields can provide useful information about the climatology and the systematic error of the model's rainfall.

4.1 The zonal distribution

Before looking at the global maps, it is useful to consider the mean latitudinal distribution of rainfall. Fig.1 shows the zonal means of monthly precipitation in January, April, July and October for forecasts at D1 and D7, compared with the mean zonal values deduced from Jaeger's climatology (1976). The main deviations of the forecast climatology from Jaeger's are an underestimation of rainfall in the intertropical band and an overestimation over the extratropical northern hemisphere. An underestimation of rainfall in the middle latitudes of the southern hemisphere is also evident, but here Jaeger's climatology is less reliable due to the lack of date over most of the areas. These differences are present in all the four months and for all the forecast times; however, as the forecast time increases from D1 to D7, they tend to be smaller in the tropics and in the northern midlatitude summer, whereas they increase between 20° and 50°S.

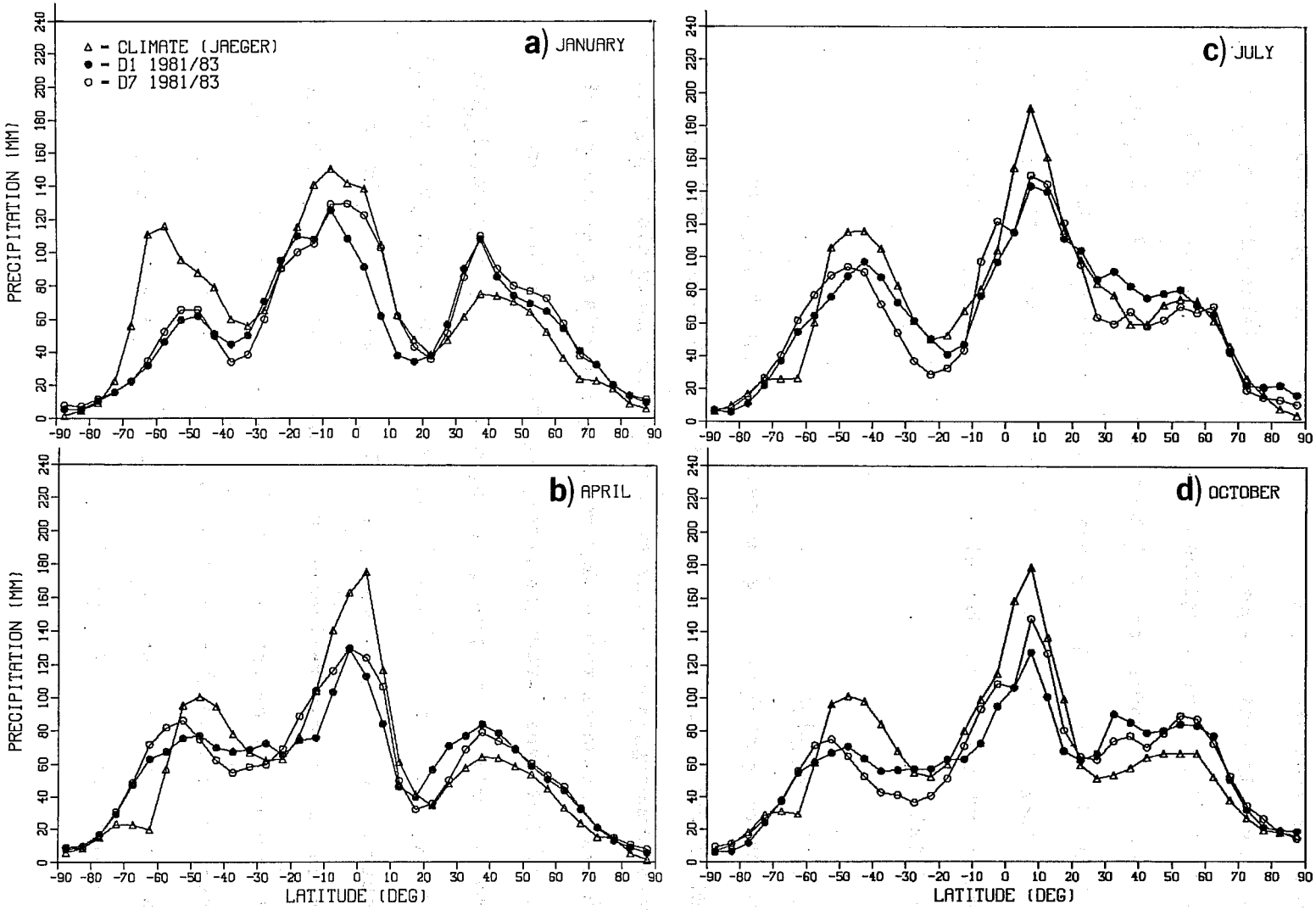

Fig. 1 Zonal means of monthly rainfall in January (a), April (b), July (c) and October (d), deduced from Jaeger's climatology (1976), D1 and D7 ECMWF forecasts.

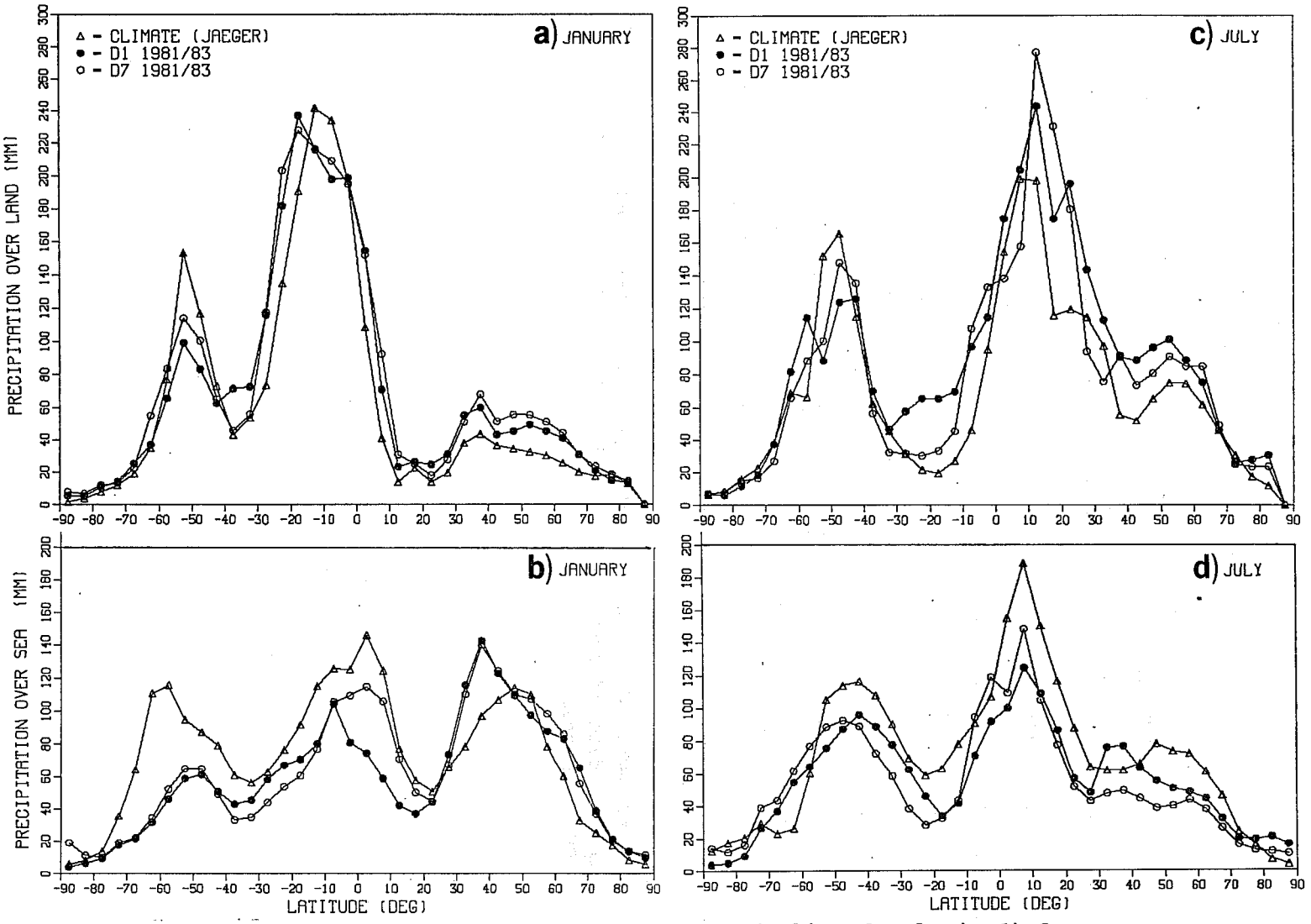

Fig. 2 Zonal means of monthly rainfall in January (a,b) and July (c,d) from Jaeger's climatology (1976), D1 and D7 forecasts, computed over continental (a,c) and oceanic (b,d) areas.

	JANUARY	APRIL	JULY	OCTOBER
JAEGER	80.2	74.4	86.1	79.2
D+1	67.9	69.6	79.6	71.4
D+2	70.6	70.4	79.3	72.0
D+4	70.5	69.5	74.9	70.4
D+7	72.4	70.6	75.3	71.8

Table 1. Global means of monthly rainfall (mm) in January, April, July and October deduced from Jaeger's climatology (1976), D1, D2, D4 and D7 ECMWF forecasts.

The global mean values of rainfall are compared in Table 1. One can see that the short range forecast underestimates global rainfall in all months. However, the global mean increases from D1 to D7 in January, decreases in July, while there is no significant trend in April and October. Fig. 1 shows that the January trend is mainly due to an increase of rainfall in the tropics, while in July the variations in the tropical distribution are small and the main effect is the decrease of precipitation in middle latitudes. In the intermediate months, the tropical and extratropical variations balance each other.

A better understanding of the model's behaviour can be obtained by separating the zonal rainfall means over the continents and over the oceans. Fig. 2 shows these values for January and July. Fig. 2a shows that in January, the strong peak over land in the tropics is well reproduced by the model, but the maximum is displaced about 5° southwards and the latitudinal width of this peak is too large. This causes an overestimation of about 40%-50% in the continental rainfall between 0° and 10°N, and between 20° and 30°S. Also in the continental northern mid-latitudes the comparison with Jaeger's results shows a relatively large overestimation, especially for D7 forecasts, while D7 seems better than D1 in the southern hemisphere. However, the main differences between the forecast and Jaeger's climatology in January can be found over the tropical oceans (see Fig. 2b). Here, D1 values are only about half Jaeger's estimate and the maximum is displaced 10° to the south. D7 forecasts are much better between 5°S and 25°N, with the maximum correctly located between 0° and 5°N. In the northern midlatitudes, the maximum intensity of the oceanic storm tracks is located at about 40°N in the forecast, with no appreciable difference developing during the forecast; Jaeger puts the track at about 50°N. It is interesting to note that, for the forecasts, this maximum is even higher than the tropical one.

In July over land (Fig. 2c), the forecast amounts considerably exceed Jaeger's data between 60°N and 25°S. The main differences are between 10° and 30°N, and in this band D1 forecasts are better; in particular they have a local minimum at 20°N which corresponds to the Sahara desert. This feature is present in Jaeger's data and also in D2 forecasts but not at D4 and D7. Over the oceans (Fig. 2d), rainfall forecasts are once again much lower than Jaeger's value, but the ratio between tropical and extratropical precipitation is more similar to Jaeger's value than is found in January. D7 forecasts are higher than D1 in the tropics and lower in the northern mid-latitudes; the relative maximum in the latter area is again further south in the forecasts than in Jaeger's data, but its amplitude decreases during the forecast cycle.

Before drawing conclusions from these comparisons with Jaeger's data, it would be useful to check the forecasts against other estimates of mean monthly rainfall. It is also important to compare the differences between the forecast and the 'observed' climatologies with the interannual variability of the monthly values, since part of these differences may be simply due to the small number of years available for the rainfall forecasts. Due to the limitations of the observed data, such a comparison is possible only over the continents.

Corona (1978) computed means and standard deviations of zonal means of monthly rainfall over the northern continents for January and July. He used monthly observations from about 1300 stations in the period 1935-1975 and his results were computed for 5° latitude bands in two areas: Europe-Asia-North Africa (EANAF) and North America (NAM). Fig.3 compares his values with Jaeger's data, and with the D1 and D7 forecasts.

In January (Figs. 3a and 3b), Jaeger's data are systematically lower than Corona's except near the pole and, over NAM, south of 25°N. In that area there is a surprising difference between the two "observed" climatologies, but one must remember that here the data refer to a very small area whose station network is probably far from ideal. Over EANAF (Fig.3a), D1 forecasts fit Corona's data better than Jaeger's, the differences being of the order of the interannual variability. The only exception is between 0° and 5°N, where the forecast values are about twice the observed ones. Over NAM (Fig.3b), south of 30°N, Corona's data have fluctuations that sometimes bring his values closer to Jaeger's and sometimes closer to the forecasts. The forecasts diverge south of 30°N, but apart from a clear overestimation between 20° and 25°N, it is impossible to have a good estimate of the forecast errors in that area due to the enormous difference between Jaeger's and Corona's data.

In July, there is a better agreement between the two observed climatologies. Over EANAF (Fig.3c) D1 forecasts constantly overestimate the observed data, but the latitudinal distribution is better (more regular than that of D7 forecasts) and the errors, at least in the tropics, are again of the order of the interannual variability. The D1 forecasts also reproduce well the relative minimum at 15°-20°N in Jaeger's data due to the Sahara desert, which seems reasonable even though it is missing in Corona's results. Over NAM (Fig.3d) the forecast distribution has very large errors over the tropics, with a maximum displaced 10° to the south with respect to Jaeger's data, and a general overestimation which is particularly high for D1. Of course, due to the different area coverage, especially in the tropics, the northern parts of the zonal profiles shown in Fig.2a and 2c are mainly representative of EANAF.

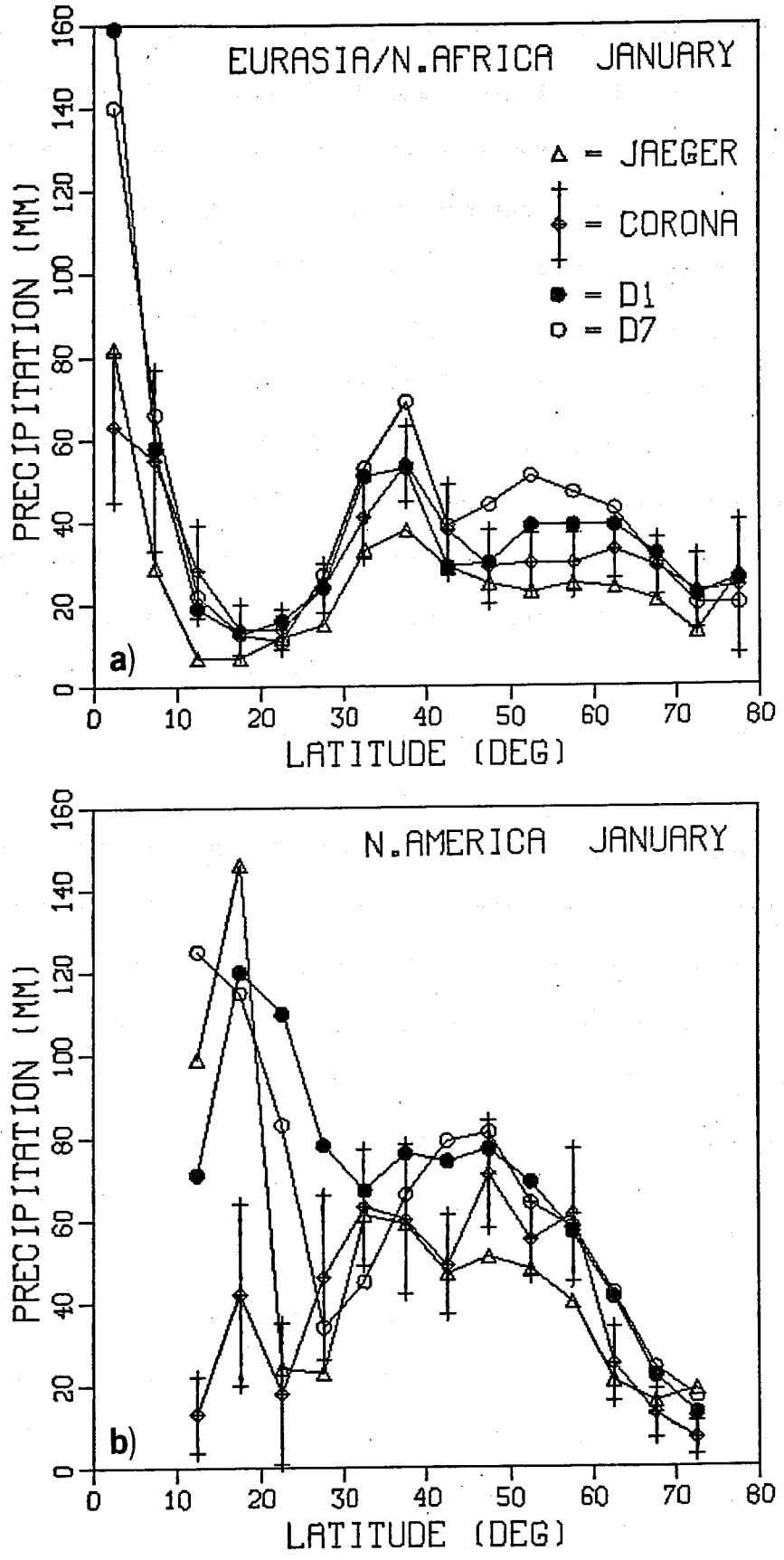

Fig. 3 Zonal means and standard deviations of monthly rainfall over Europe-Asia-North Africa (a,c) and North America (b,d) in January (a,b) and July (c,d) computed by Corona (1978), compared with mean values from Jaeger (1976) and with ECMWF D1 and D7 forecasts.

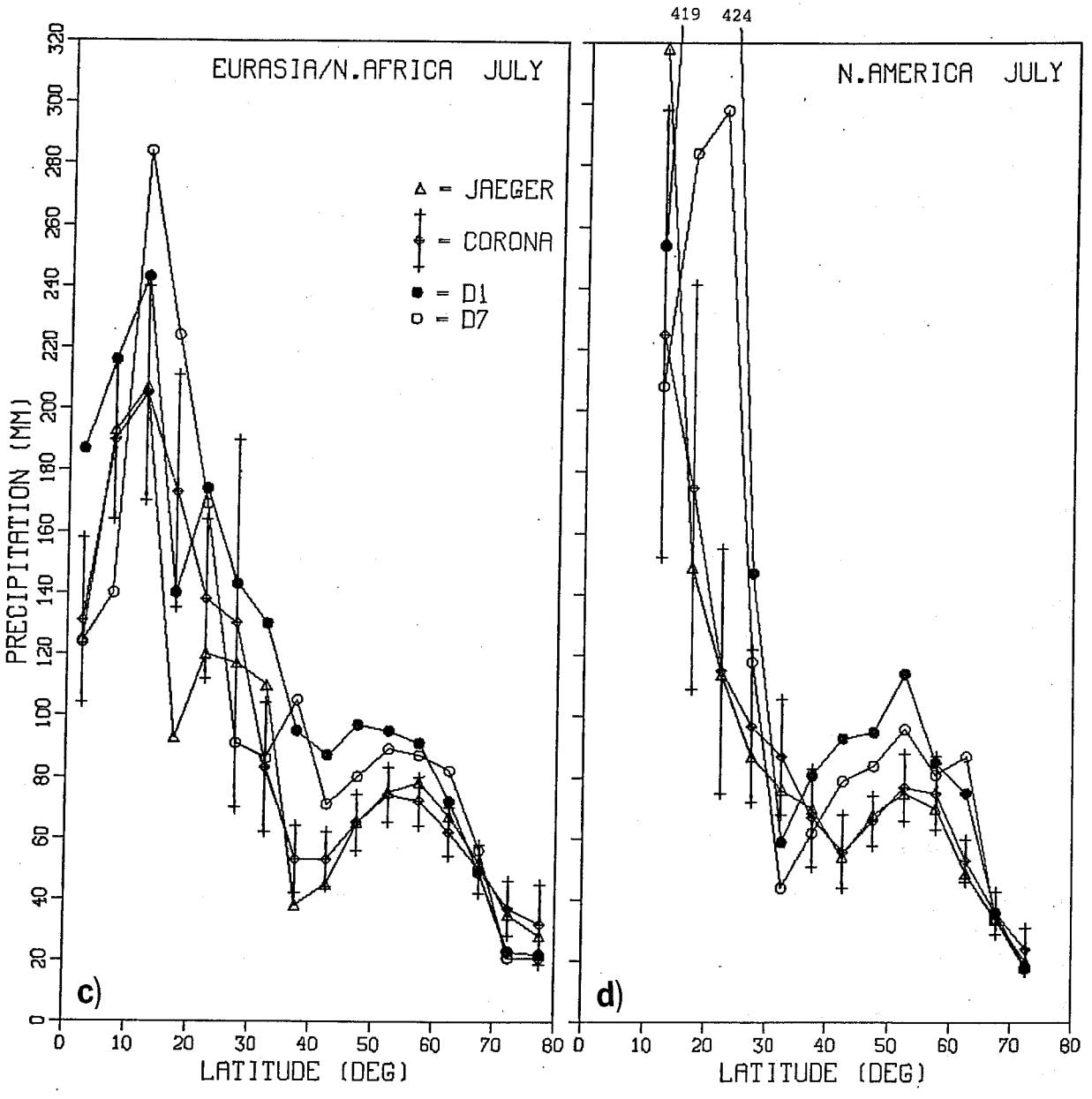
EURASIA/N.AFRICA JULY
N.AMERICA JULY
419 424
Δ = JAEGER
+ = CORONA
● = D1
○ = D7
PRECIPITATION (MM)
LATITUDE (DEG)
LATITUDE (DEG)
c)
d)

Fig. 3 c) and d)

The main conclusions that can be drawn from the comparisons discussed above can be summarised as follows:

(a) In the tropics the forecasts produce too much rainfall over land (with a clear tendency to increase the width of the intertropical convergence zone over the continents) and too little over the oceans; the former effect being stronger in July, the latter in January. The forecast error over tropical oceans is progressively reduced from D1 to D7, especially in January; over land there is no significant difference arising during the forecast cycle in winter, whereas in summer the effect of the desert areas is reduced from D1 to D7.

(b) In the northern mid-latitudes, precipitation is overestimated both over land and over sea in winter, while it is overestimated over land and underestimated over sea in summer. However, according to Corona's data the overestimation over land in winter is not so strong as it appears when Jaeger's climatology is used as a comparison, and its magnitude is of the order of the interannual variability. With the exception of the continents in July, the D1 forecasts seem to give a better representation of the precipitation in this area.

(c) In the southern extratropics, the forecasts (especially D7) give reasonable estimates over land, but underestimate oceanic rainfall over the oceans, particularly in winter. However, comparison with other observational studies, besides Jaeger's one, are necessary to have a reliable estimate of the magnitude of this error.

It is difficult to explain the systematic errors in the rainfall forecasts in terms of the physical processes simulated by the model only in terms precipitation data. However, the fact that the systematic error over the northern middle latitudes has the same features as the tropical error clearly indicates that the convection processes are not properly simulated in the model, and too much convection is being generated over land and too little over the oceans.

The case study presented in Sect.5, in which the balance between precipitation and evaporation will be considered, will give a clearer indication about the possible causes of these errors.

4.2 The global patterns of precipitation

We can now compare in more detail the geographical distribution of rainfall in the forecast 3-year means and in Jaeger's climatology.

(a) January

Fig.4 shows the D1 and D7 forecasts, the differences between the two, and Jaeger's data for January. One can easily see that the main differences between D1 and D7 are in the oceanic patterns. The D7 forecasts show a number of features that are more similar to Jaeger's data than those represented in D1; most of them are included in the wide band of high rainfall that covers the southern part of Africa, the central Indian Ocean, Indonesia and New Guinea (over which a maximum of more than 500 mm is present in the forecasts), most of the western border of the Pacific, and from there extends both eastwards through the equatorial Pacific, and northwards to connect with the North Pacific storm track. Over this wide band, D7 forecast amounts often

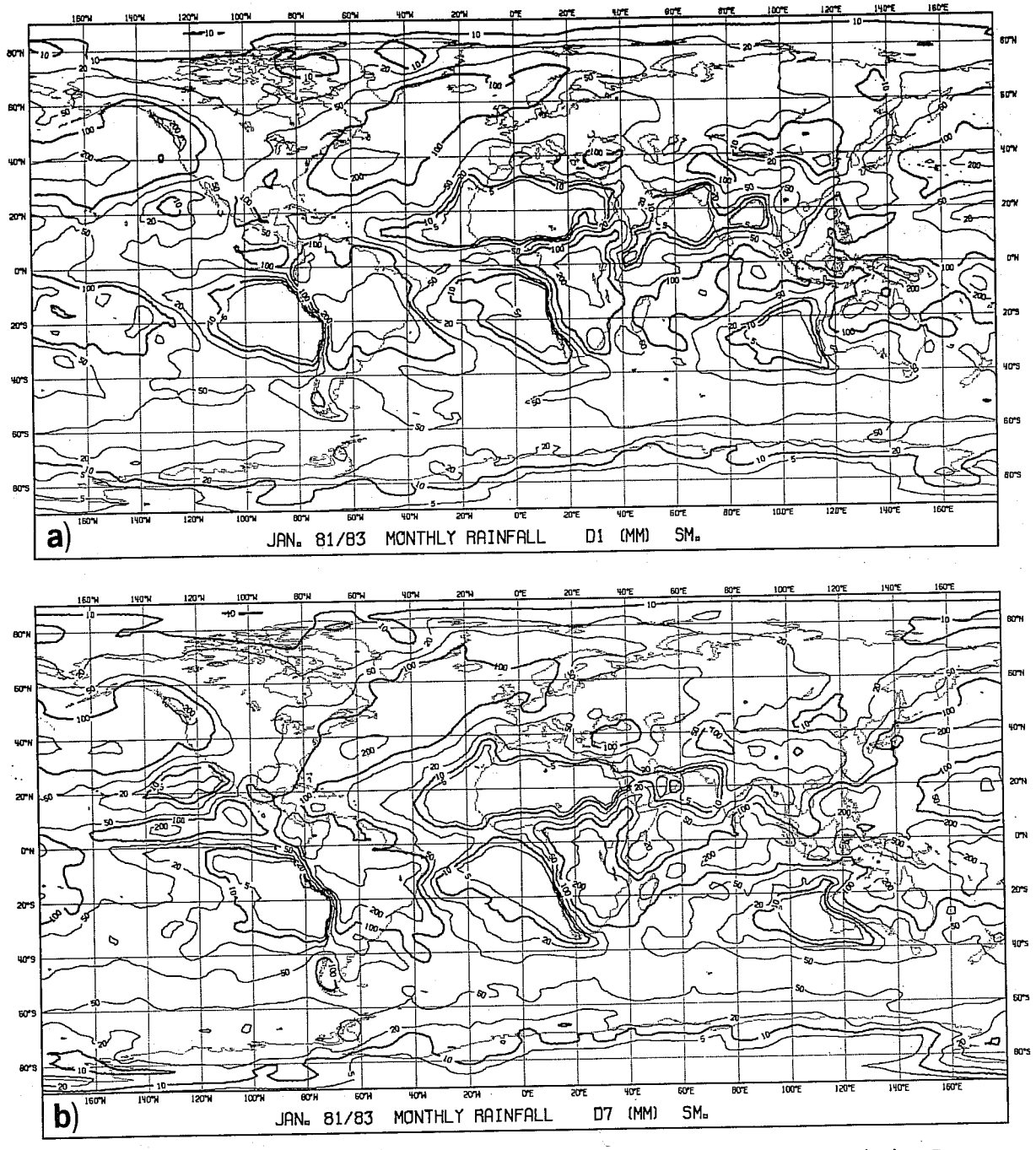

Fig. 4 (a) Mean global distribution of monthly rainfall (mm) in January, deduced from D1 ECMWF forecasts. (b) As in (a), from D7 forecasts. (c) Difference between (b) and (a). (d) As in (a), from Jaeger (1976).

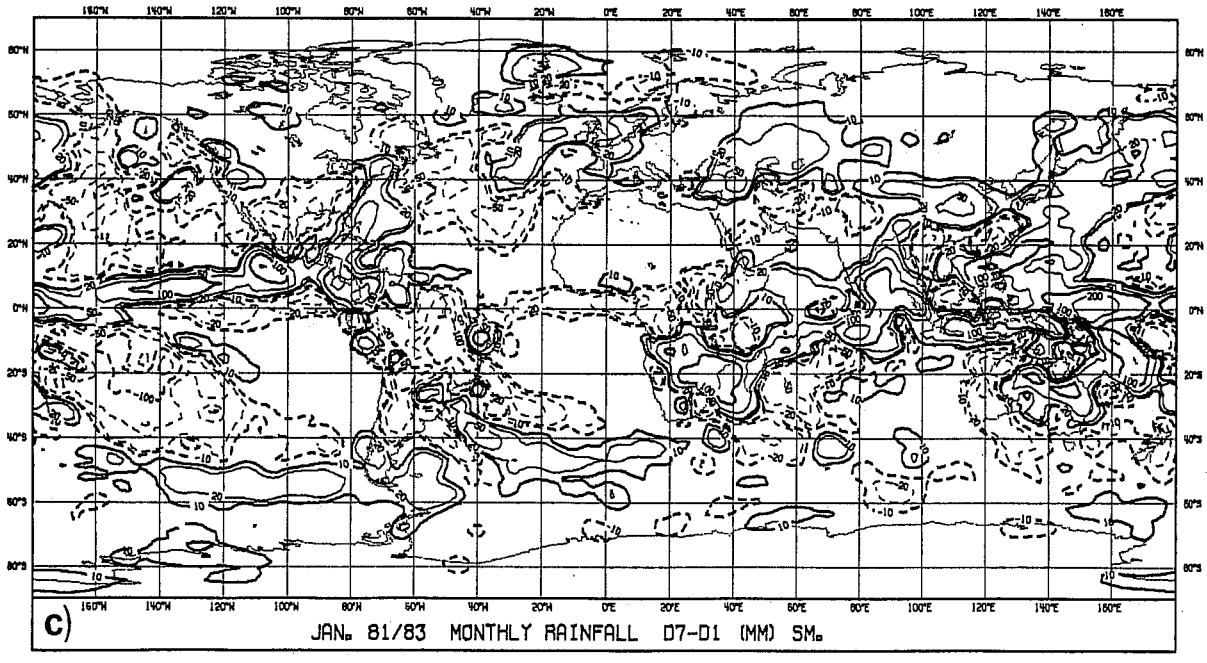
c)
JAN. 81/83 MONTHLY RAINFALL D7-D1 (MM) SM.

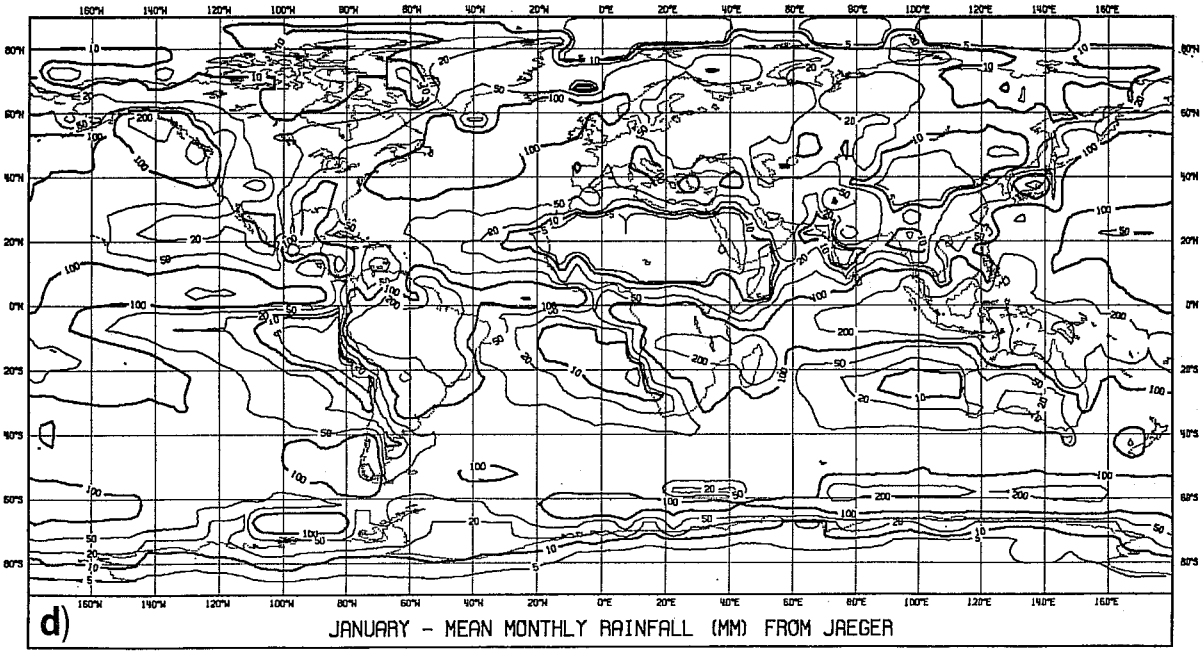
d)
JANUARY - MEAN MONTHLY RAINFALL (MM) FROM JAEGER

Fig. 4 c) and d)

exceed those in D1. However there is a significant difference between the forecasts over the eastern tropical Pacific, where D1 better represents the South Pacific convergence zone (SPCZ) around 20°S, and the D7 the intertropical convergence zone (ITCZ) between 0° and 20°N.

An oceanic feature that is more intense in the forecasts than in Jaeger's map is the North Atlantic storm track, particularly at D7, where it links with the high rainfall area over Central and South America; it is also more intense in the northern part. Another remarkable difference is associated with the high rainfall band in the southern ocean around 60°S in Jaeger's map which is much weaker and displaced 5°-10° northwards in the forecasts. This band is the source of the marked difference that was noticed in the zonal profile of the oceanic rainfall in January.

Despite the differences described above, we can say that on a global scale the agreement between D7 forecasts and Jaeger's climatology is quite good. The main differences that arise during the forecast cycle are due to an increase in convective activity in the intertropical band over the Indian and Pacific Oceans. The difference map suggests that this increase is mainly fed by an intensified water vapour transport from the surrounding areas; this is particularly clear over the eastern Pacific where an intensifying Hadley circulation produces more convergence in the ITCZ and removes moisture from the subtropical areas. Variations in the poleward water vapour transport appear also to be responsible for the intensification of the northern part of the Atlantic storm track and the rain belt located around 50°S in the south-eastern Pacific and southern Atlantic oceans. However, not all the differences between D7 and D1 can be explained in terms of water vapour transport or intensified meridional circulation. Sect. 5 will show that the

increase of globally averaged precipitation shown in Table 1 is fed by an increase in evaporation which is concentrated over the tropical oceans.

(b) July

Fig. 5 shows the D1 and D7 forecasts, the difference between the two, and Jaeger's data for July. The differences between the D7 and D1 forecasts have a similar pattern to those found in January (compare Figs 4c and 5c), but they are stronger over many areas. The convective activity in the ITCZ clearly increases in intensity from D1 to D7 over almost the whole equatorial region; in particular, this also occurs in the Atlantic, whereas in January the opposite trend appears in the forecasts over this area. It is also evident from Fig. 5c that the rainfall increase is supported by an increase in the moisture convergence due to a stronger Hadley circulation which removes water vapour from the subtropics. However, even if the poleward motion in the extratropics is considered, the water vapour transport cannot account for the large areas in the subtropics and mid-latitudes where the rainfall is significantly higher in D1: actually, the mean global precipitation decreases by about 5% from D1 to D7. A remarkable decrease can be seen over South America, and this is also apparent (see Fig.2c) in the zonal profile between 10°S and 30°S. Large areas over the northern continents experience a less intense but clear decrease in rainfall during the forecast cycle. Therefore the comparison with Jaeger's data suggests that an excess in convection over land in the first few days of the forecast removes water vapour from the atmosphere over the continents at such a rate that evaporation and moisture convergence from the sea are not able to compensate, and consequently this gradually reduces the convective activity itself. Even though the D1 global mean is closer to Jaeger's value, the local reductions in rainfall from D1 to D7 tend to improve the rainfall distribution.

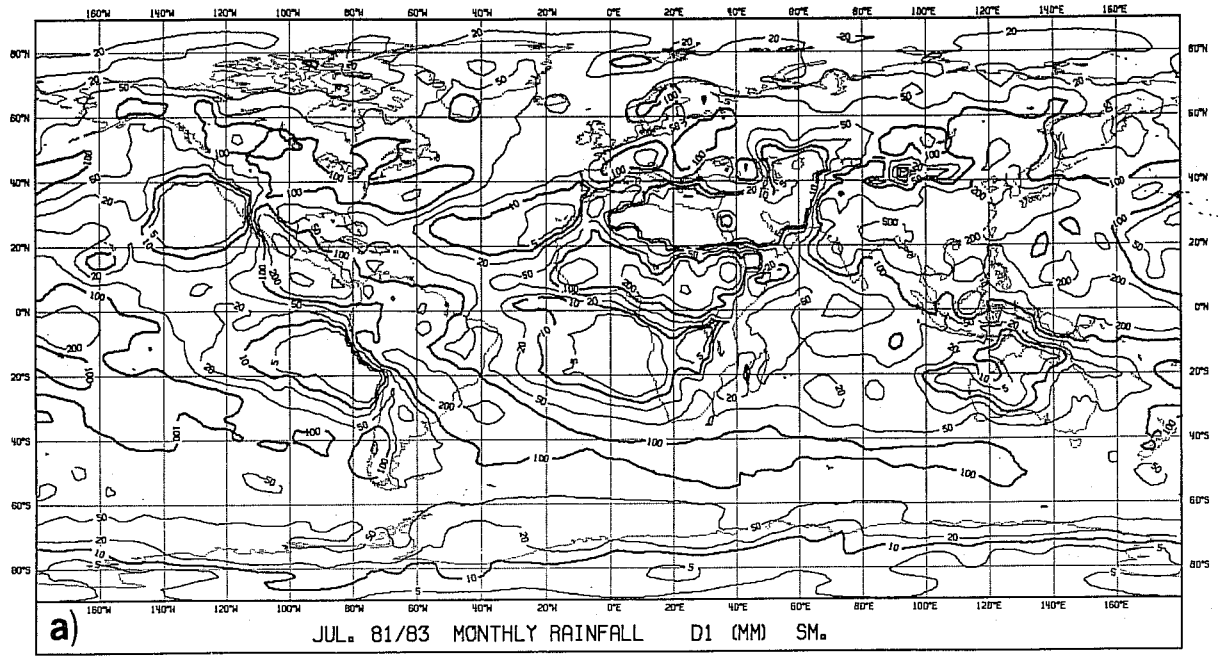

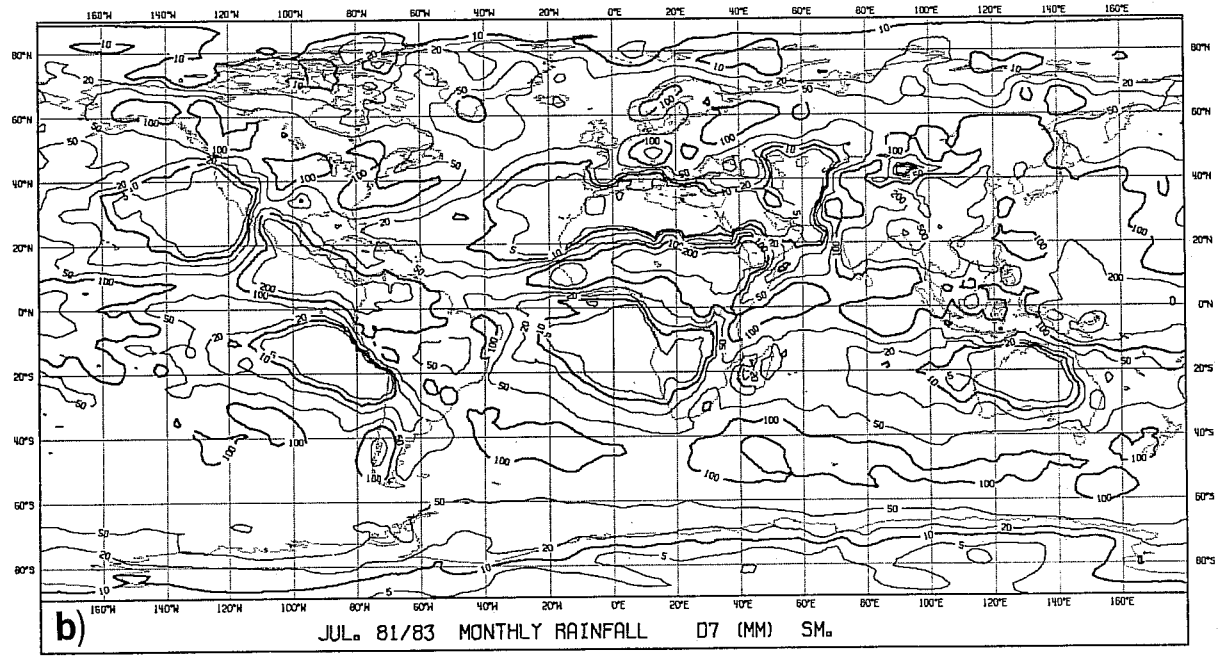

Fig. 5 (a) Mean global distribution of monthly rainfall (mm) in July, deduced from D1 ECMWF forecasts. (b) As in (a), from D7 forecasts. (c) Difference between (b) and (a). (d) As in (a), from Jaeger (1976).

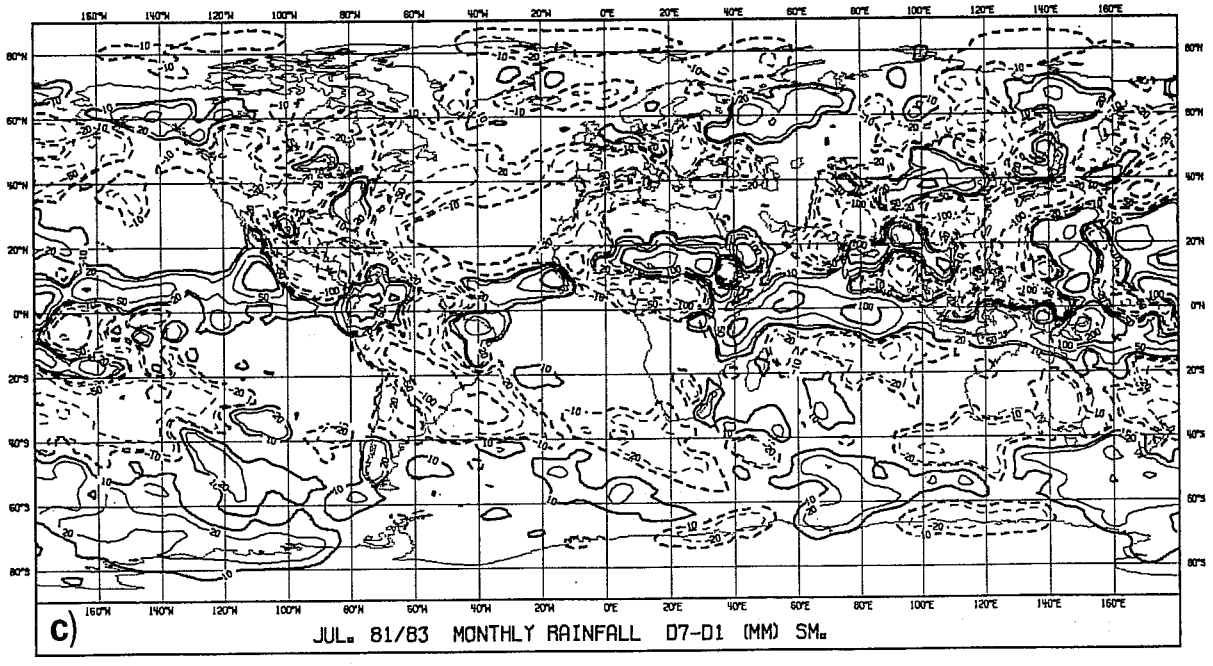
c)
JUL. 81/83 MONTHLY RAINFALL D7-D1 (MM) SM.

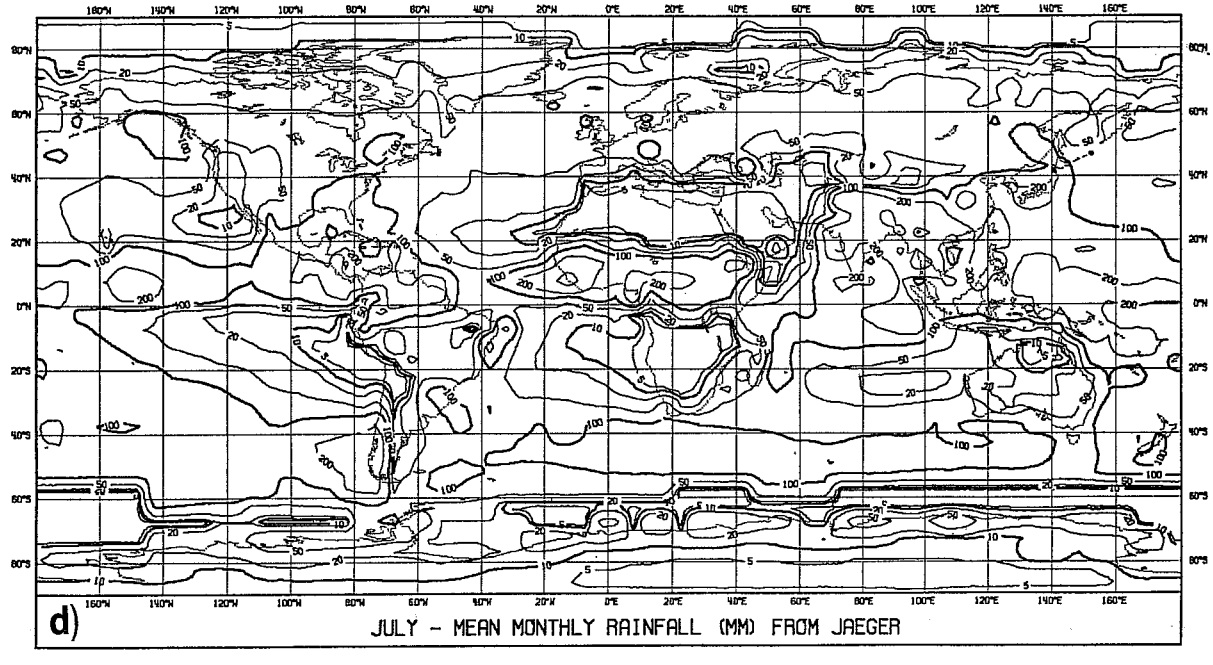
d)
JULY - MEAN MONTHLY RAINFALL (MM) FROM JAEGER

Fig. 5 c) and d)

4.3 The partitioning amongst rainfall classes

We now briefly discuss the contribution of rainfall events of different intensity to the monthly totals. As mentioned in Sect.3, we have divided daily rainfall into three classes (0-2 mm/day, 2-20 mm/day, above 20 mm/day) and have computed the total monthly amount due to each class. Let us first look at the mean global values for January and July (see Table 2). The fractional contributions of the three classes to the total monthly values show only small variations during the forecast cycle and between different months, the values ranging between 9-10% for Class I, 55-59% for Class II and 30-36% for Class III. However, in January a small but constant trend can be noted towards an increase in Class III and a decrease of the other two. This is due to the fact that Class III accounts for most of the increasing trend in January global precipitation, while the contributions of the other two classes are nearly constant. In July, no significant trend can be found; the decrease in global rainfall from D1 to D7 is almost equally distributed between Class II and Class III.

The geographical distribution of rainfall for the three classes is shown in Figs. 6,7,8; each of these shows the D7 distribution and D7-D1 difference for January and July. Fig.6 shows that the forecast rainfall in Class I mainly occurs in two bands - one in the ITCZ and another one over the winter high latitudes, the latter being more realistic than the former. The main variations during the forecast cycle occur in the ITCZ: in both months there is an increase over Brazil and Central Africa. However, the January maps show a general decrease over the oceans, while in July areas with positive variations are also present in the Indian and the Pacific Oceans.

JANUARY

	CLASS I	CLASS II	CLASS III	TOTAL
D1	6.9 (10.2%)	40.2 (59.2%)	20.8 (30.6%)	67.9
D2	7.0 (9.9%)	41.4 (58.6%)	22.2 (31.5%)	70.6
D4	6.9 (9.8%)	40.4 (57.3%)	23.2 (32.9%)	70.5
D7	6.6 (9.1%)	39.9 (55.1%)	25.9 (35.8%)	72.4

JULY

	CLASS I	CLASS II	CLASS III	TOTAL
D1	6.8 (8.5%)	43.8 (55.0%)	29.0 (36.5%)	79.6
D2	6.9 (8.7%)	45.5 (57.4%)	26.9 (33.9%)	79.3
D4	7.0 (9.3%)	42.8 (57.1%)	25.1 (33.6%)	74.9
D7	6.8 (9.0%)	41.8 (55.5%)	26.7 (35.5%)	75.3

Table 2. Globally averaged contributions to the mean monthly precipitation (mm) in January and July due to daily rainfall less than 2 mm (Class I), between 2 and 20 mm (Class II), greater than 20 mm (Class III), deduced from D1, D2, D4 and D7 forecasts. In parentheses, these values are expressed as percentage of the total amounts.

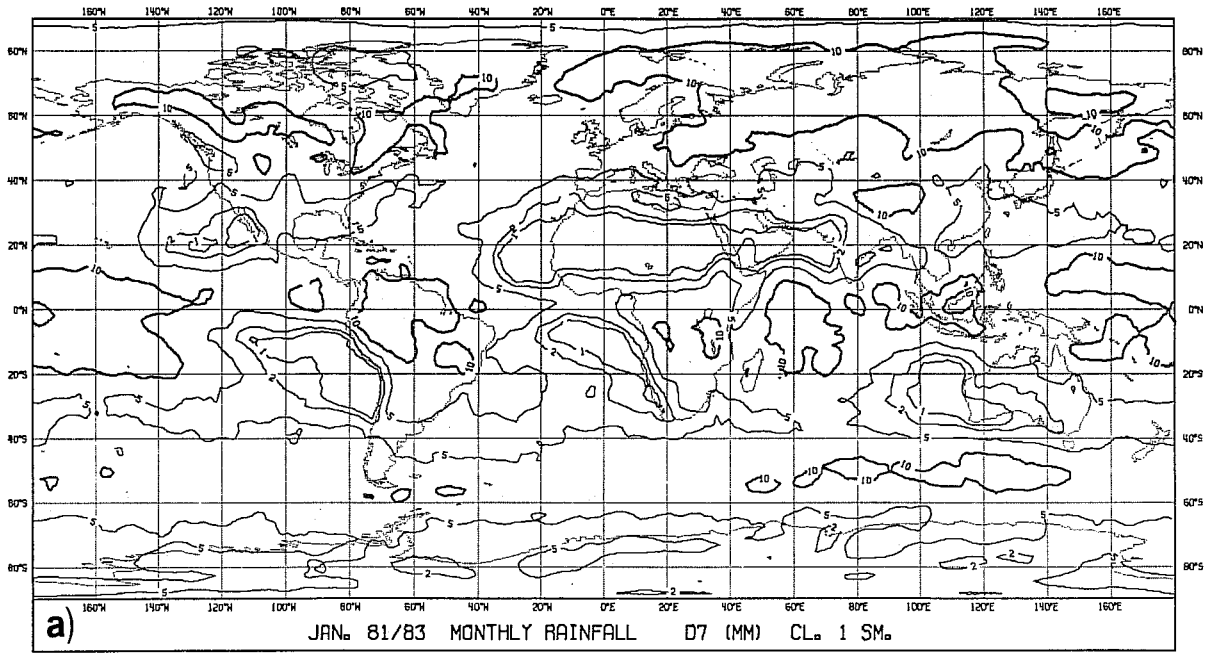

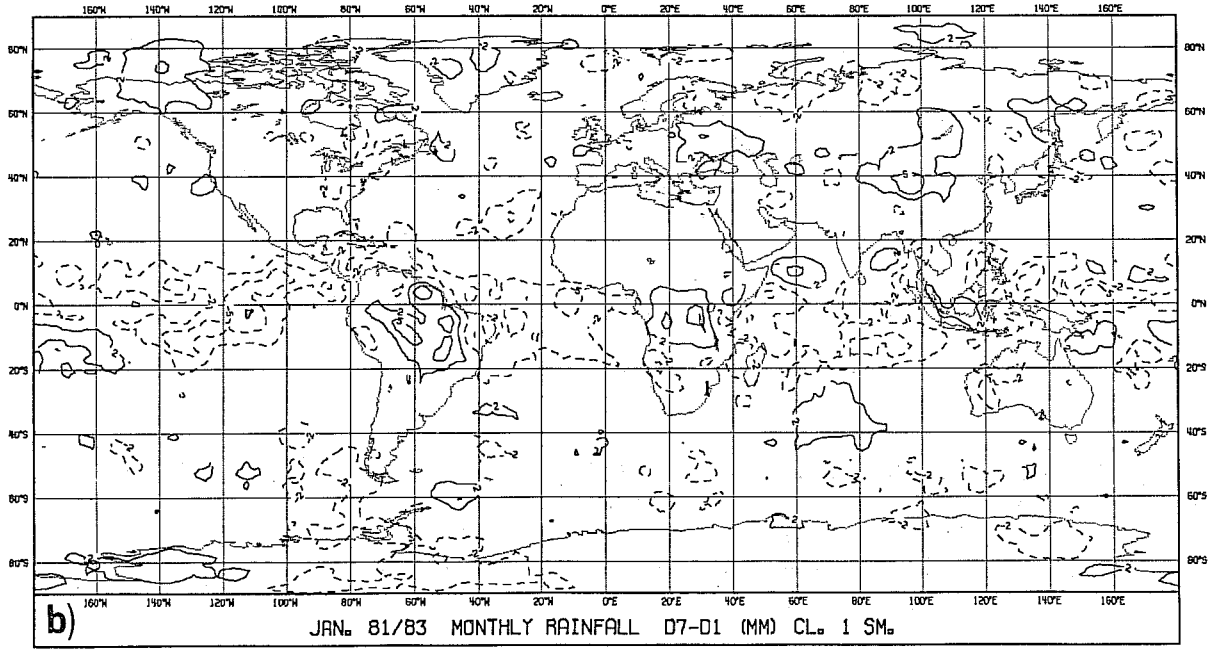

Fig. 6 Contribution to the mean monthly precipitation (mm) due to daily rainfall less than 2 mm (Class I).
(a) in January, from D7 forecasts; (b) in January, difference between D7 and 91 forecasts; (c) and (d) as in (a) and (b), for July.

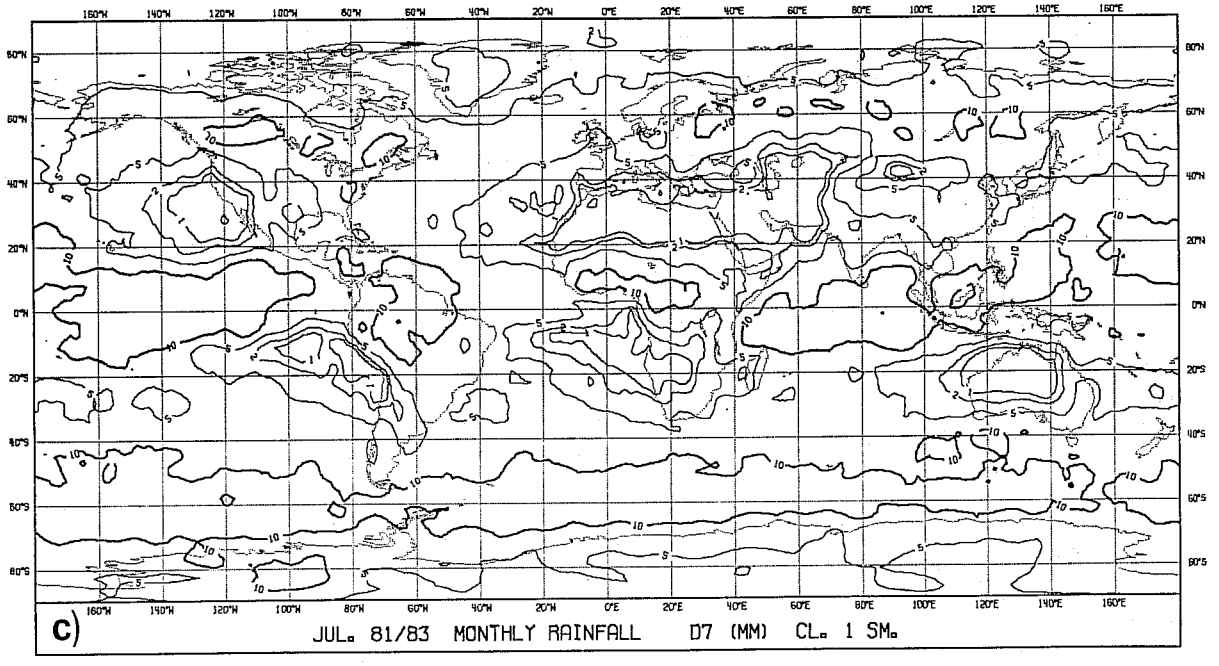
c)
JUL. 81/83 MONTHLY RAINFALL D7 (MM) CL. 1 SM.

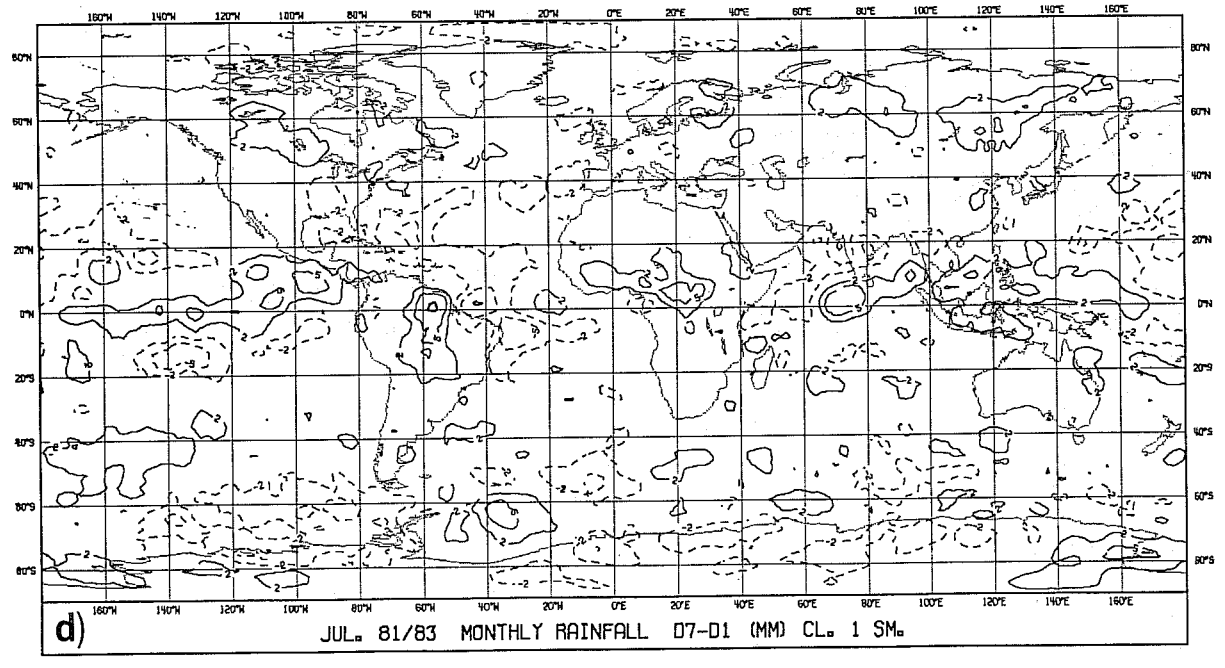
d)
JUL. 81/83 MONTHLY RAINFALL D7-D1 (MM) CL. 1 SM.

Fig. 6 c) and d)

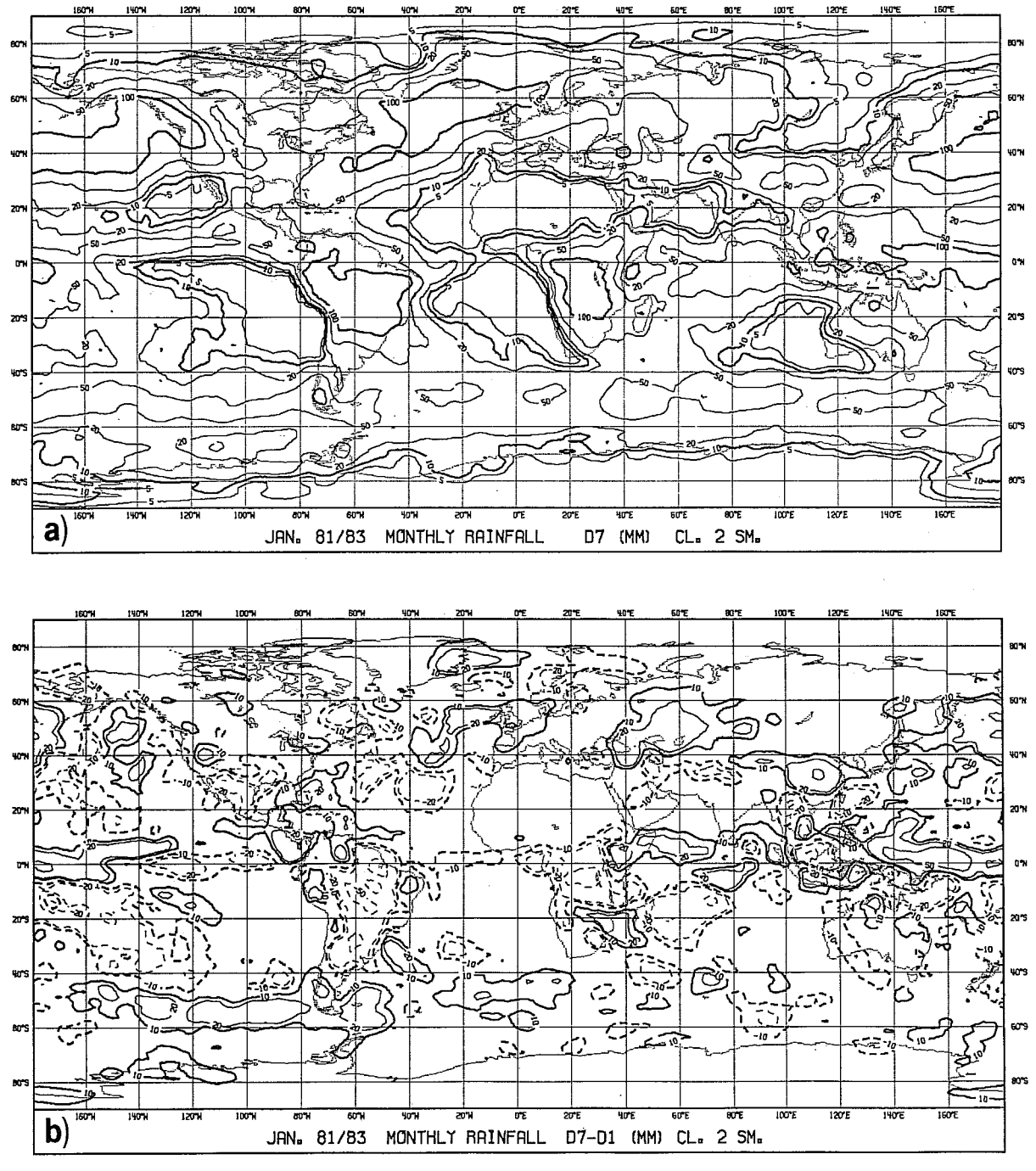

Fig. 7 As in Fig. 6, but for daily rainfall between 2 and 20 mm (class II).

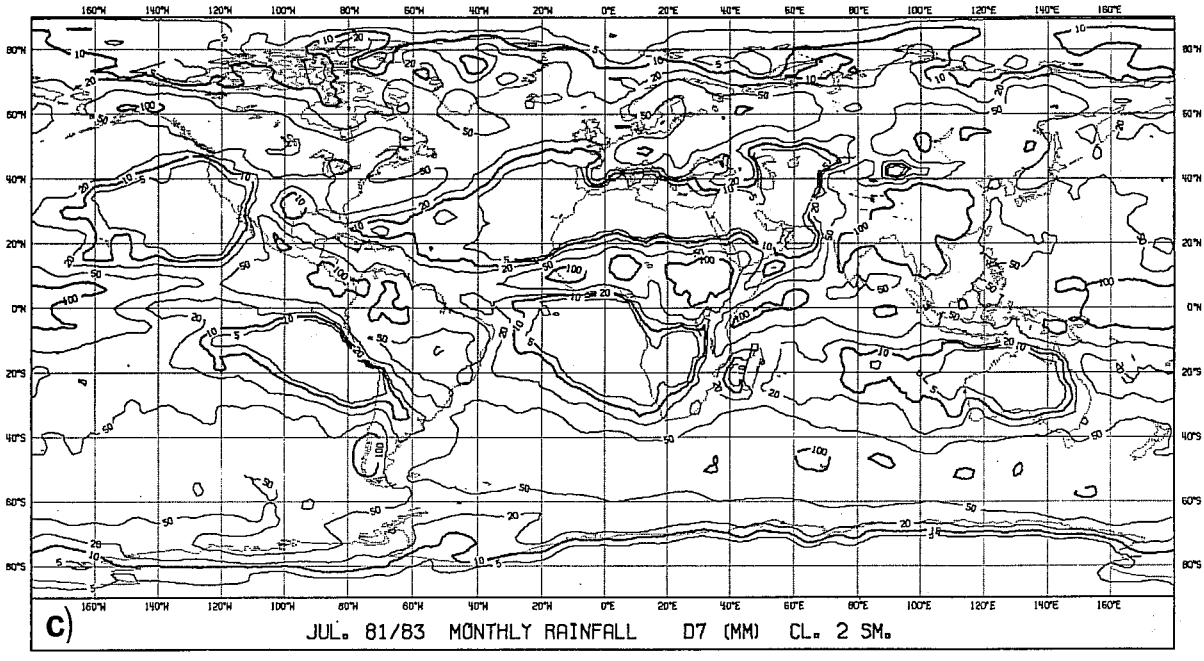
c)
JUL. 81/83 MONTHLY RAINFALL D7 (MM) CL. 2 SM.

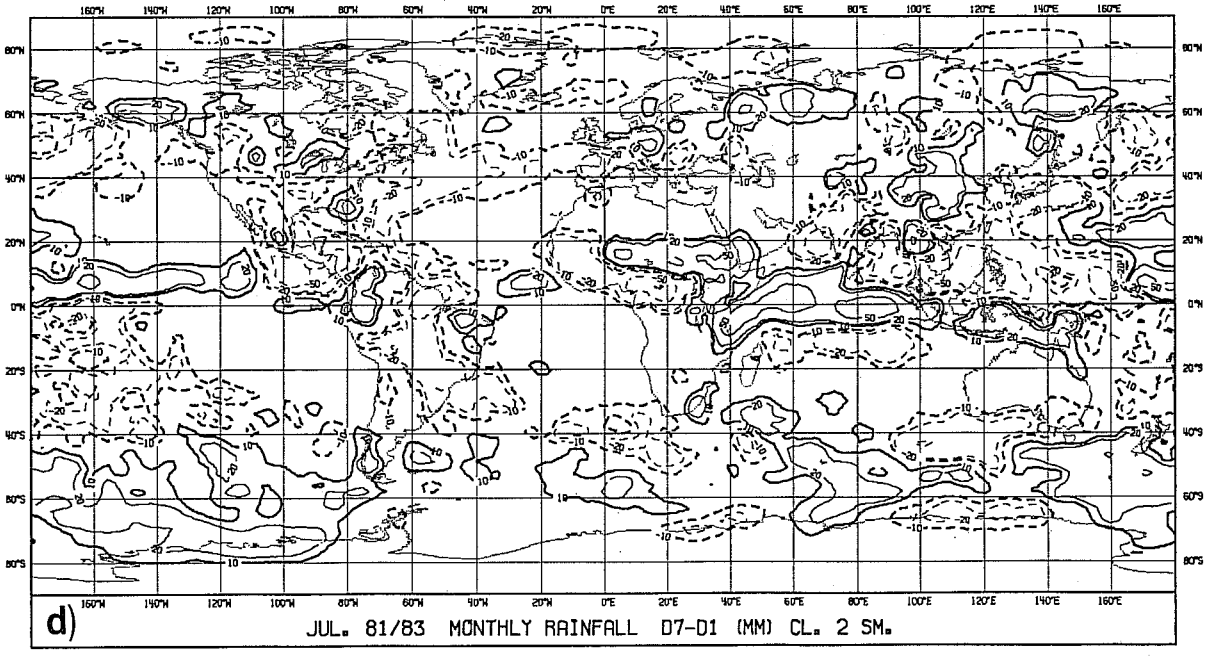
d)
JUL. 81/83 MONTHLY RAINFALL D7-D1 (MM) CL. 2 SM.

Fig. 7 c) and d)

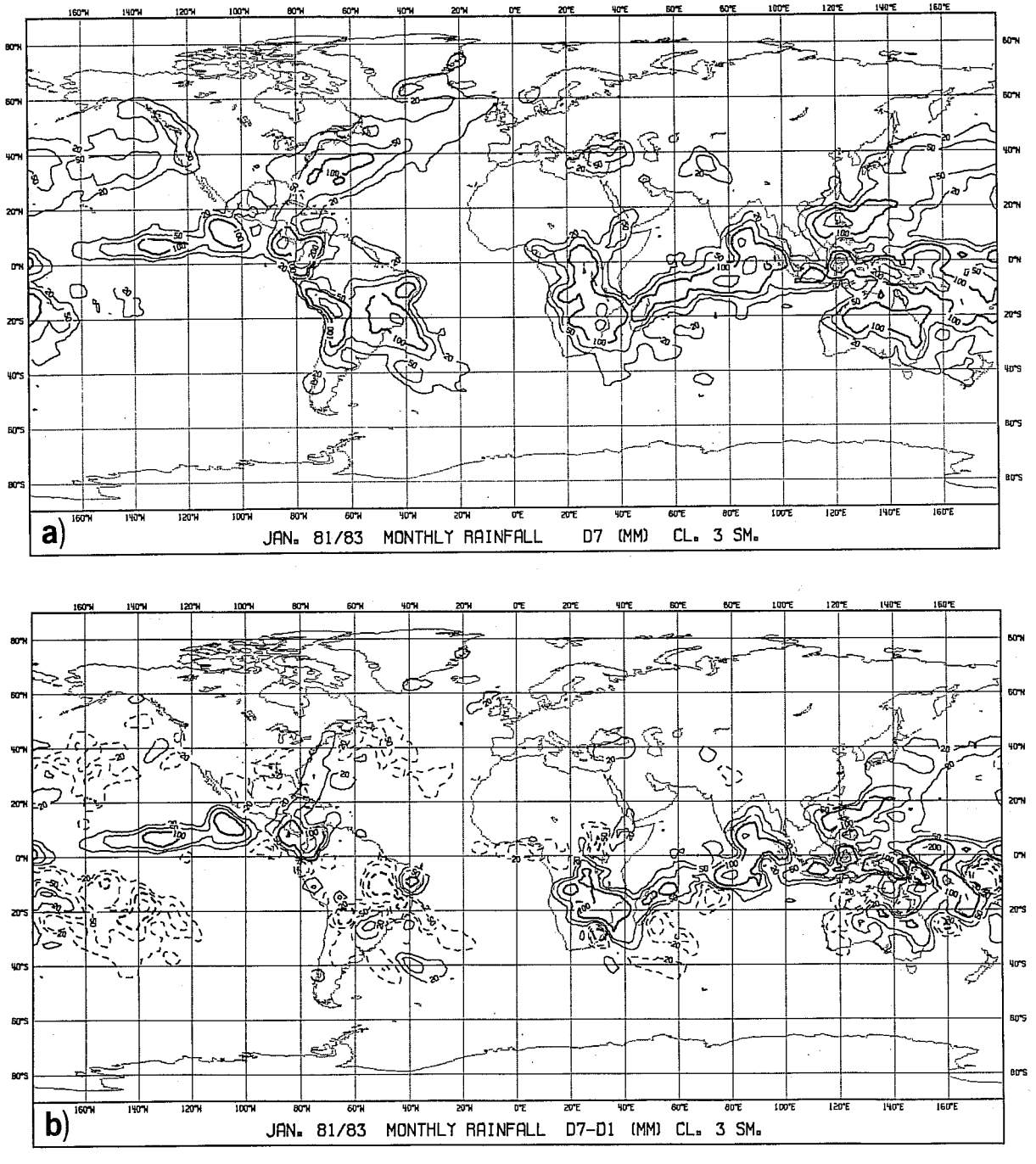

Fig. 8 As in Fig. 6, but for daily rainfall greater than 20 mm (Class III).

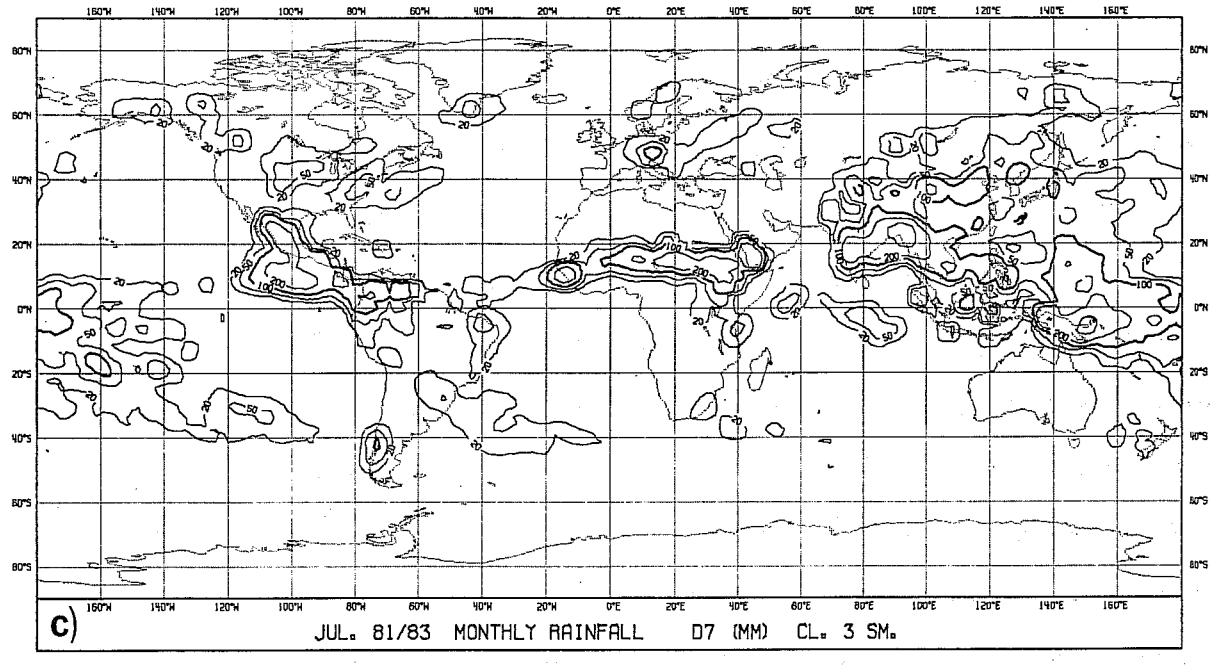
c)
JUL. 81/83 MONTHLY RAINFALL D7 (MM) CL. 3 SM.

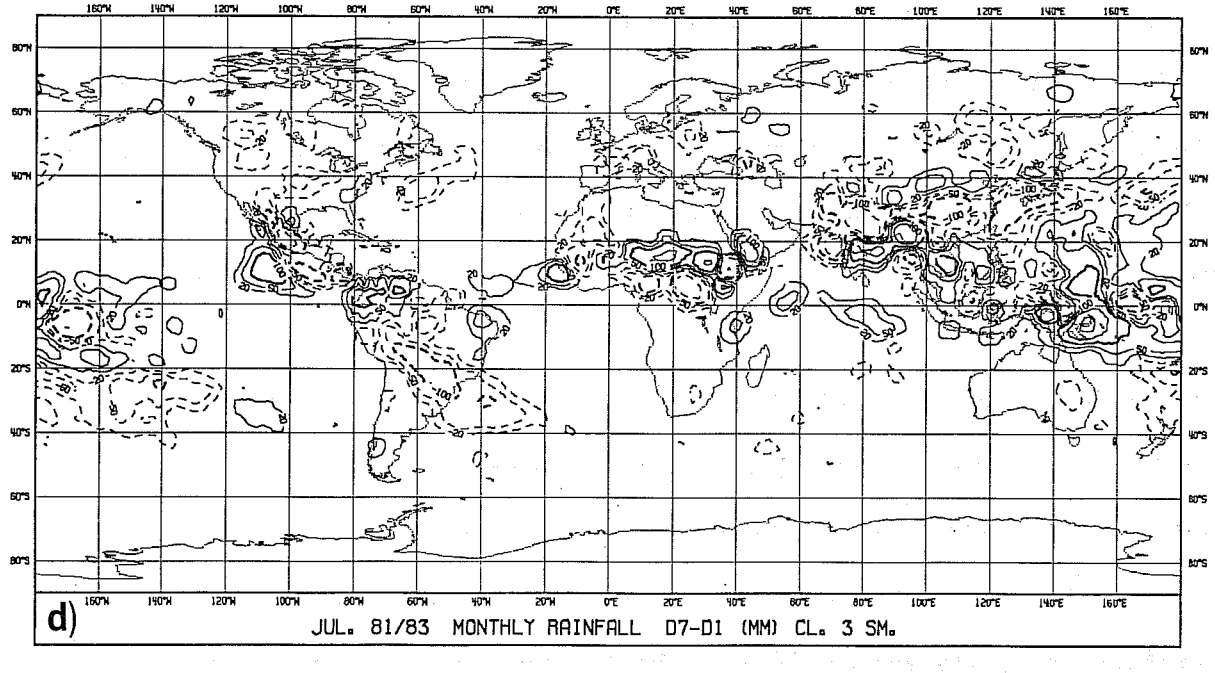
d)
JUL. 81/83 MONTHLY RAINFALL D7-D1 (MM) CL. 3 SM.

Fig. 8 c) and d)

Class II rainfall accounts for most of the total rainfall so the maps in Fig.7 resemble very closely the maps of total rainfall given in Figs. 4 and 5. It is, however, more interesting to consider the Class III rainfall. Fig.8 clearly shows that in the forecasts high rainfall cases are concentrated in the tropical areas and in the oceanic storm tracks. A remarkable feature is the almost complete absence of intense rainfall over the middle latitude continental areas in January. It is evident from these maps that rainfall over 20 mm/day is generated by the model almost exclusively by convection; conversely, we know that over the northern extratropics in winter, intense rainfall can also be generated by large scale or orographic ascent, and give a considerable contribution to the monthly totals. This feature of the systematic error in the model rainfall forecasts had already been detected in the previous verifications referenced in Sect.3 and will be clearly evidenced in Sect.6, where the forecasts will be compared with observed data over Europe.

The evolution of Class III during the forecasts cycle is different in the two months. In January, Class III variations account for a great part of the total monthly variation in the tropics, as can be seen by comparing Fig. 8b with Fig.4c. The comparison with Fig.8a also shows that some of the intense rainfall areas present at D7 over the tropical oceans are almost entirely generated during the forecast cycle; the belt in the equatorial eastern Pacific is particularly evident. On the other hand, in July the tropical variations are accounted for by both Class II and Class III in nearly equal proportions; a notable exception is the extinction of the high rainfall area over South America, which was generated by intense convective rainfall. Also, the convective activity over the midlatitude northern continents shows a general decrease.

5. A CASE STUDY OF THE HYDROLOGICAL BALANCE IN JANUARY AND JULY 1983

A further insight into the possible causes of the systematic error in rainfall forecasts can be obtained from the investigation of the balance between precipitation and evaporation in the model. A detailed study of the full hydrological cycle of the model is beyond the scope of this report, so we shall mostly limit ourselves to the comparison of global and zonal means of precipitation and evaporation for January and July 1983.

5.1 January results

The results concerning the forecasts hydrological balance in January 1983 are presented in Figs. 9a, 10, 11 and 12. Fig. 9a shows the global means of monthly forecasts of precipitation and evaporation. The zonal means of precipitation for the whole globe, the continents and the oceans are presented in Fig. 10, while the corresponding values of evaporation and precipitation minus evaporation are shown in Figs. 11 and 12 respectively.

For the precipitation data, a first comparison can be made with the values for the 3-year means shown in Table 1 and in Figs. 1 and 2, in order to check if strong anomalies are present in the 1983 forecasts. Actually, even though the global means for January 1983 are less than those for the 3-year climatology, and some small improvements can be seen in the representation of tropical rainfall, the trend during the forecast cycle and the zonal distribution are very similar.

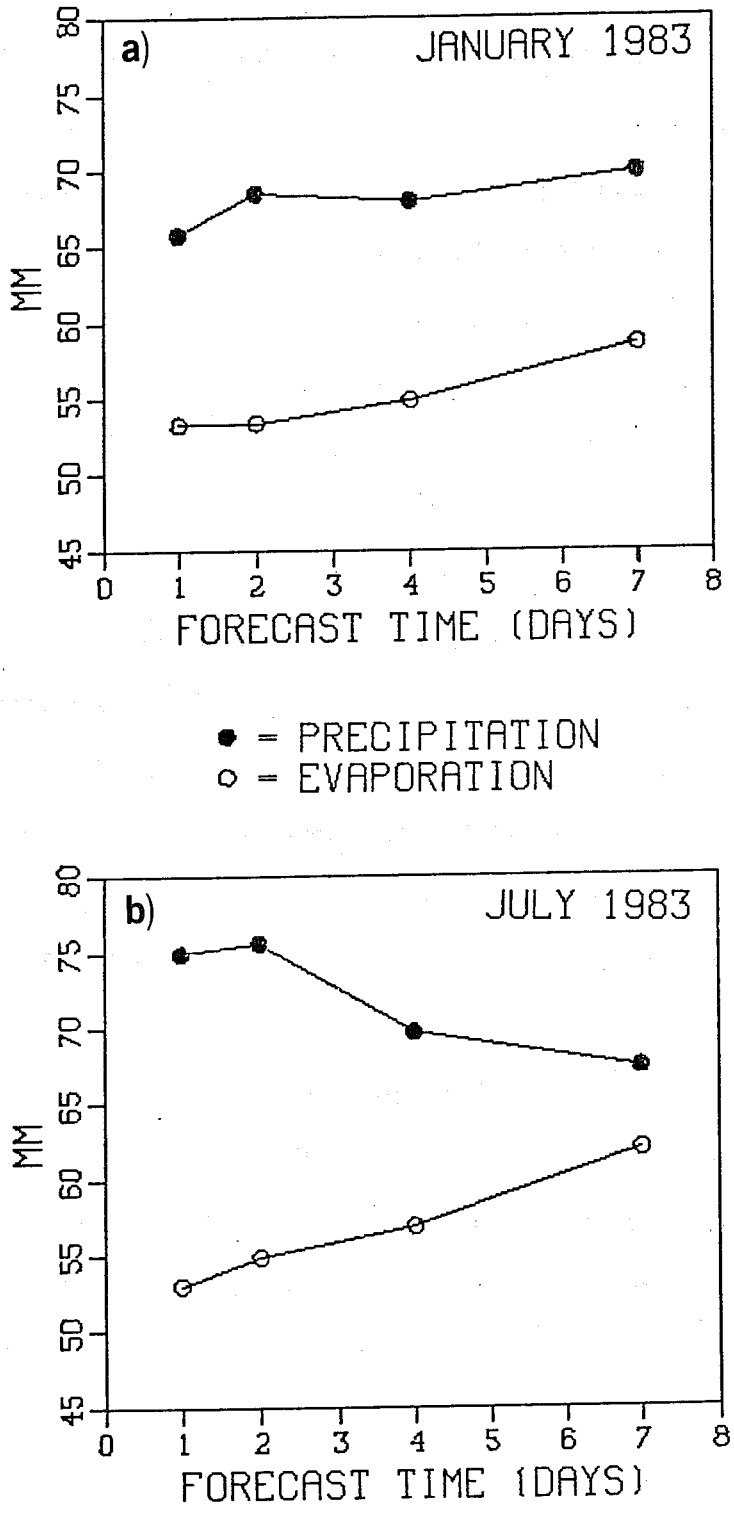

Fig. 9 Variety with forecast time of global monthly means (mm) of precipitation and evaporation forecasts in January 1983 (a) and in July 1983 (b).

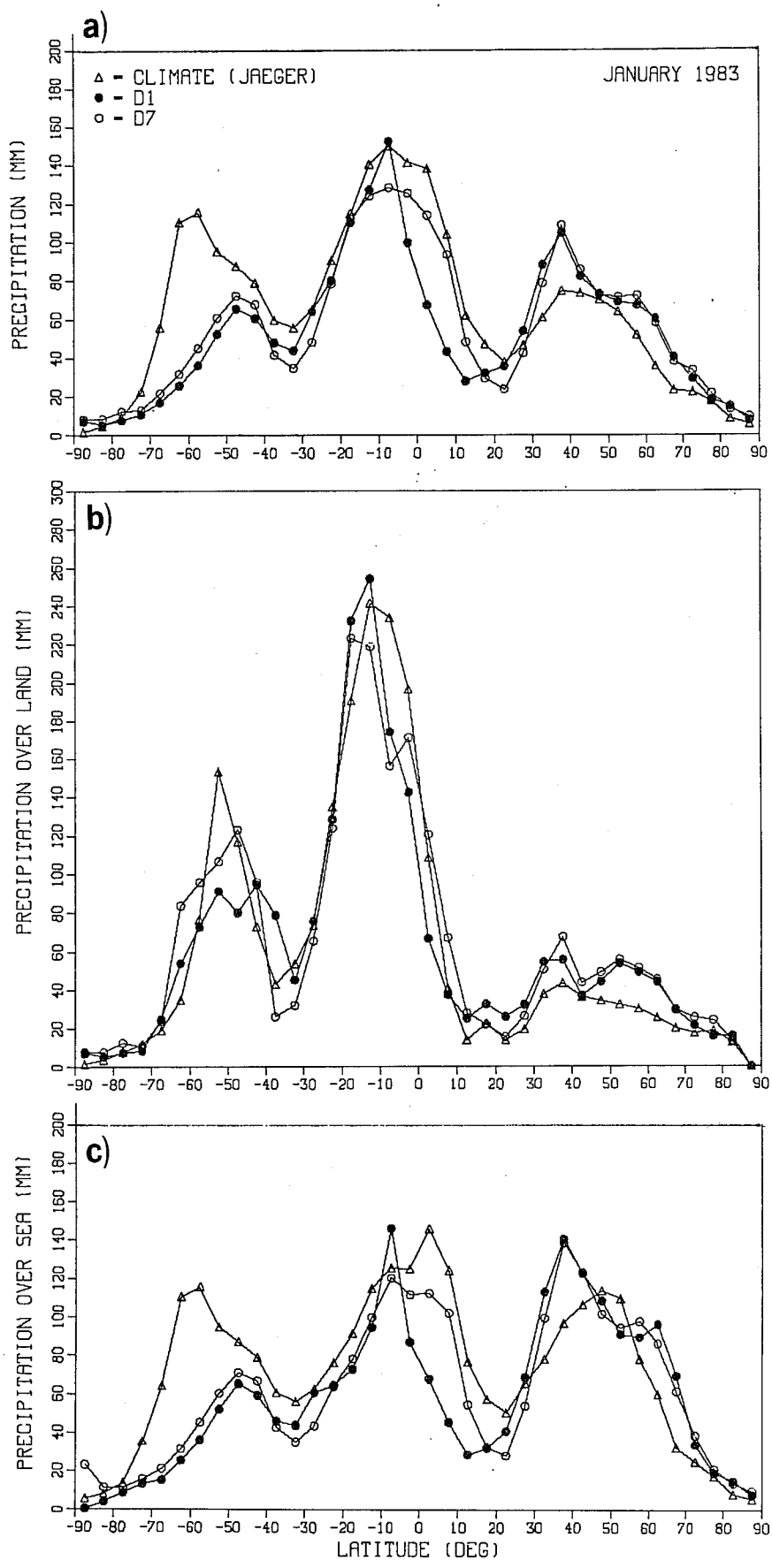

Fig.10 (a) Zonal means of monthly precipitation (mm) in January 1983 from D1 and D7 forecasts compared with Jaeger's climatology (1976) for January; (b) as in (a) but only for continental areas; (c) as in (a) but only for oceanic areas.

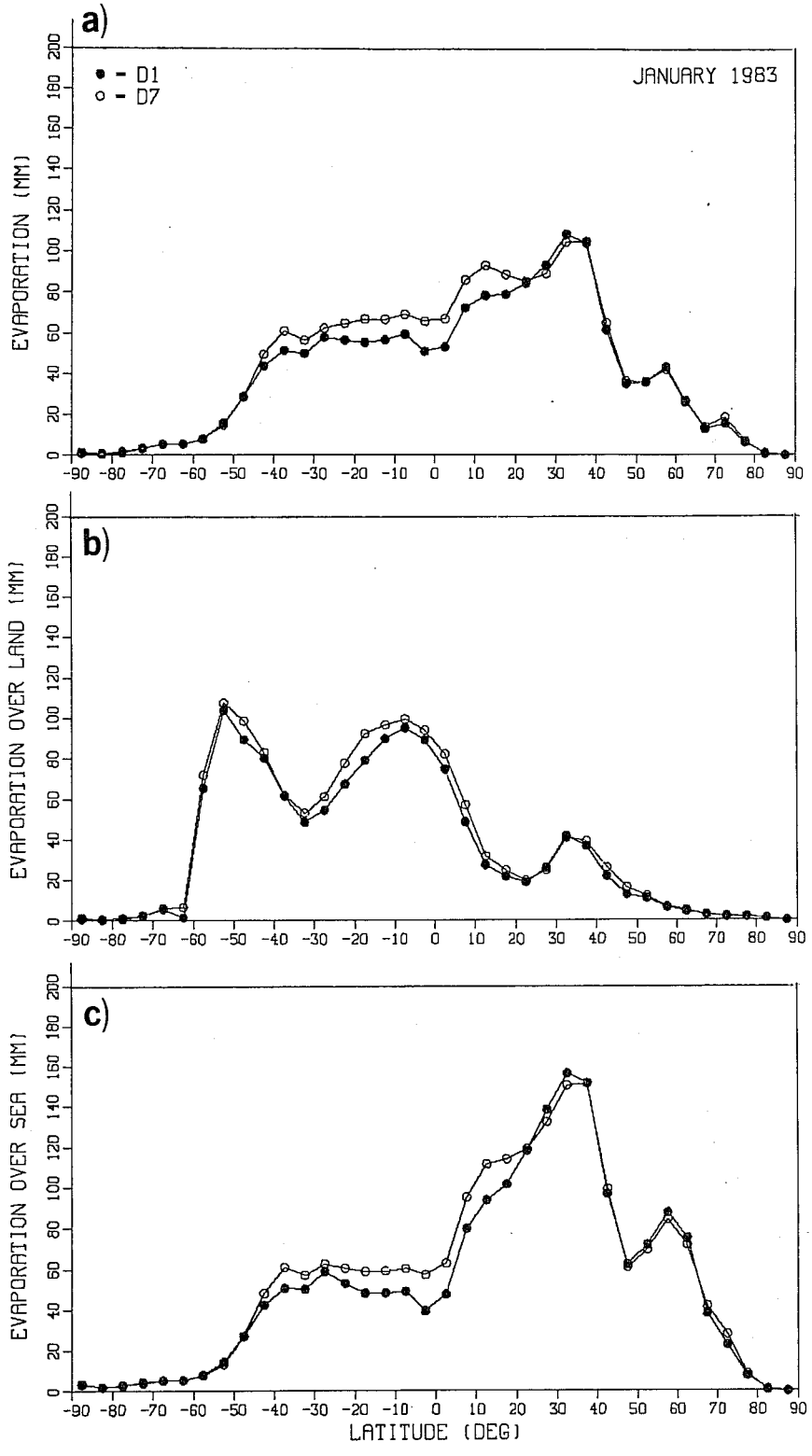

Fig.11 (a) Zonal means of monthly evaporation (mm) in January 1983 from D1 and D7 forecasts; (b) as in (a), but only for continental areas; (c) as in (a) but only for oceanic areas.

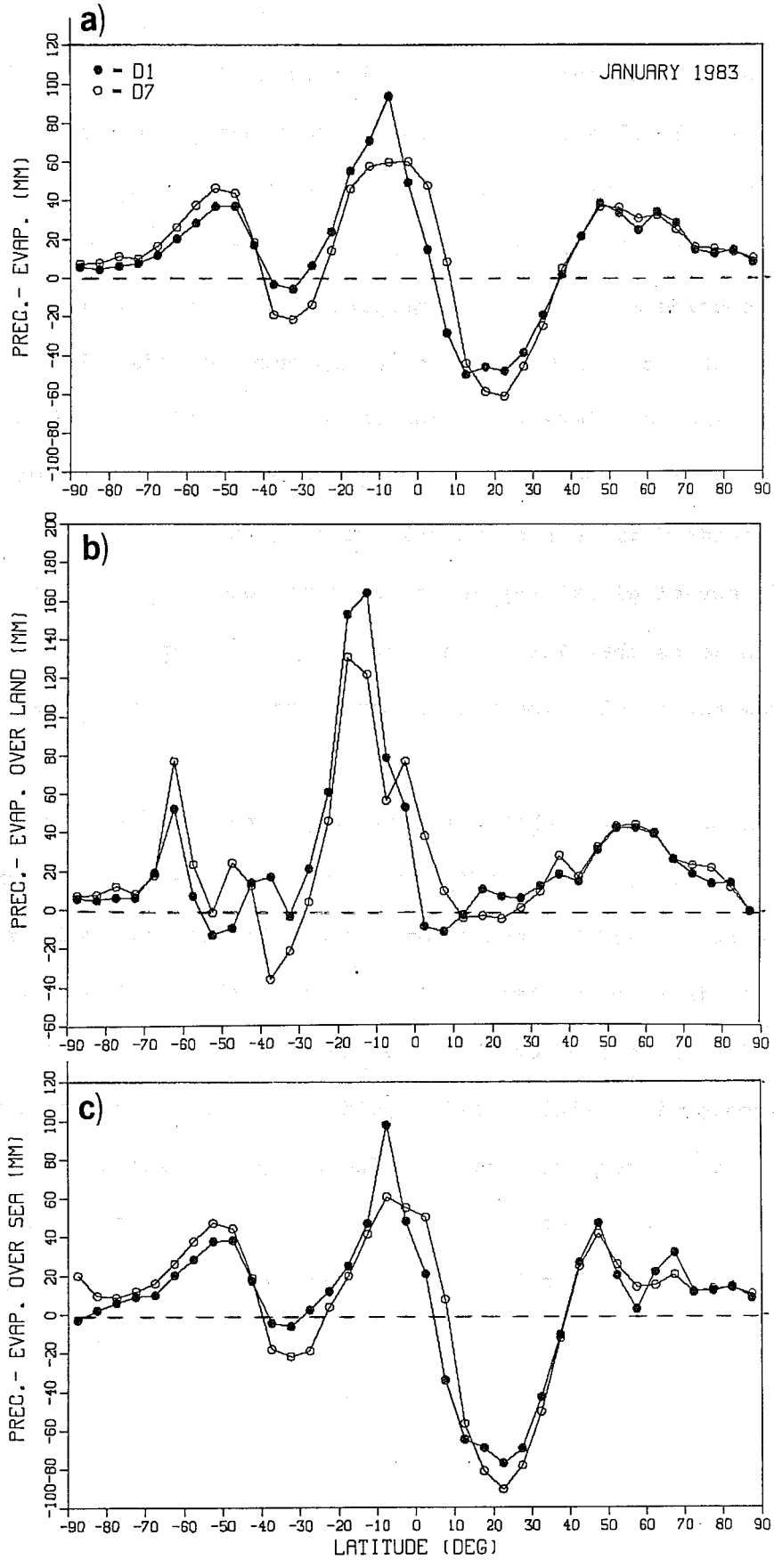

Fig.12 (a) Zonal means of monthly differences between precipitation and evaporation (mm) in January 1983 from D1 and D7 forecasts; (b) as in (a) but only for continental areas; (c) as in (a), but only for oceanic areas.

Figs. 9a and 11 show that this increasing trend in January rainfall is fed by an increase in global evaporation that occurs mainly between 20°N and 40°S, and is particularly evident over the oceans. Despite the fact that from D2 to D7 the increase in global evaporation exceeds that in global precipitation, there is a considerable excess of precipitation (16-19%) during the first days of the forecast cycle with only a slow tendency towards a balance. When mean daily values are considered, a rough calculation indicates that, during the first 180 hours of integration, the model removes from the atmosphere a global average of about 3 mm of precipitable water. According to Peixoto and Oort (1983), the actual global average of precipitable water in January is about 24 mm, which means that 12% of the actual global content of water vapour is removed from the model atmosphere in the first seven and a half days.

From Fig. 9a one can see that there is only a negligible change in evaporation from D1 to D2, whereas a significant increase in precipitation occurs. When zonal means for D1 and D2 (not shown) forecasts are compared, we can see that this increase is concentrated in the ITCZ over the continents and is probably due to an intensification of the divergent circulation in the model - in other words, D1 convective rainfall still suffers from spin-up problems. After D2, the decrease of atmospheric moisture due to the imbalance between precipitation and evaporation prevents a further increase in the former, but intensifies the latter until, from D4 to D7, a new increase in precipitation is possible due to an enhanced supply of water from the surface, particularly from the oceans.

It is not only the global value of evaporation that appears to be incorrect. From Fig.11 and Fig.12 it is evident that over the continents evaporation mainly occurs in the Southern Hemisphere (as seems reasonable); however, over the oceans values considerably greater than the global mean occur only between 10°N and 45°N, and at D1 this oceanic band appears to be the only part of the globe in which in January the model produces an excess of evaporation over precipitation. On the contrary, the evaporation over the oceanic southern extratropics is very low. When Fig.11c is compared with Fig.10c, which shows the precipitation over the sea, one can easily see that the strong peak between 30°N and 40°N, the relative maximum around 60°N and the very low values of evaporation south of 40°S have a clear correspondence in the overestimation or an underestimation of rainfall in comparison with Jaeger's data. A comparison (not shown) between values of convergence of water vapour flux computed from uninitialised analyses and D1 and D7 forecasts indicates that errors in the meridional transport of moisture can only account for 25-50% of the difference between forecast precipitation and Jaeger's climatology between 20°N and 10°S, while negligible errors occur in the extratropics. Despite the uncertainties that affect Jaeger's climatology, it seems plausible to argue that the anomalous distribution of evaporation over the oceans is related to a large part of the systematic error in the rainfall forecasts, even though this does not necessarily mean that the former is the ultimate cause of the latter.

5.2 July results

The global means shown in Fig. 9b for July 1983 indicate a general decrease of rainfall during the forecast, particularly strong between D2 and D4, as can be seen also in Table 1 for the 3-year means. Between D1 and D2 the global rainfall is nearly stationary (1983 values show a small increase, while the

3-year means an even smaller decrease); between D4 and D7 rainfall is again nearly constant in the 3-year value, whereas the 1983 data show a further, but more limited, decrease. Apart from the trend, the 1983 values are systematically 5-10% lower than the 3-year means.

From the global means of evaporation shown in the same figure, one can deduce that the rainfall decrease is related to a strong excess of precipitation over evaporation in the first days of the forecast. Despite the fact that this imbalance is much stronger than in January in the first 2 days (28%), the linear increase in evaporation and the decrease of precipitation produce, by D7, a much better balance than in January; however, while in January the global value of precipitation tends (slowly) towards Jaeger's climatology as the forecast proceeds, in July the balance is (more rapidly) reached and this increases the gap between Jaeger's data and the forecasts. In the first 180 hours, about 3.5 mm of precipitable water is removed from the atmosphere, which represent 13% of the actual mean value of 26 mm deduced for July by Peixoto and Oort (1983).

We now examine the latitudinal distribution of precipitation (Fig. 13) and evaporation (Fig. 14) in July 1983, and the difference between precipitation and evaporation (Fig.15). Comparing Fig. 13 with Figs. 1 and 2 (which show the same fields for the 3-year climatology), it is evident that, as in the January case, the zonal distribution of rainfall is very similar. In general a better agreement between 1983 forecasts and Jaeger's data can be seen in the equatorial region, but greater discrepancies are present over the ocean in the Southern Hemisphere.

Also many features of the evaporation distribution have a clear counterpart in the January profiles. Over the continents the evaporation has its maxima in the equatorial band and in the summer hemisphere (in this case the northern) and shows very little variability during the forecast. The evaporation over the oceans has a maximum near 20°S and very little evaporation in the extratropics of the summer hemisphere; a considerable increase occurs between D1 and D7 in all the tropical areas, a more limited one in the southern mid-latitudes. However, the main difference from the January distribution is that the relative minimum at the equator and the secondary maximum between 10°N and 20°N are more evident than their counterparts in the January profile. This secondary maximum has a very strong increase during the forecast cycle. Therefore, if at D1 the oceanic band between 10°S and 30°S is the only part of the globe in which the model generates a significant excess of evaporation over precipitation, then at D7 also the band between 15°N and 30°N acts as a considerable net source of water vapour for the model atmosphere. It is worthwhile noting that in their respective winter periods, the southern mid-latitude continents are a much stronger 'sink' of atmospheric water vapour than the northern ones, which partially compensates their more limited extent.

In the July forecasts an interpretation of local errors of precipitation in terms of evaporation deficit is more arguable than in the January case, since the stronger discrepancies between the forecasts and Jaeger's data occur in the Southern Hemisphere where evaporation has its maximum and Jaeger's climatology is less reliable. Besides, differences between moisture convergence in the analysis and the forecasts (not shown) are able to account for a good part of the rainfall error north of 40°N and near the equator. So, the deficiency in moisture supply from the surface seems to be concentrated in the subtropics, where one can see the greatest increase in evaporation from D1

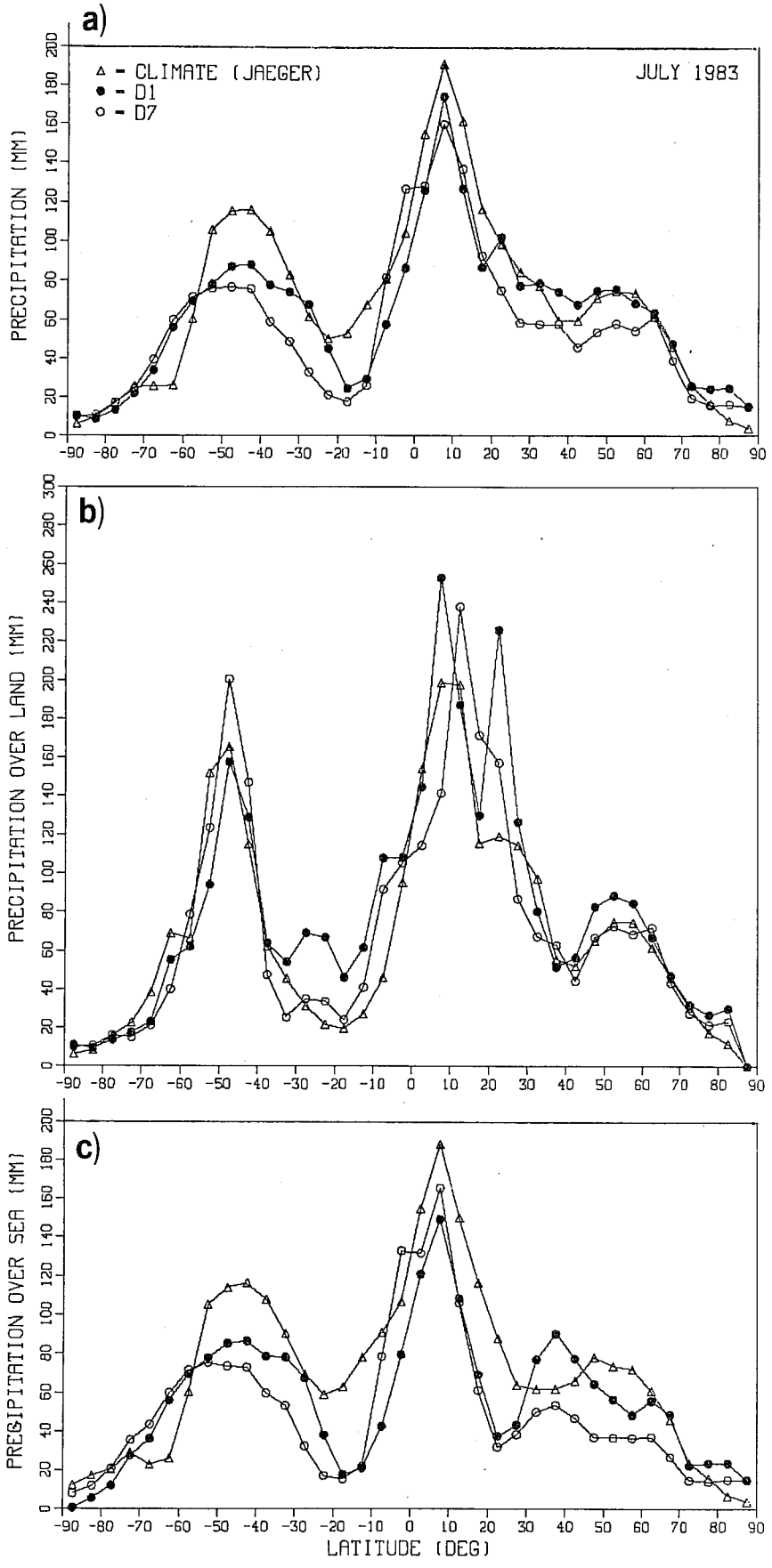

Fig. 13 (a) Zonal means of monthly precipitation (mm) in July 1983 from D1 and D7 forecasts compared with Jaeger's climatology (1976) for July; (b) as in (a) but only for continental areas; (c) as in (a) but only for oceanic areas.

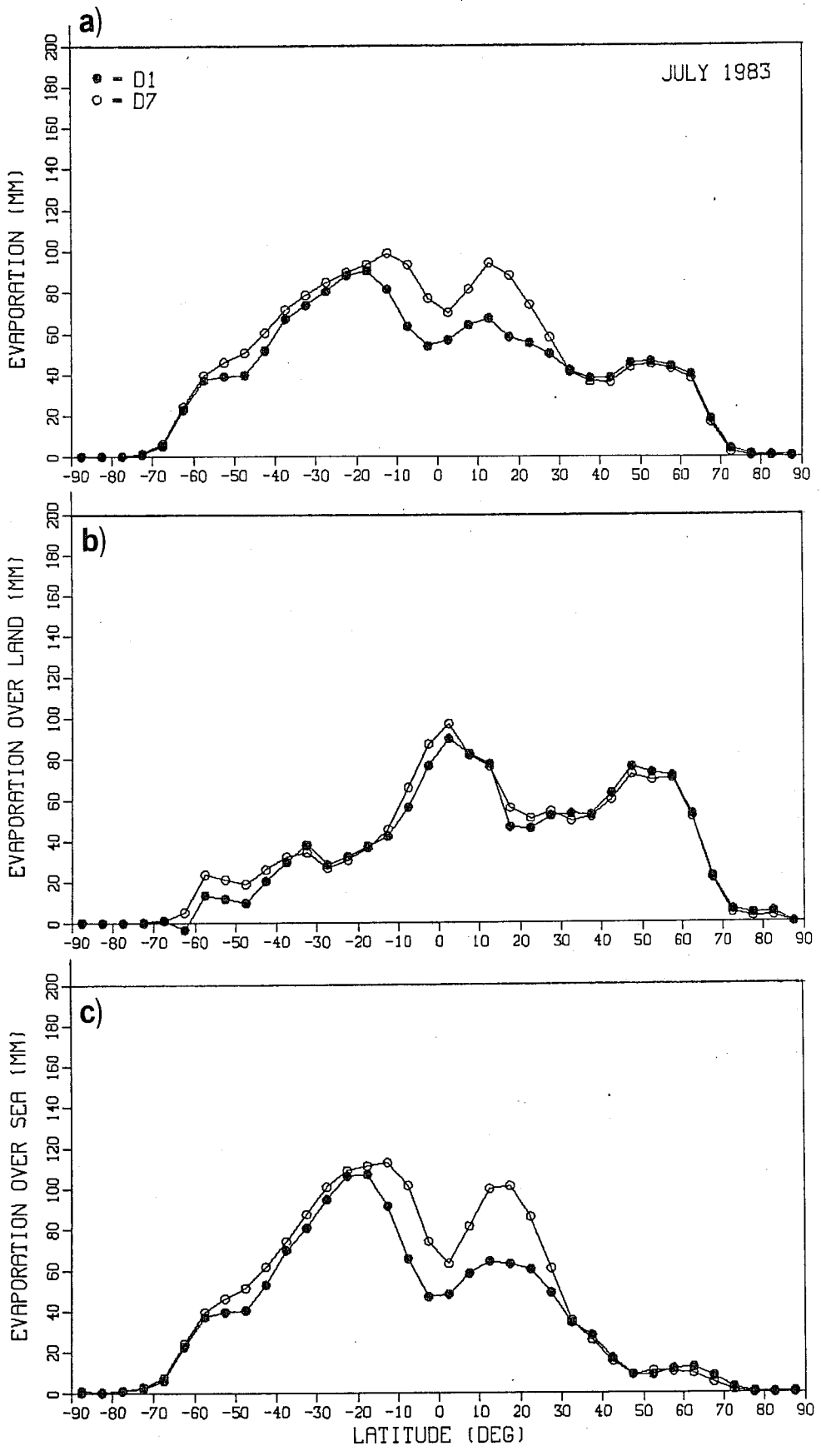

Fig.14 (a) Zonal means of monthly evaporation (mm) in January 1983 from D1 and D7 forecasts; (b) as in (a), but only for continental areas; (c) as in (a) but only for oceanic areas.

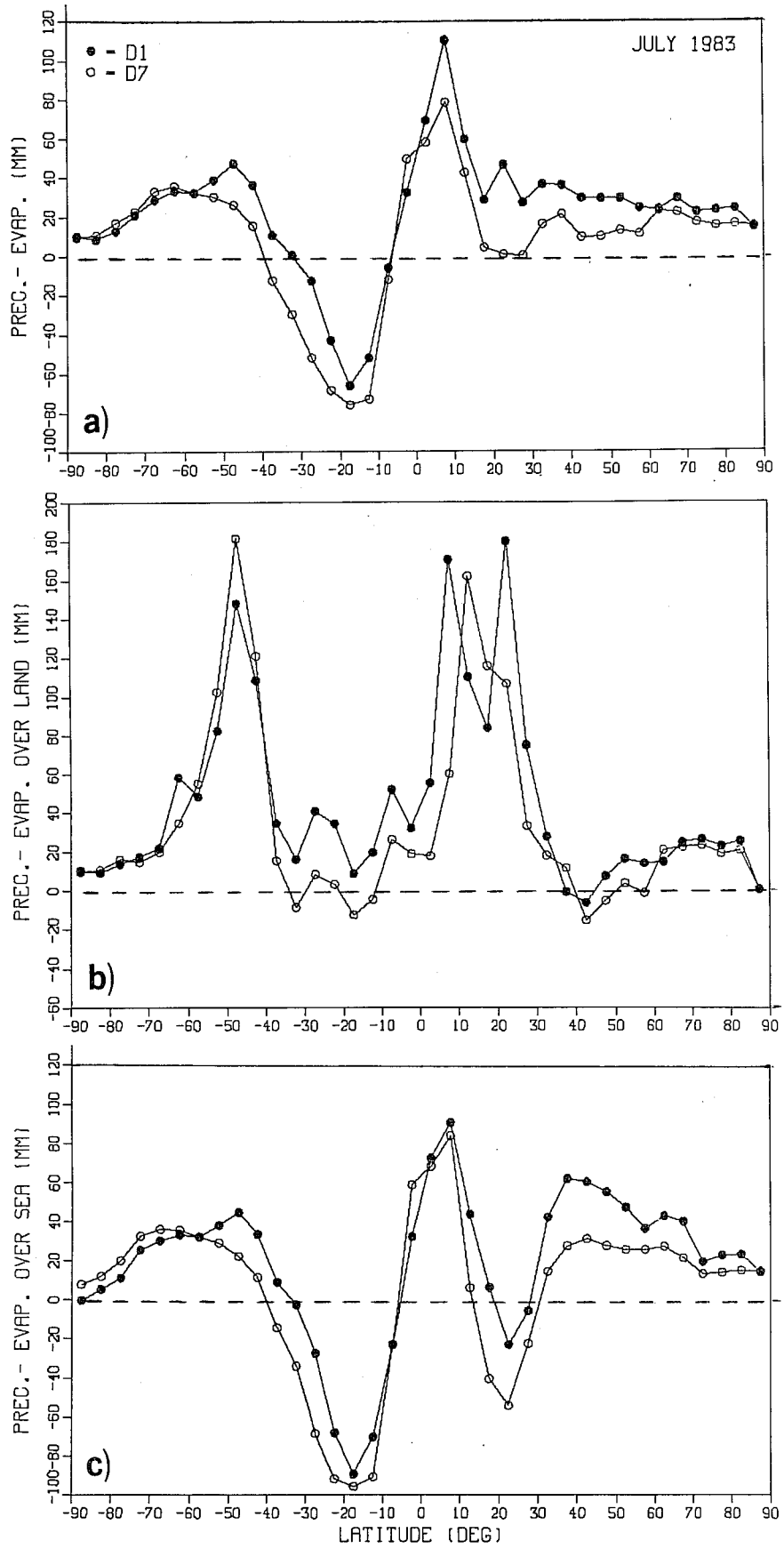

Fig. 15 (a) Zonal means of monthly differences between precipitation and evaporation (mm) in January 1983 from D1 and D7 forecasts; (b) as in (a), but only for continental areas; (c) as in (a) but only for oceanic areas.

to D7. Since prediction precipitation actually decreases from D1 to D7 over most of the globe, it is clear that this increase in evaporation simply compensates for part of the moisture which is removed from the model atmosphere in the first part of the forecast.

5.3 Discussion of the results

We have seen so far that the imbalance between precipitation and evaporation can account for most of the discrepancies between predicted rainfall and Jaeger's climatology, at least on a global scale. To find the cause of such low values of evaporation (both in January and in July) becomes therefore the key question. Heckley (1985) identifies the cause as being an excess of moisture in the model atmosphere at low levels. This excess could be generated by the excess of evaporation over precipitation in the first 6 hours of forecast due to the spin-up problems characteristic of the model convection; over the oceans, the lack of reliable data (or an incorrect treatment of the few available ones, mostly surface data) prevents an adequate correction of the first guess during the analysis step. More importantly, Heckley (1985) suggests that the absence of a parameterisation of the effects of a shallow convection may be the main cause of the model's inability to transport moisture upwards, from the lowest levels to the top and out of the boundary layer, so as to allow new moisture to evaporate from the underlying surface. Tiedtke (1984) also pointed out the need for a shallow convection parameterisation in order to ensure a realistic structure of the planetary boundary layer in the subtropics. Shallow convection allows the accumulation of water vapour at the top of the mixed layer, below the inversion caused by large-scale subsidence and its transport by trade winds into the ITCZ. Tiedtke (1984) showed that the effects of shallow convection can be represented in the model by means of an adequate parameterisation of turbulent fluxes of heat and moisture.

The need for an improvement in the representation of vertical diffusion of waer vapour is also evident from our results.

In southern mid-latitudes in January and in northern mid-latitudes in July, the oceanic evaporation is very low, and remains low on D7 despite the excess of precipitation over evaporation. Also in the tropics, the oceanic evaporation, even though it increases during the forecast, remains below the value required for a global balance during the entire 10-day period despite the excess of precipitation.

So if the excess of water vapour in the lowest level of the model is maintained up to D7 while the overlying layers become increasingly drier, the vertical diffusion in the boundary layer must clearly be insufficient. However, since evaporation is simply the lower boundary condition for the vertical water vapour flux, we are induced to suppose that, with the present scheme, the evaporation in oceanic areas would be insufficient even in the presence of a correct initial distribution of low-level atmospheric moisture.

Evaporation, on the other hand, is not insufficient everywhere. Another problem is represented by the large amount of evaporation over the oceans between 30° and 40°N in January, which is related to excessive (compared to climatology) rainfall in the storm tracks. Since the observed climatology is less reliable over the oceans and the evaporation is on average underestimated, is tempting to suppose that the actual rainfall in those areas might be underestimated by Jaeger's data. However, even taking this into account, the difference in oceanic evaporation between the mid-latitudes of

the two hemispheres remains very high. A possible alternative explanation is that the dependence of the drag and exchange coefficients on the static stability near the surface is too strong. Over the oceans this would cause an excess of evaporation in winter and a deficit in summer; this agrees with the model's behaviour.

To conclude this discussion about the systematic errors in the hydrological balance, we can consider what part of the systematic error in the model's large-scale circulation is the model's own dynamical response to the erroneous latent heat release. The link between the deficit in tropical precipitation and the cooling of the tropical mid-troposphere has been documented by Heckley (1985). Kanamitsu (personal communication) showed by a numerical experiment that the systematic error in the tropics is strongly reduced when a 'climatological' release of latent heat replaces the thermal forcing produced by the convection scheme. It is not unrealistic, therefore, to suppose that the systematic error in the tropics may have an effect also on the extratropical circulation after some time.

Systematic errors in latent heat release occur also in mid-latitudes. If we assume that the vertical distribution of the erroneous (positive or negative) latent heat release is similar to the one deduced by Newell et al. (1974) for the actual atmospheric field, we can convert it into an equivalent daily error in thickness of the 500-1000 mb layer, and compare it with the observed growth rate of the systematic error of this quantity during the same forecast interval. Fig.16 shows the corresponding maps for January deduced by D1 forecasts in 1981/83; as usual, Jaeger's climatology has been used to compute the rainfall systematic error. One can see that some of the large scale

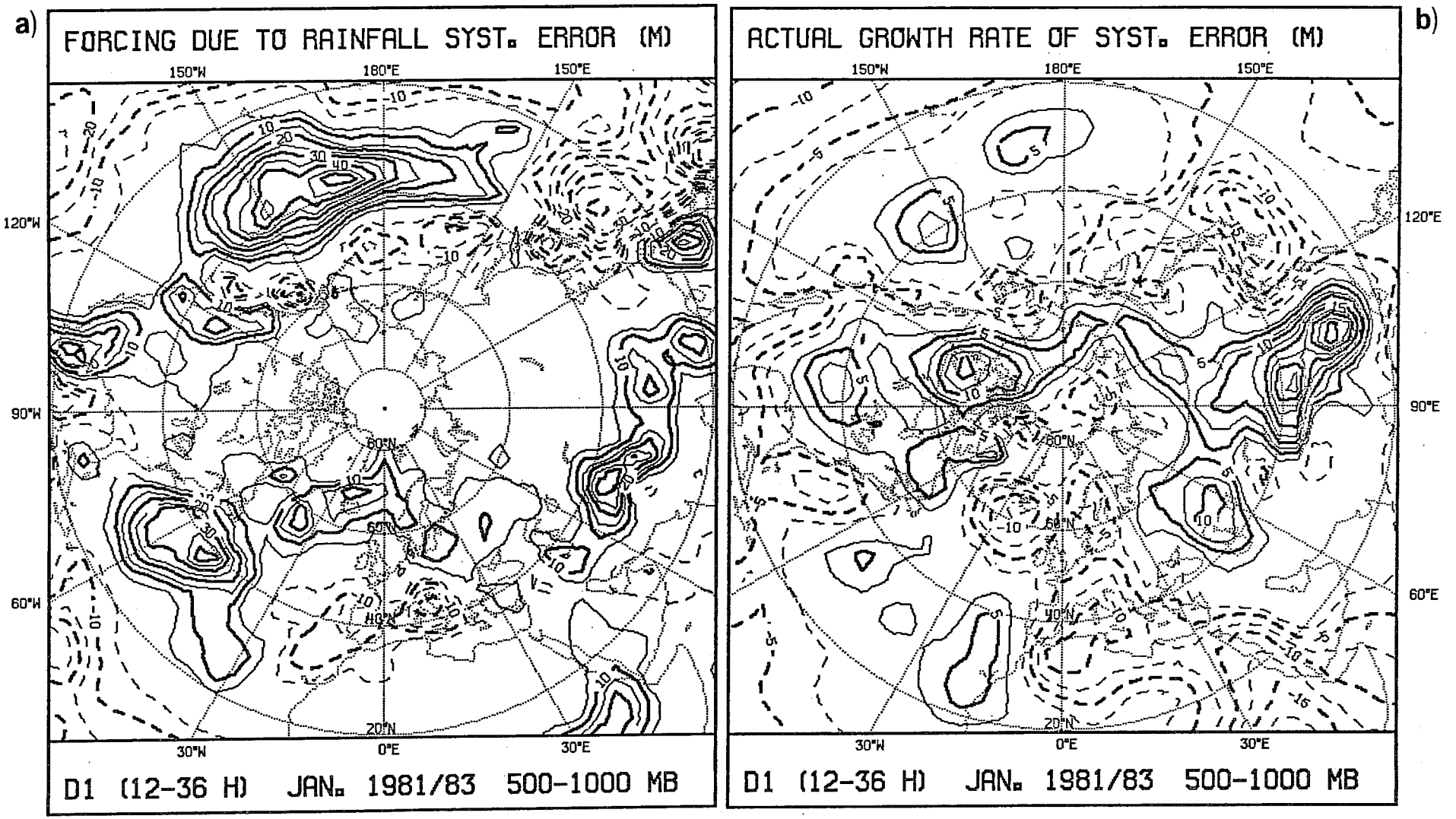

Fig.16 (a) Mean forcing in the 500-1000 mb thickness (m/day) in January due to the systematic error in D1 rainfall forecasts (Jaeger's climatology (1976) is assumed as a reference); (b) actual growth rate of the systematic error of 500-1000 mb thickness in the same month and forecast time.

features have a quite good correspondence in the two maps, especially over Asia and the Western Pacific Ocean. Obviously, many of the main features in the observed thickness error have (totally or partially) a dynamical origin (see, for example, Wallace et al. 1983) and the error in precipitation may be a consequence of this dynamical error. On the other hand, the poor correspondence between the amplitude of the positive errors over the Atlantic and the Central and Eastern Pacific Ocean might be due either to the uncertainty in rainfall climatology or to compensating effects, such as an excess of cold air advection or adiabatic cooling, that could counterbalance the anomalous release of latent heat.

In conclusion, it seems that the error in latent heat release can give a significant contribution to the climate drift of the model atmosphere. A number of sensitivity experiments are therefore needed to clarify the role of the hydrological cycle in determining the long-term climate of the model, not only in the tropics but also in the mid-latitudes.

6. COMPARISON BETWEEN OBSERVED AND PREDICTED MEAN FIELDS OVER EUROPE

In the previous sections, we have compared the mean rainfall fields computed from three years of short range forecasts with the long term global climatology. These comparisons showed the main features of the systematic error of the rainfall forecasts but they were affected by two sources of uncertainty:

(a) the limited reliability of the observed climatology;

(b) the fact that a three-year mean may significantly deviate from a long term mean because of the limitation of the sample.

For these reasons, it is interesting to compare the mean predicted fields with actual observations recorded in the same period in an area where a dense network of stations exist. Europe was chosen for this verification, and in Sect.3 the procedure used to produce grid point values from station reports was explained. As already indicated, the grid used is that of the N48 grid-point model, which has a resolution of 1.875° in latitude and longitude. We also recall that each grid point value was derived from data of at least two stations, and only grid points with values for all the three years were considered. The resulting number of points used in the verification was 184 in January, 203 in July, 204 in April and October. The geographical distribution of these points is shown in Fig.17a, where the number above each point indicates in how many of the four months the data were available in all the three years. Figs. 17b, c and d show the three different representations of the orography used in the ECMWF model during the three year period.

6.1 Variations in the skill of the forecast

Before discussing the maps of the observed and predicted fields, let us consider some indices of the skill of the precipitation forecasts over the whole area. In Table 3 the following values are listed for all the months, forecast times and classes of precipitation considered in this study.

$\bar{P}_o$ spatial mean of the observed precipitation

$\bar{P}_F$ spatial mean of the forecast precipitation

$\bar{\varepsilon} = \bar{P}_F - \bar{P}_o$ spatial mean of the forecast error

$|\bar{\varepsilon}|$ spatial mean of the absolute forecast error

For the total monthly rainfall, the percentage of points over which the monthly value is correctly estimated (CES) underestimated (UES) or overestimated (OES) by the forecasts are also indicated. A forecast was considered correct if:

$$\frac{1}{1.5} \leqslant \frac{P_F}{P_o} \leqslant 1.5 \quad \text{or} \quad |P_F - P_o| \leqslant 10 \text{ mm}$$

The following can be deduced from Table 3:

- The model gives a quite good estimate of the mean rainfall over Europe in January but overestimates it in the other months. This overestimation is tolerable in October and from D4 onwards in July; it is however considerable in April and in the first part of the forecast in July.

- The number of grid point values correctly estimated is quite good, ranging from 67.6 at D1 in October to 45.1 at D7 in April; the percentages are always above 50%, except at D7 in April and July.

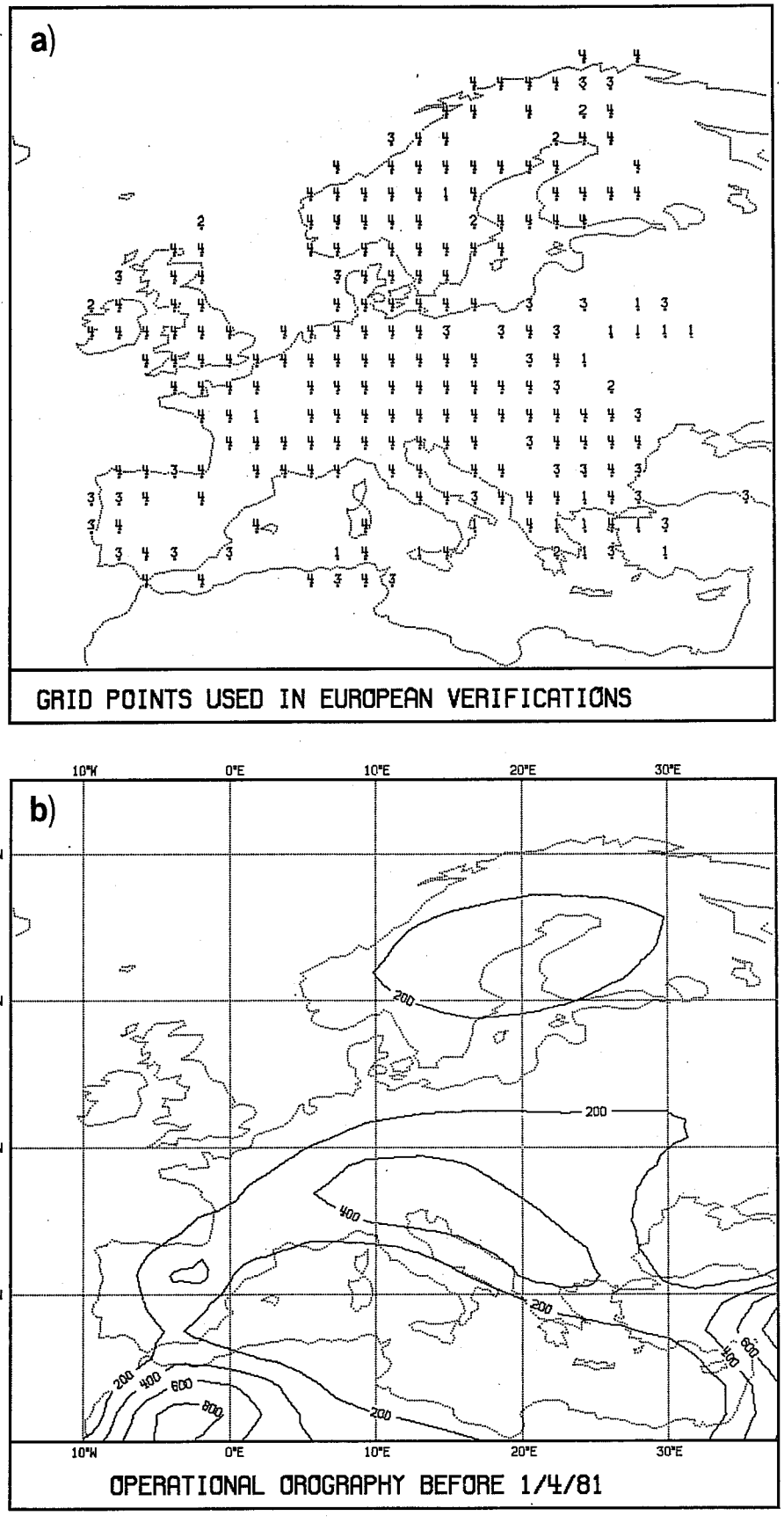

Fig.17 (a) Grid points used in the European verifications; the number above each point indicates for how many of the four months (January, April, July, October) it was possible to compute a 3-year mean of observed date. Three areas selected for a comparison of errors in mountain and plain areas are also shown. (b,c,d) Different representations of the orography in the European area used in ECMWF models before 1/4/1981 (b); from 1/4/1981 to 20/2/83 (c, mean orography); from 20/4/1983 to 31/1/1984 (d, envelope orography).

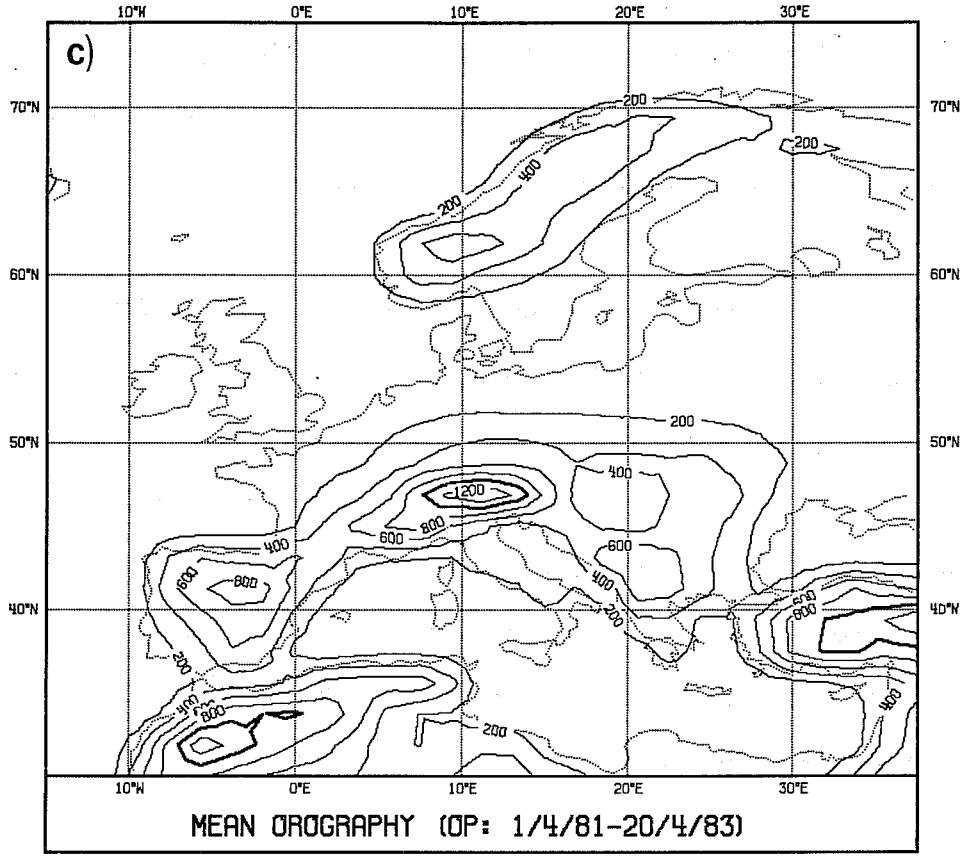
c)
10°W
0°E
10°E
20°E
30°E
70°N
60°N
50°N
40°N
MEAN OROGRAPHY (OP: 1/4/81-20/4/83)

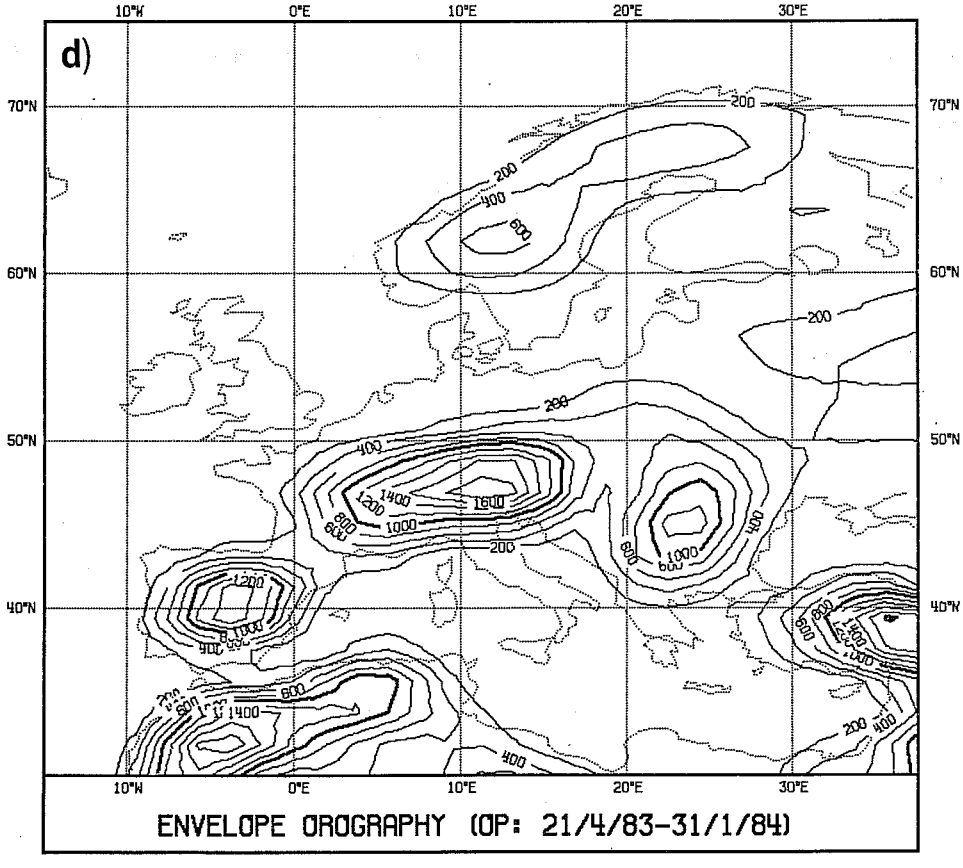
d)
10°W
0°E
10°E
20°E
30°E
70°N
60°N
50°N
40°N
ENVELOPE OROGRAPHY (OP: 21/4/83-31/1/84)

Fig. 17 c) and d)

- The mean absolute error is of the order of 30 mm in all months and ranges from 27.0 (32.0% of the mean actual value) and D1 in October to 38.9 (66.3%) on D1 in July (the worst relative value is 69.9% on D7 in April).

- During the year there is a continuous shift of the forecast time at which the forecasts have the best skill. In October, D1 forecasts are the best according to all the three scores ($\bar{\varepsilon}$, $|\bar{\varepsilon}|$ and CES), with a clear decrease of skill between D1 and D2; in January D1 and D2 are nearly equivalent, the main decrease in skill being between D2 and D4; in April the skill on D1, D2 and D4 is nearly identical, and considerably better than on D7 especially with regard to CES; finally, in July, the skill clearly increases from D1 to D4 (which is the best forecast time according to both $|\bar{\varepsilon}|$ and CES), then decreases again on D7.

- Rainfall Class I is overestimated by about a factor of 2 during the whole year. This overestimation is uniform over all Europe, as can be seen by the fact that $\bar{\varepsilon}$ and $|\bar{\varepsilon}|$ are nearly identical in all months and all forecast times.

- Rainfall Class II is also overestimated in all months, but the mean error is only a fraction of the actual mean value and there are areas where an underestimation occurs: the mean proportional error during the forecast cycle ranges from 28% in July to 56% in April, and the absolute error from 42% in October to 71% in April.

EUROPEAN MONTHLY RAINFALL 1981/83		TOTAL							CLASS I				CLASS II				CLASS III			
		$\bar{P}_o$	$\bar{P}_F$	$\bar{\varepsilon}$	$\overline{\lvert\varepsilon\rvert}$	UES%	CES%	OES%	$\bar{P}_o$	$\bar{P}_F$	$\bar{\varepsilon}$	$\overline{\lvert\varepsilon\rvert}$	$\bar{P}_o$	$\bar{P}_F$	$\bar{\varepsilon}$	$\overline{\lvert\varepsilon\rvert}$	$\bar{P}_o$	$\bar{P}_F$	$\bar{\varepsilon}$	$\overline{\lvert\varepsilon\rvert}$
JANUARY	D1	77.5	71.1	-6.3	27.0	20.1	60.9	19.0	4.5	7.5	3.0	3.2	44.2	58.8	14.6	18.9	28.8	4.8	-24.0	25.3
	D2		74.8	-2.6	27.6	18.5	60.9	20.7		7.8	3.3	3.4		60.5	16.3	20.0		6.5	-22.3	24.0
	D4		79.6	2.1	31.1	19.6	54.9	25.5		7.4	2.9	3.0		66.8	22.7	25.8		5.4	-23.5	25.3
	D7		76.7	-0.8	31.0	22.8	56.0	21.2		7.5	3.1	3.2		61.2	17.0	21.2		8.0	-20.8	24.0
APRIL	D1	52.5	72.5	20.0	31.2	11.3	53.4	35.3	3.5	6.8	3.3	3.4	34.0	50.2	16.2	21.5	15.0	15.6	0.5	14.7
	D2		74.6	22.1	31.4	7.4	54.4	38.2		6.7	3.2	3.3		53.1	19.2	24.2		14.7	-0.3	15.7
	D4		71.8	19.3	31.1	11.8	53.4	34.8		7.0	3.5	3.6		50.6	16.7	22.5		14.1	-1.0	15.0
	D7		77.9	25.4	36.7	12.3	45.1	42.6		7.0	3.5	3.6		57.4	23.5	28.8		13.5	-1.6	15.9
JULY	D1	58.7	79.1	20.4	38.9	21.2	52.7	26.1	2.6	5.2	2.6	2.8	33.4	43.3	9.9	19.4	22.7	30.6	7.9	25.6
	D2		75.8	17.2	35.2	21.7	55.2	23.2		5.1	2.5	2.6		44.4	11.0	18.6		26.3	3.6	23.3
	D4		67.4	8.8	28.7	24.1	56.2	19.7		5.1	2.5	2.7		42.3	8.9	17.0		20.0	-2.7	18.1
	D7		64.0	5.3	33.9	33.5	46.8	19.7		5.0	2.4	2.6		40.5	7.1	18.1		18.5	-4.2	22.4
OCTOBER	D1	84.3	91.9	7.7	27.0	11.3	67.6	21.1	3.6	7.7	4.1	4.1	52.5	68.8	16.3	20.3	28.1	15.5	-12.7	19.1
	D2		98.3	14.0	31.5	9.3	63.7	27.0		7.5	3.9	3.9		73.6	21.1	25.1		17.2	-10.9	19.4
	D4		97.3	13.1	31.4	8.8	62.7	28.4		7.6	4.0	4.1		72.3	19.8	22.4		17.4	-10.8	20.3
	D7		95.6	11.4	34.0	11.8	60.8	27.5		7.3	3.7	3.7		67.7	15.2	21.3		20.7	-7.5	21.1

Table 3. Statistics derived from the comparison between 3-year means of monthly rainfall (and contributions from 3 rainfall classes) deduced from observed data and D1, D2, D4, D7 forecasts over ~200 European grid points.

$\bar{P}$: mean observed value (mm); $\bar{P}_F$: mean forecast value (mm); $\bar{\varepsilon}$ mean error (mm); $\overline{\lvert\varepsilon\rvert}$: mean absolute error (mm); UES, CES, OES: percentages of underestimated, correctly estimated and overestimated values. See text for a precise definition of the scores, the grid point values and the rainfall classes.

- Rainfall Class III is poorly estimated during the whole year. The mean absolute error has nearly the same magnitude of the actual value, except in October, when it is about 70%. In April and July both overestimations and underestimations occur locally, so that the mean error is small, while the underestimation is prevailing in October and strongly dominant in January, when the forecasts account for only 20-30% of the mean observed value in this class.

6.2 Geographical distribution of the systematic error

We now examine the geographical distribution of the systematic error over Europe. Fig.18 shows the actual mean values, the mean forecast field on D1, the mean error of these forecasts and the ratio between forecasts and observations for January. In the ratio map the values are expressed as percentages and a small number of stations that had an observed rainfall less than 20 mm have been excluded so that a value between 67 and 150 indicates a correct estimate according to our criterion.

It is evident from Fig.18 that the main source of error in the forecast is the excessive smoothness of the model's orography. In the observed fields, the highest values are obviously over the mountains, and particularly on the western side of the mountain chains which are close to the Atlantic coast. The maxima are reached in the south-western part of Norway, with values of the order of 300 mm. A strong decrease of rainfall can be seen in the lee (generally, the eastern) side of the mountains. Again, the effect is particularly evident in Scandinavia, but the difference can be seen also in Scotland and even between the western and the eastern coast of Italy. Over the Alps, the mean flow in January is from north-west, and the strongest

gradient of precipitation can be found along this direction. The variations in the rainfall distribution caused by the mountains are heavily underestimated in the forecasts as was already noted by Johannessen (1982) for the Alpine region and by Heckley (1981) for the Andes. Predicted rainfall is much below the observed values over the Alps, in western Spain and on the Norwegian coast. Even though the forecasts show a difference between the western and the eastern part of Scandinavia, and the maxima can be found close to the observed ones, the gradient is too weak and rainfall over central Scandinavia is strongly overestimated.

Conversely, the skill of the forecasts is good over the plains. We can compare the percentage of correct estimates over the whole of Europe with the same score computed in three selected regions shown in Fig.17a, each one including 25 stations: western Scandinavia (WS), the Alps and the central Mediterranean coasts (AM) and the plain in northwestern Europe (PB). Over WS and AM, there are two areas with strong orographic gradients, CES are 44% and 40% respectively, whereas they are 80% over PB; the value computed from all the European stations is 60.9%, as shown in Table 3.

The verification maps for July, which compare observations with D4 forecasts, are shown in Fig.19. They indicate that in summer the orography is again the main source of error but with the opposite effect, too much convective rainfall being generated over the mountains, particularly over the Alps. Comparing Fig.19b with Fig.17c,d one sees that the forecast rainfall pattern over Europe closely resembles that of the orography used in the model. Tibaldi (1982) showed that the erroneous diffusion of temperature and moisture over sigma surfaces in mountain areas was the main source of the strong excess of convection generated by the model after the introduction of a more

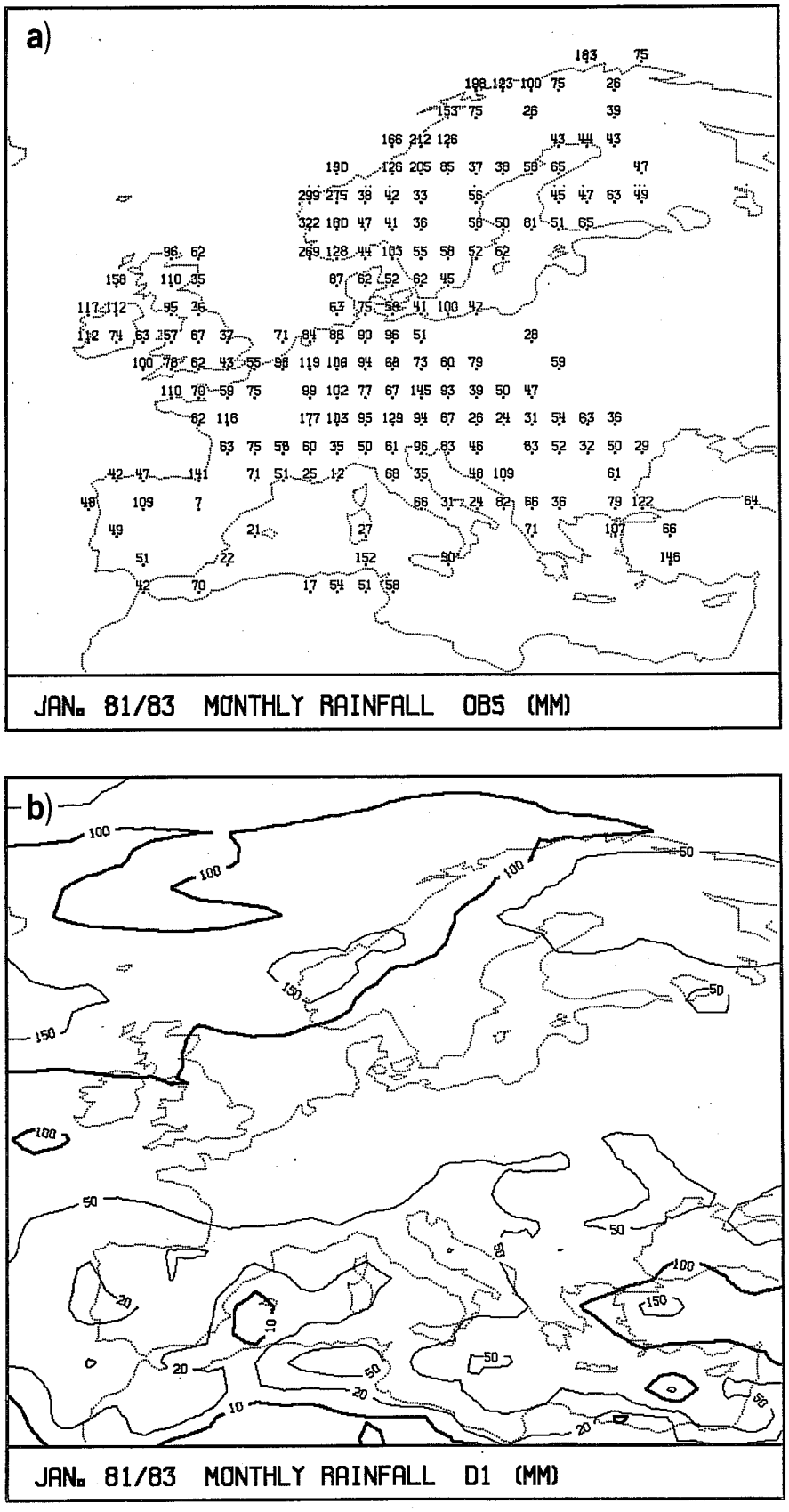

Fig.18 (a) 3-year means of monthly rainfall (mm) in January deduced from observed data; (b) as in (a) but computed from D1 forecasts; (c) mean forecast error; (d) ratio of predicted to observed values, in percentages.

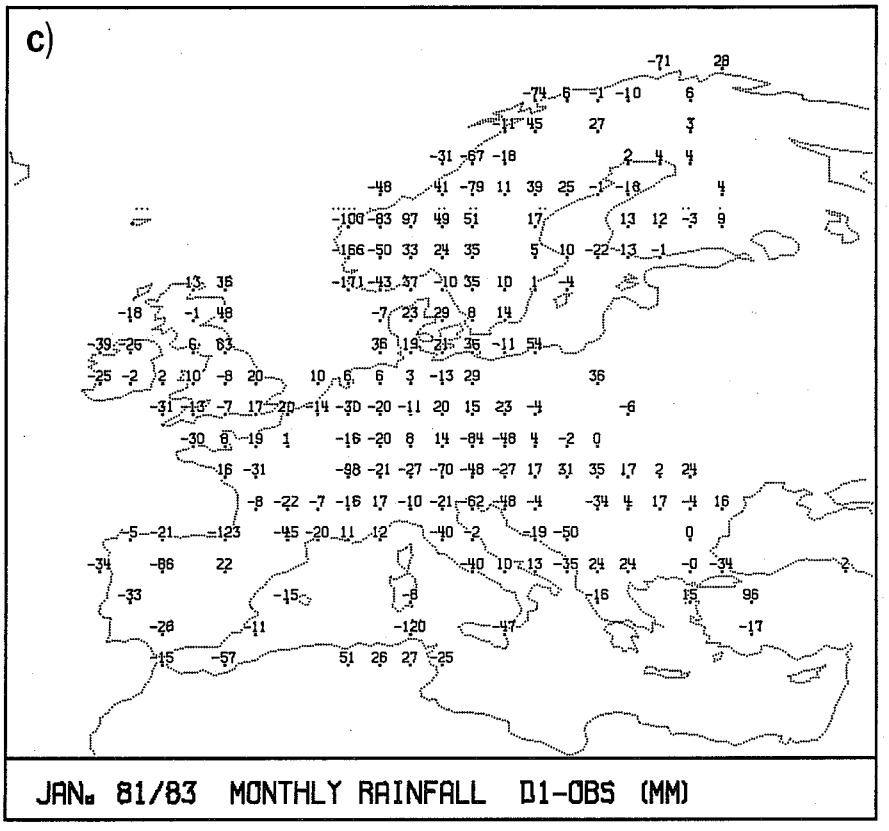
c)
JAN. 81/83 MONTHLY RAINFALL D1-OBS (MM)

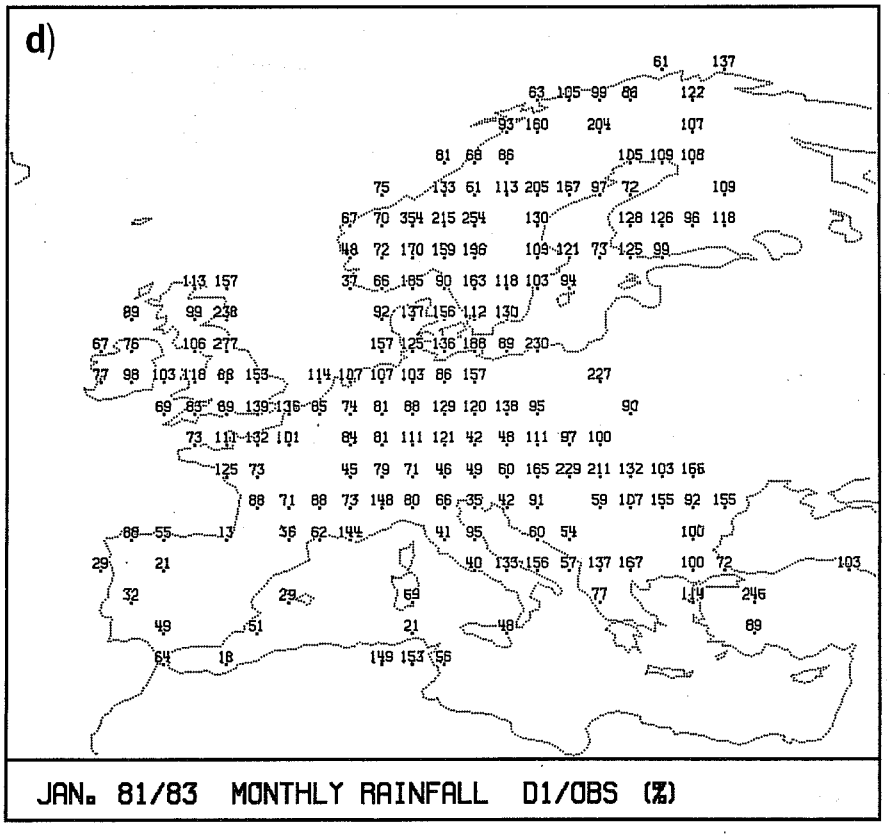
d)
JAN. 81/83 MONTHLY RAINFALL D1/OBS (%)

Fig. 18 c) and d)

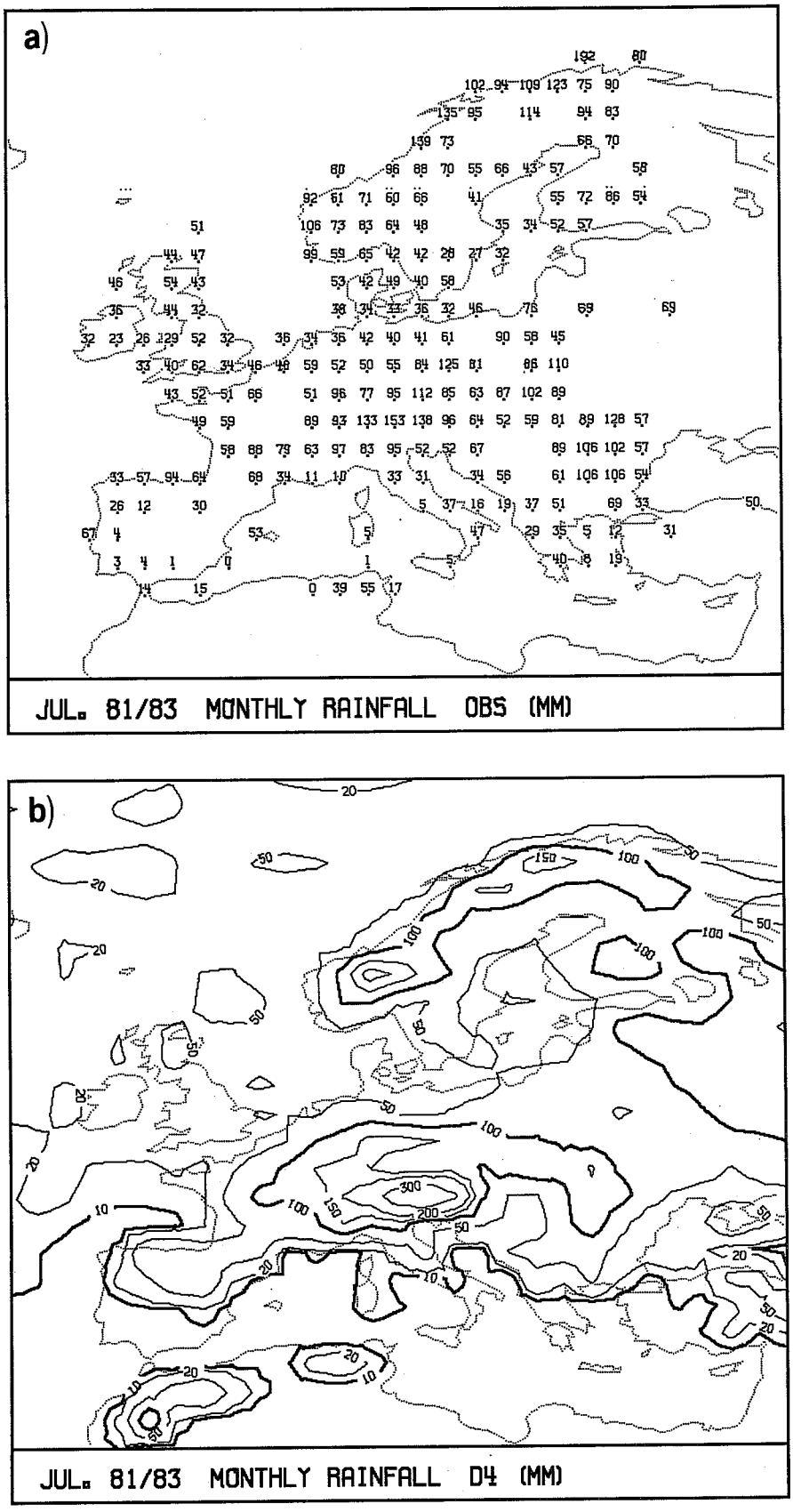

Fig. 19 (a) 3-year mean of monthly rainfall (mm) in July deduced from observed data; (b) as in (a) but computed from D4 forecasts; (c) mean forecast errors; (d) ratio of predicted to observed values, in percentages.

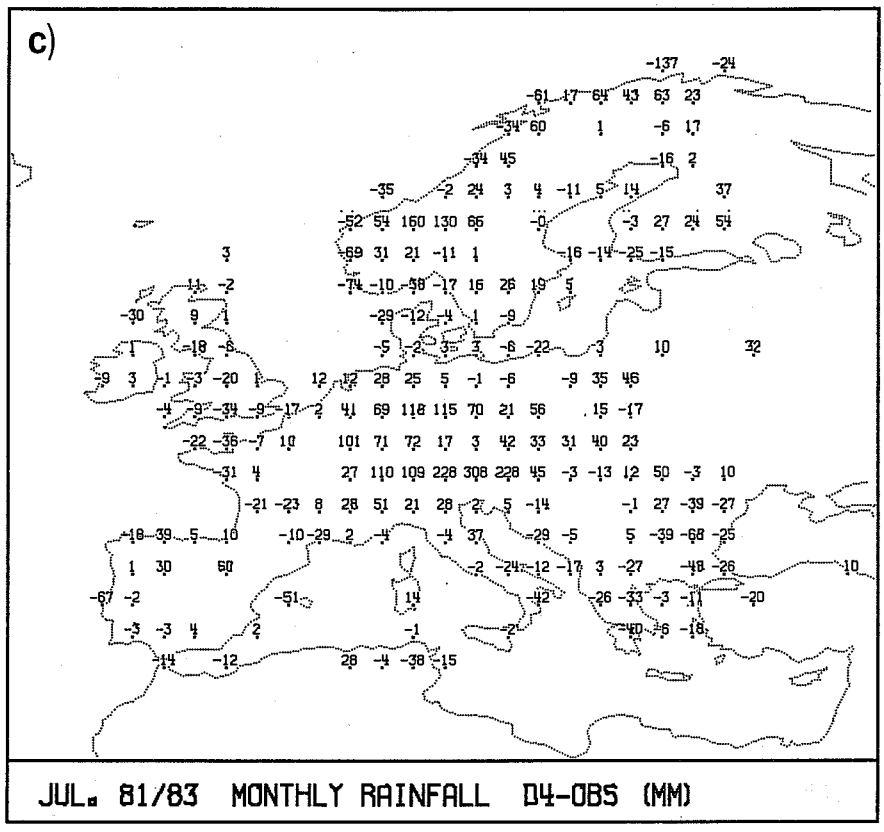
c)
JUL. 81/83 MONTHLY RAINFALL D4-OBS (MM)

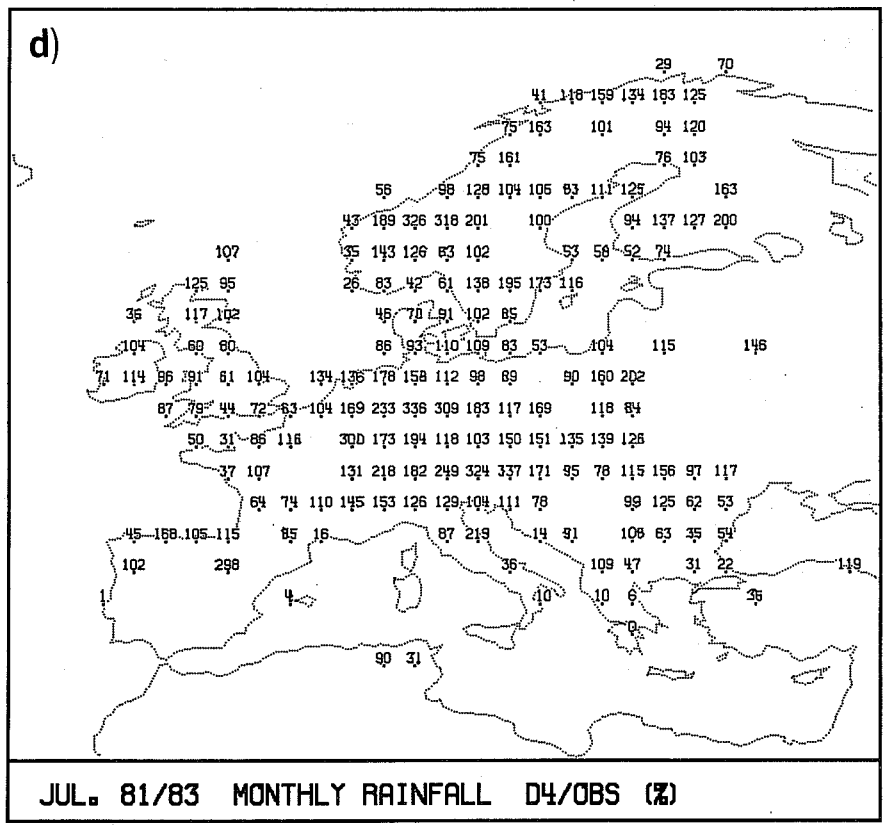
d)
JUL. 81/83 MONTHLY RAINFALL D4/OBS (%)

Fig. 19 c) and d)

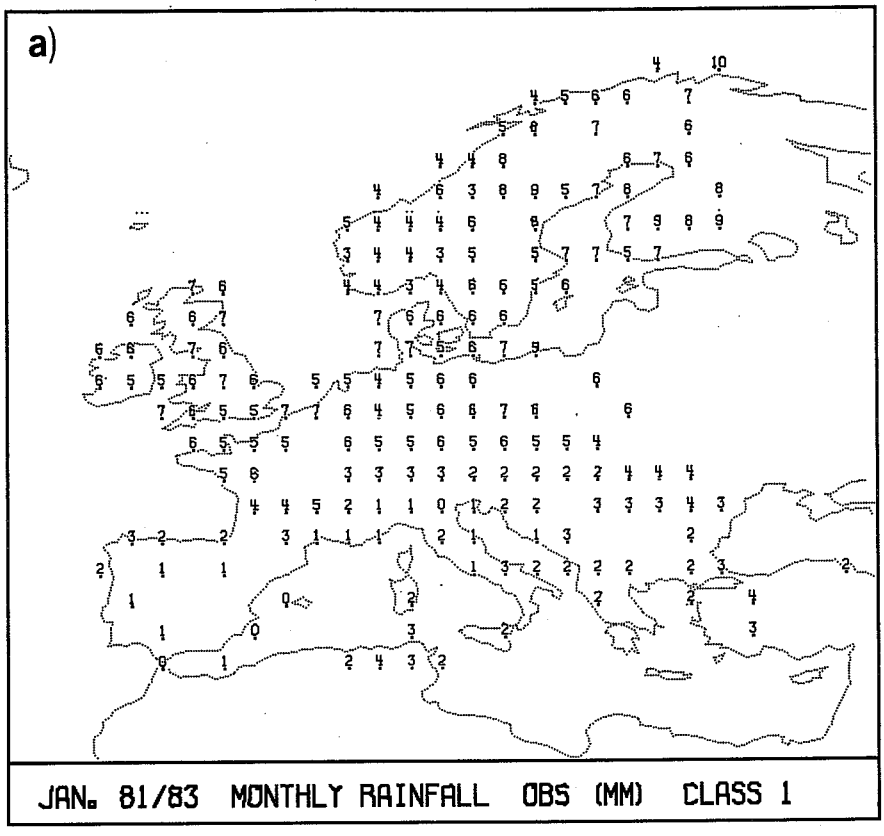

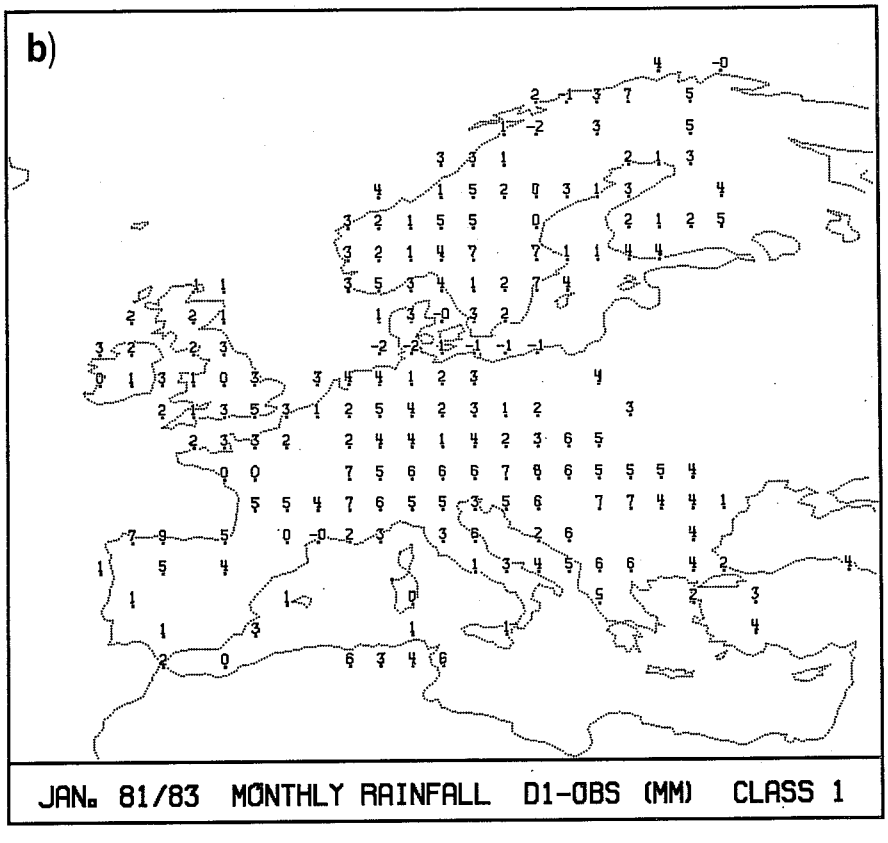

Fig.20 Contribution to the 3-year means of monthly precipitation (mm) over Europe due to daily rainfall less than 2 mm (Class I). (a) observed values in January; (b) D1 forecasts minus observed values in January; (c) observed values in July; (d) D4 forecasts minus observed in July.

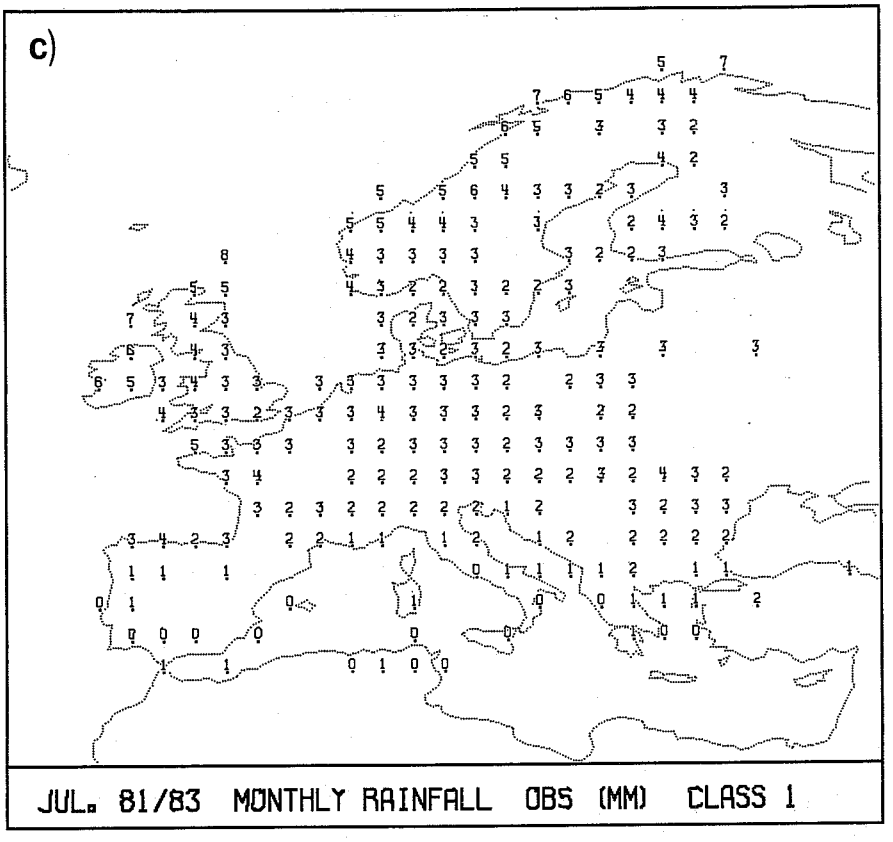
c)
JUL. 81/83 MONTHLY RAINFALL OBS (MM) CLASS 1

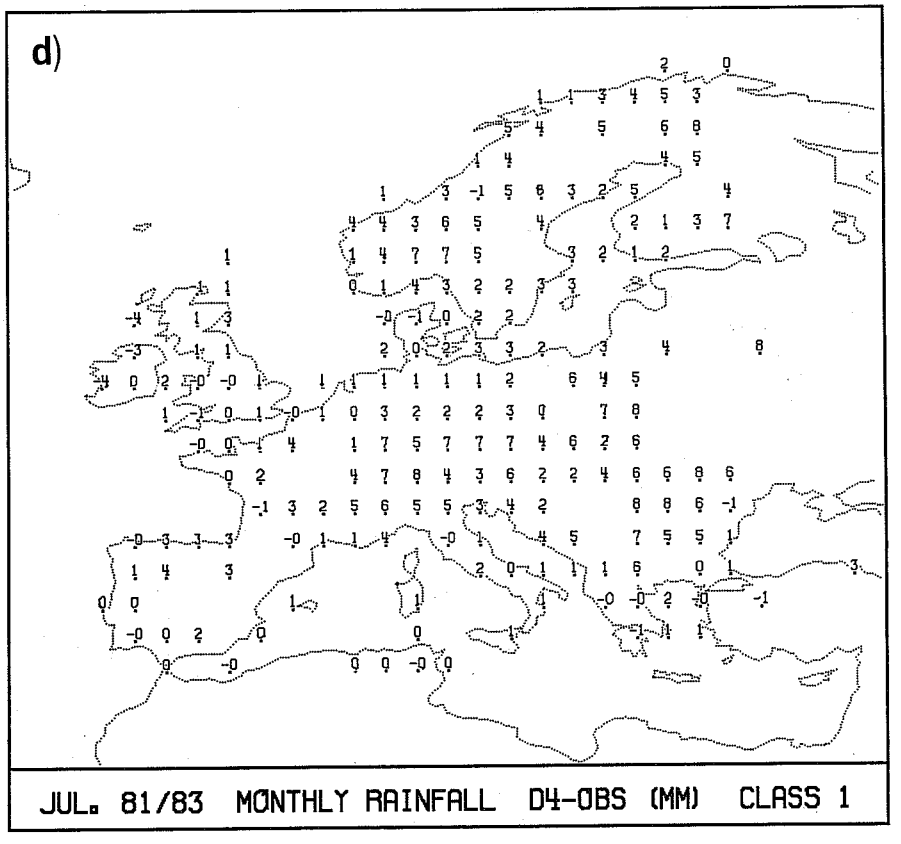
d)
JUL. 81/83 MONTHLY RAINFALL D4-OBS (MM) CLASS 1

Fig. 20 c) and d)

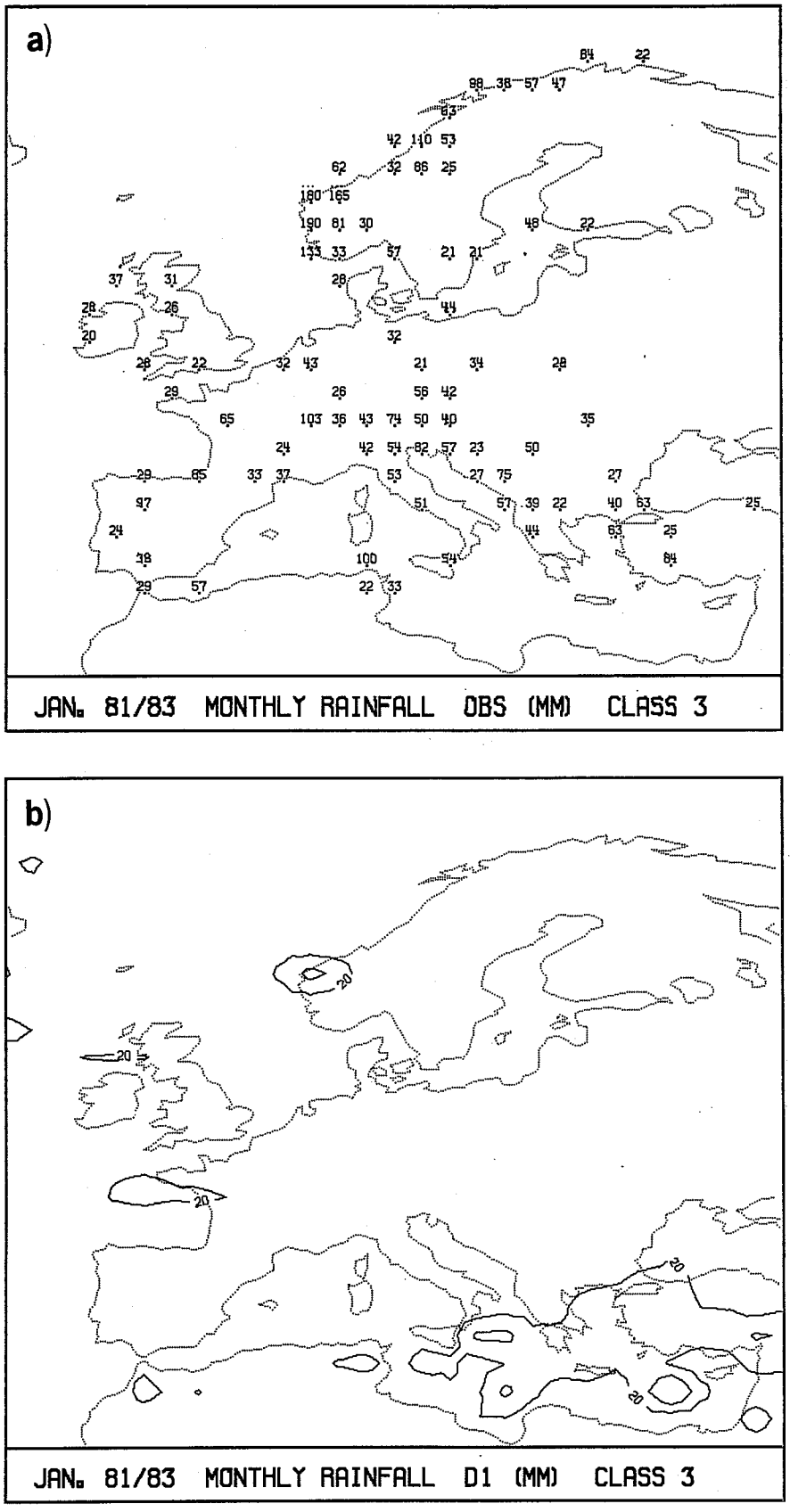

Fig. 21 Contribution to the 3-year means of monthly precipitation (mm) over Europe due to daily rainfall greater than 20 mm (Class III).
(a) observed values in January; (b) D1 forecasts in January;
(c) observed values in July; (d) D4 forecasts in July.

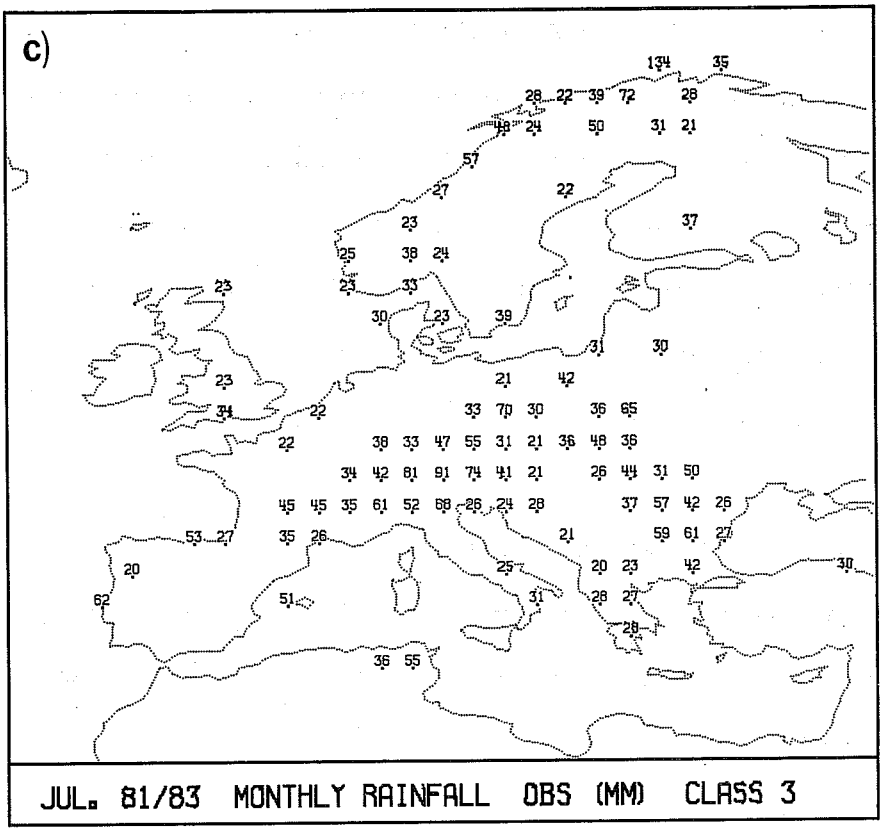
c)
JUL. 81/83 MONTHLY RAINFALL OBS (MM) CLASS 3

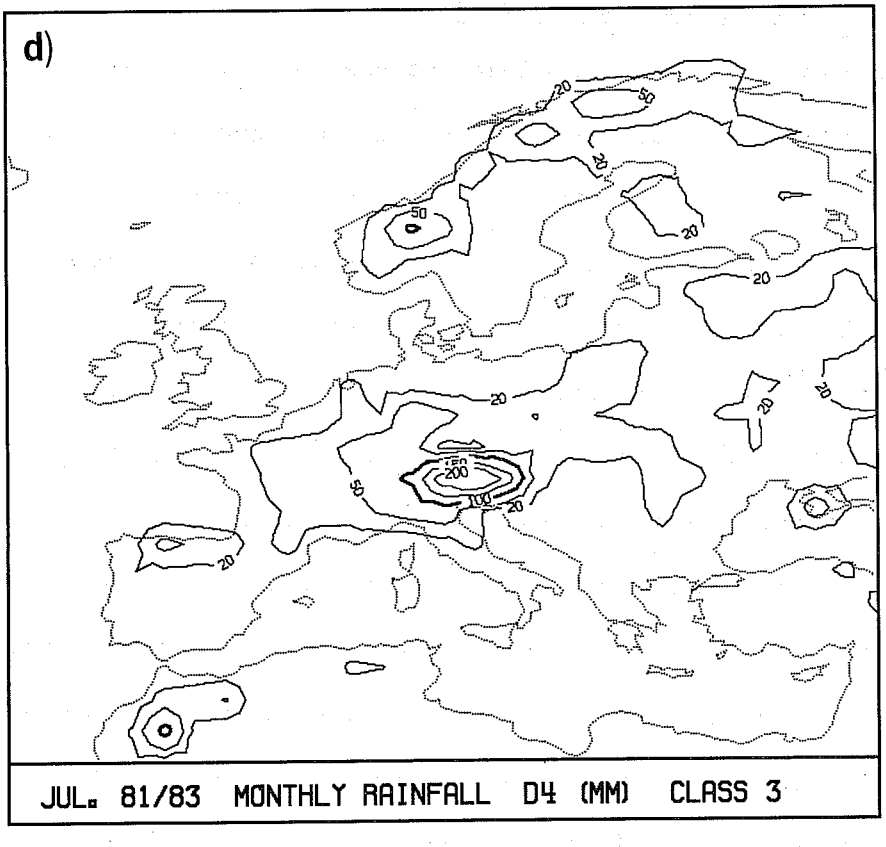
d)
JUL. 81/83 MONTHLY RAINFALL D4 (MM) CLASS 3

Fig. 21 c) and d)

realistic orography in April 1981 (Fig.17c). Since a new horizontal diffusion scheme, which approximates diffusion over constant pressure surfaces, was introduced at the end of September 1981, the excessive convection over mountains has been reduced but not eliminated. This seems to indicate that a number of different causes, including natural oversensitivity of the Kuo scheme and residual spurious diffusion, contribute to the incorrect behaviour of the convection scheme in mountain areas.

The percentages of CES over the three selected areas are 44% (WS), 48% (AM), 68% (PB) while the total European value is 56.2%. Also in July, the skill of the forecasts over the plains is considerably better than over or close to the mountains, but the difference is not as noticeable as in winter.

6.3 The results by rainfall classes

We can now examine how the contributions due to light (Class I) or heavy (Class III) daily rainfall are simulated in the forecasts. Fig.20 shows the observed values in Class I and the corresponding errors for January and July. One can see that this rainfall class is overestimated at almost all the stations, the errors being of the same order of magnitude of the observed values. In Fig.21, the observed and the forecast values of rainfall Class III are compared for January and July. In all the maps only the points (or the areas) with a three-year mean value greater than 20 mm are plotted and one can see a clear correspondence between the distribution of the observed values and the orography. In July, the distribution of the forecast values is rather similar to that of the observed ones, even though there is an underestimation in the Balkan region and an overestimation on the eastern Alps; conversely, in January there is very little rainfall in Class III forecasts over the whole of Europe so that the three-year mean is below 20 mm on almost all points.

6.4 Concluding remarks

We conclude that, over Europe, deficiencies in the representation of the orographic and convective processes are the main sources of systematic error in the rainfall forecasts. In winter, the excessive smoothness of the model orography produces an underestimation on the windward side of the mountains and an overestimation on the lee side, and prevents the simulation of intense rainfall due to orographic lifting. In summer, the diffusion scheme and the parameterisation of convection interact negatively and generate an excess of precipitation over the areas in which the model orography is steep. Over areas with smooth topography, an underestimation of rainfall prevails, even if a number of local exceptions still exist (the mean error over PB areas is only -4 m). The underestimation is stronger where the model orography fails to represent the actual topographic gradients. These results are in good agreement with the conclusions of the large scale verifications over the northern extratropical continents, presented in Sects. 4 and 5, and with those of the previous verification studies referred to in Sect.2.

7. THE INTERANNUAL VARIABILITY OF RAINFALL FORECASTS

In all the previous verifications, three-year means of rainfall forecasts were compared with climatological or observed fields. In this section, monthly fields computed from forecasts in individual years (1981, 1982, 1983), as well as differences between two different years, will be compared with the corresponding observed fields over Europe. The reasons for doing this are the following:

- to evaluate the impact of the model changes which occurred in the three-year period, especially changes in orography, and to see whether the skill of rainfall forecasts improved from 1981 to 1983;

- to verify whether the results deduced from three-year mean fields are valid also for single-year fields;

- to evaluate the skill of the forecasts in reproducing the observed interannual variability of monthly rainfall.

To discuss these problems we need to refer to Table 4, where the mean observed rainfall $\bar{P}_o$, the mean forecast rainfall $\bar{P}_F$, the mean error $\bar{\varepsilon}$, the mean absolute error $\overline{|\varepsilon|}$ and the percentage of correct estimates CES are listed for all the three years, the four months and the four verification times considered in this study; values for the 3-year means are also listed for comparison.

EUROPEAN MONTHLY RAINFALL 1981/83		OB	D1				D2				D4				D7			
		$\bar{P}_o$	$\bar{P}_F$	$\bar{\varepsilon}$	$\overline{\lvert\varepsilon\rvert}$	CES%	$\bar{P}_F$	$\bar{\varepsilon}$	$\overline{\lvert\varepsilon\rvert}$	CES%	$\bar{P}_F$	$\bar{\varepsilon}$	$\overline{\lvert\varepsilon\rvert}$	CES%	$\bar{P}_F$	$\bar{\varepsilon}$	$\overline{\lvert\varepsilon\rvert}$	CES%
JANUARY	1981/83	77.5	71.1	-6.3	27.0	60.9	74.8	-2.6	27.6	60.9	79.6	2.1	31.1	54.9	76.7	-0.8	31.0	56.0
	81	72.9	72.6	-.3	36.7	48.4	73.9	1.0	37.8	52.7	81.7	8.7	43.0	44.6	83.2	10.3	49.9	32.1
	82	84.4	63.5	-20.9	40.0	47.8	69.8	-14.5	40.9	49.5	73.9	-10.4	43.7	46.2	67.4	-17.0	43.1	43.5
	83	75.1	77.2	2.1	31.6	52.2	80.7	5.6	33.8	52.2	83.1	8.1	35.0	56.5	79.6	4.5	33.1	54.9
APRIL	1981/83	52.5	72.5	20.0	31.2	53.4	74.6	22.1	31.4	54.4	71.8	19.3	31.1	53.4	77.9	25.4	36.7	45.1
	81	39.4	73.7	34.3	50.7	31.9	74.3	34.9	51.4	37.3	72.5	33.1	49.3	30.9	84.6	45.2	58.0	20.6
	82	53.2	59.0	6.8	28.3	48.5	62.8	9.7	29.4	47.5	63.9	10.7	34.5	42.2	67.8	14.7	41.9	30.4
	83	64.9	83.9	18.9	33.3	51.0	86.7	21.7	35.7	50.0	78.8	13.9	33.2	50.5	81.2	16.3	38.6	44.1
JULY	1981/83	58.7	79.1	20.4	38.9	52.7	75.8	17.2	35.2	55.2	67.4	8.8	28.7	56.2	64.0	5.3	33.9	46.8
	81	72.6	113.4	40.8	73.7	35.5	103.9	31.4	66.2	37.9	90.7	18.1	54.5	44.8	81.9	9.3	56.9	40.4
	82	58.2	68.1	10.0	38.4	42.4	71.8	13.6	41.6	44.8	64.3	6.2	34.8	49.3	58.9	0.8	36.4	38.4
	83	45.3	55.9	10.6	39.0	43.8	51.8	6.5	36.8	38.9	47.3	2.0	37.1	41.9	51.3	5.9	43.9	37.9
OCTOBER	1981/83	84.3	91.9	7.7	27.0	67.6	98.3	14.0	31.5	63.7	97.3	13.1	31.4	62.7	95.6	11.4	34.0	60.8
	81	94.9	109.7	14.8	33.8	68.1	114.7	19.7	38.1	61.3	117.2	22.3	41.1	61.8	121.1	26.2	51.1	53.4
	82	83.3	80.9	-2.4	34.7	51.5	93.4	10.2	37.6	55.4	95.5	12.2	42.6	51.5	82.9	-0.4	48.5	37.7
	83	74.6	85.1	10.6	38.8	47.1	86.7	12.2	40.8	45.6	79.3	4.8	38.6	51.0	82.9	8.4	46.4	36.3

Table 4. Statistics derived from the comparison between monthly rainfall deduced from observed data and D1, D2, D4, D7 forecasts in 1981, 1982, 1983 on ~200 European grid-points. Values for 3-year means are also listed for comparison.

$\bar{P}_o$: mean observed value (mm); $\bar{P}_F$: mean forecast value (mm); $\bar{\varepsilon}$: mean error (mm); $\overline{\lvert\varepsilon\rvert}$: mean absolute error (mm); CES: percentage of correctly estimated values.

7.1 Effect of model changes

Let us first discuss the effect of the changes that occurred in the model during the three years; the three changes that had the strongest impact on rainfall distribution in the 1981-83 period were:

- the introduction of the mean orography (Fig.17c) in the grid point model on 1 April 1981;

- the modification of the horizontal diffusion scheme for temperature and moisture on 29 September 1981;

- the introduction of the new spectral model with an envelope orography (Fig.17d) on 21 April 1983.

It is useful to remember that in the new spectral model rainfall is calculated on a Gaussian grid in which the latitude lines do not coincide with those of the previous N48 grid. Therefore, the grid point values used in this verification from 21 April 1983 onwards are linearly interpolated from the two nearest Gaussian grid points on the same meridian. This may cause a little smoothing of the rainfall forecasts in July and October 1983.

The effect of the changes which occurred in April and September 1981 are evident by comparing the scores for 1981 months with those for the following two years, see Table 4. Whereas the scores are not very different in January and October (surprisingly, October 1981 has the highest percentage of correct estimates in the entire sample), the forecasts in April and July 1981 (when the mean orography but still the uncorrected diffusion scheme was used) were much worse than in the following years.

Conversely, no significant change can be seen after the introduction of the spectral model; if there was a small improvement, this has been masked by the interpolation.

7.2 Comparison of individual years with the 3-year mean

We now compare the skill of the forecasts in individual years with that of the 3-year mean, see again Table 4. In January, on D1 and D2 both $|\bar{\varepsilon}|$ and CES were significantly better for the 3-year mean than for any individual year. In general, the mean absolute error has its minimum on D1 and CES its maximum on D2 but, as in the 3-year mean, the scores of D1 and D2 are very similar. An improvement of the scores from 1981 to 1983 becomes much more evident when going from D1 to D7, and by D7 the skill of the 3-year mean is comparable with that of 1983.

In April, the skill of the 3-year mean is influenced by the large errors which occurred in 1981, and it is similar to that of the last two years on D1 and D2. On D4 and D7 there is again an improvement from 1981 to 1983 and the scores of the 3-year mean are only slightly better than those of 1983. The scores of D1, D2 and D4 are practically the same for the 3-year mean, and are also very similar in the individual years, even if a slight decrease of skill from D1 onwards can be seen in 1982.

For July, despite the errors in the 1981 forecasts, the 3-year mean has significantly better scores than both 1982 and 1983 (with the exception of $|\bar{\varepsilon}|$ on D1). D4 forecasts generally have the best skill in individual years, even if in 1983 D1, D2 and D4 are comparable. However, this is due to D4 scores being worse in 1983 than in 1982, rather than because the skill improved on D1 and D2 in 1983.

In October, the three years have similar mean absolute errors, but the percentage of CES is surprisingly better for 1981 than for the other two years. The scores of the 3-year mean are considerably better than those in individual years, except for the CES of 1981. The clear decrease of skill from D1 onwards seen in the 3-year mean is mainly a reflection of the trend in 1981, since in the other two years the scores show comparable values on D1, D2 and D4.

Summarising the results in individual years, and excluding extreme cases, conclude that the percentage of correct estimates according to our criterion is about 50% on D1, D2 and D4 in all months except July, when it is about 40% on D1 and D2 and 45% on D4. These scores are about 10% lower than the corresponding values for the 3-year means, except in April, when the influence of the 1981 data is stronger and the difference is reduced.

7.3 Examination of the interannual variations in observed and forecast rainfall

If we examine the correspondence between the interannual variations in the mean observed rainfall $\bar{P}_o$ and in the mean forecast rainfall $\bar{P}_F$, the results are not very encouraging. However, in order to have a better idea of the skill of the model in reproducing the interannual variability, the following values have been computed for the three pairs of years available (1982-81, 1983-82, 1983-81), the four forecast times and the months of January and July:

$$\delta_o = \overline{\left| p'_o - p''_o \right|}$$

$$\delta_F = \overline{\left| p'_F - p''_F \right|}$$

$$\eta = \overline{\left| p'_F - p''_F - (p'_o - p''_o) \right|}$$

$$\rho = \frac{\overline{(\sqrt{p'_F} - \sqrt{p''_F}) \cdot (\sqrt{p'_o} - \sqrt{p_o})}}{\left[\overline{(\sqrt{p'_F} - \sqrt{p''_F})^2} \cdot \overline{(\sqrt{p'_o} - \sqrt{p''_o})^2} \right]^{\frac{1}{2}}}$$

where ' and " indicate values in different years and the overbar the spatial average. Here, δ_o and δ_F are the mean absolute values of the interannual variations in the observed and the forecast rainfall, η is the mean absolute error of the forecast variation and ρ is a correlation coefficient between the two variations computed using square roots of rainfall data in order to avoid an excessive influence of the high values. These statistics are shown in Table 5.

Unfortunately, the strong excess of rainfall over the mountains in July 1981 limits the significance of the July data in two of the three cases, but at least the correlation coefficients can give some useful indications. If we compare δ_o with δ_F and η in the three January cases and in the July 1983-82 case, we see that the mean amplitude of the interannual variability is correctly reproduced in the forecasts, but the errors are of the same order of magnitude of the variability. In all cases the correspondence between observed and forecast variations decreases progressively from D1 to D7, with only few deviations from this trend.

		D1			D2			D4			D7		
	δ_o	δ_F	η	ρ	δ_F	η	ρ	δ_F	η	ρ	δ_F	η	ρ
JAN													
82-81	47.1	35.3	50.1	.395	38.3	53.4	.359	31.9	57.3	.225	37.8	64.0	.072
83-82	51.8	43.9	46.4	.645	48.1	48.3	.618	42.2	48.8	.572	37.2	46.0	.590
83-81	37.2	40.4	38.3	.530	40.5	41.0	.474	38.5	42.4	.381	35.6	49.0	.189
JULY													
82-81	42.6	77.5	78.0	.361	71.3	75.1	.286	57.1	62.5	.229	47.4	61.0	.090
83-82	34.6	36.3	43.7	.327	36.0	44.5	.290	31.7	47.1	.113	31.6	50.2	.013
83-81	45.8	81.5	78.2	.430	74.8	72.2	.448	67.9	68.1	.310	61.4	68.6	.129

Table 5. Indices of interannual variations deduced from observed and predicted values of monthly rainfall in different years over ~200 European grid points. Predicted values are computed from D1, D2, D4 and D7 forecasts.

δ_o observed mean absolute variation (mm)

δ_F predicted mean absolute variation (mm)

η mean absolute error in the interannual variations (mm)

ρ spatial correlation coefficient between the observed and predicted interannual variations.

The correlation coefficients are rather poor in July, though they improve in January (particularly for the 1983-82 case). Apart from the fact that the forecasts are more skillful in January, these differences also reflect the changes which occurred in the model: the January 1983-82 variation is the only case in which no significant change occurred in the model in that period, and the corresponding correlation coefficients are by far the best, especially on D4 and D7. With the exception of this case, correlation coefficients on D7 are not statistically significant.

The results discussed above seem to leave little hope for a practical use of the operational short range forecasts in studies about the interannual variability of precipitation. A necessary condition for such studies to be useful is the stability of the model, which is not always possible for obvious operational reasons. However, since the most important factor that can change the rainfall distribution is the choice of orography, the possibility remains that the short range forecast could reproduce the interannual variability over the oceans, despite the large systematic errors occurring in those areas. To test this possibility, we compared the difference in D1 precipitation over the Pacific between January 1983 and January 1982 with the anomalous outgoing longwave radiation in January 1983 as deduced from NOAA satellite data. As is well known, a strong "El Niño" anomaly occurred in the autumn of 1982 and in winter of 1983 in the surface temperature of the tropical Pacific. Fig.22 compares the rainfall difference deduced from D1 forecasts with the anomaly anomaly of outgoing radiation deduced from satellite data and published in the Climate Diagnostics Bulletin (NOAA, 1983). This anomaly can be interpreted in terms of anomalous cloudiness. Areas with increased rainfall and cloudiness are shaded in the figure.

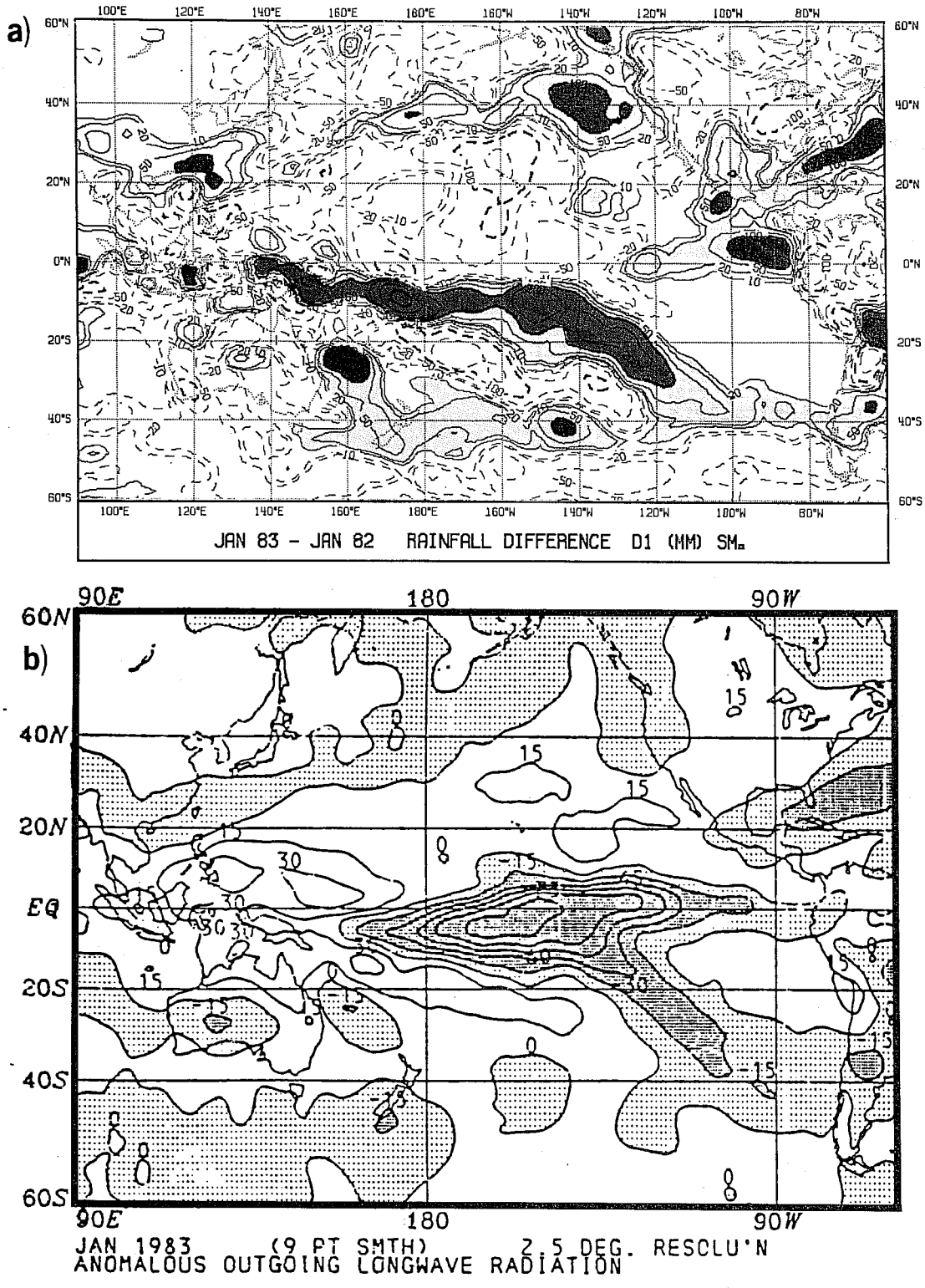

Fig.22 (a) Difference in D1 rainfall forecasts (mm) between monthly values in January 1983 (El Niño case) and in January 1982 over the Pacific Ocean; (b) mean anomalous outgoing longwave radiation (W/m^2) in January 1983 as deduced from NOAA satellite data (from Climate Diagnostics Bulletin, NOAA 1983).

It is evident from the maps that at least the main structure of the rainfall anomaly, not only in the tropical area but also in the storm track, has been captured by the model. So it is reasonable to hope that, when the sources of the large systematic errors over the oceans and over the mountain area are at least partially removed, the short range rainfall forecasts will be an invaluable tool in the diagnostics of the interannual variability of precipitation, especially in the extratropics where observational satellite techniques are less useful.

8. CONCLUSIONS

In the previous sections, monthly rainfall fields deduced from short range numerical forecasts were compared with estimated rainfall climatologies on the global scale and with observed data over Europe. Even though the forecast rainfall distribution reproduces almost all the main features of the observed distribution, considerable systematic errors are present. Our results can be summarized as follows.

- The forecasts underestimate mean global rainfall during the whole year, the error ranging from 5 to 15% depending on the month and the forecast time; the amplitude of the error decreases from D1 to D7 in January, increases in July and is nearly constant in the intermediate seasons.

- Too much rainfall is forecast over the continents both in the tropics and in northern mid-latitudes in summer. A smaller overestimate over the northern extratropical continents seems to occur also in winter, but in many areas the differences between D1 forecasts and the observed climatologies are of the order of the interannual variability and/or of the observational uncertainty.

- Over the oceans, large underestimations of rainfall occur in the forecasts, especially in the tropics (where the error decreases rapidly with forecast time) and in the southern hemisphere. Over the northern extratropical oceans, the underestimation occurs only in summer, whereas in winter an excess of rainfall is observed, particularly in the region of the storm tracks between 30° and 40°N.

- Both in January and in July there is a large global excess of precipitation over evaporation, which tends to decrease with forecast time due to a roughly linear increase of evaporation. Zonally integrated forecast evaporation over the oceans shows an anomalous distribution, being much greater in the winter hemisphere than in the summer one. In January, a good correspondence can be found between these anomalies and deviations of forecast rainfall distribution from Jaeger's climatology.

- A comparison with observed data over Europe indicates that, with the exception of January, the forecasts overestimate the mean precipitation in this area. The main errors in the geographical distribution are strongly related to the orography. In January too little rainfall is generated on the windward side of mountains and too much on the lee side; in July, there is excessive convective activity over the mountains.

- The distribution of daily rainfall over Europe among classes of different intensity shows an overestimation of light rainfall (<2 mm/day) by about a factor of 2 during the whole year, and an underestimation of intense rainfall (>20 mm/day) induced by orographic lifting, particularly strong in January.

- About 50% of local monthly rainfall estimates over Europe are correct within a factor of 1.5 when data for individual years are considered; this is about 10% more than when using 3-year means. D1 forecasts give generally the best estimate. An exception to this situation occurs in July, when the scores are 5-10% lower and D4 forecasts are the most skillful.

- The operational short range forecasts fail to correctly reproduce the geographical distribution of interannual variations over Europe, mainly because of the changes continuously occurring in the model. However, the variations from January 1982 to January 1983 (a period in which no relevant model changes occurred) are well simulated both over Europe and over the Pacific. In any case, the skill in forecasting interannual variations decreases steadily with forecast time.

Apart from the problems related to the data assimilation cycle and the spin-up of the model, which mainly affect forecasts on D1 by generating an excess of moisture in the low levels, there appear to be three main sources of error which are acting more or less constantly during the forecast:

(a) An inadequacy in the parameterization of the vertical flux of moisture in the boundary layer both generates an incorrect amount of evaporation and prevents the vertical transport of the water vapour from the lowest levels.

(b) The convection scheme generates too much rainfall over land and particularly over the mountains, where its behaviour may still be influenced by deficiencies in the representation of horizontal diffusion of temperature and moisture, despite the corrections already introduced into the model.

(c) The excessive smoothness of the model orography, in addition to its dynamical consequences, has a direct impact on the distribution of precipitation in the winter mid-latitudes by preventing an adequate simulation of the orographic lifting. As pointed out before, this fact reduces the

differences between the windward and the lee side of the mountains, and prevents the model from forecasting intense daily rainfall in that season.

The two last points highlight the problems, which emerged from this study, connected to the representation of orography in ECMWF's model and they call for a further consideration: the orography seems not to be steep enough to generate enough uplift to account for the observed upwind precipitation characteristic of mountainous regions during the winter months. The same orography, however, is far too steep during the spring and summer months so that it triggers a spurious feedback between the horizontal diffusion of temperature and moisture and the Kuo-type parameterisation scheme of convective rainfall. This, together with demonstrating the need for further work in the area of the parameterisation of convection, raises doubts as to whether the numerical schemes responsible for carrying the information relative to the lower boundary condition ($w=\underline{V}.\nabla h$ at $z=h$, or $\sigma=1$) are, in fact, performing this function satisfactorily.

On the basis of all these results, we can conclude that, even if the large-scale distribution of rainfall is correctly simulated by the short range forecasts, a number of sources of systematic error (especially in the tropics and over mid-latitude continental regions) prevent the ECMWF rainfall forecasts from being a more reliable source of information than conventional or satellite observed rainfall estimates. However, in some areas their skill is at least comparable with the accuracy of other available sources. On the assumption that the current trend in model improvements will continue, it is reasonable to hope that in the near future, ECMWF short range forecast may become an important source of information for the observational study of the global hydrological cycle.

Acknowledgements

A number of ECMWF scientists gave important contributions to the present work. H. Böttger provided the computer code to retrieve rainfall observations over Europe; W. Heckley gave us useful references and data for comparisons; M. Kanamitsu showed us his results about the influence of variations in the tropical latent heat release; M. Tiedtke discussed a good part of our results with us and made valuable suggestions. We also had discussions with L. Illari about the errors in the humidity analysis, and with A. Sutera about the possible causes and effects of the large-scale rainfall systematic error. R. Riddaway carefully read the manuscript and tried to anglicise it as much as possible.

The work of F. Molteni was financially supported by the ENEL (Italian National Electricity Board) through a contract between the Centro di Ricerca Termica e Nucleare (ENEL) and Geodata.

REFERENCES

Åkesson, O., 1981: Evaluation of the ECMWF operational model precipitation forecasts in October-November 1980. ECMWF Tech.Memo.No.24, 17pp.

Åkesson, O., H. Bottger and H. Pümpel, 1982: First results of direct model output verification of near-surface weather parameters at 17 locations in Europe. ECMWF Tech.Memo.No.47, 46pp.

Arkin, P., 1983: A diagnostic precipitation index from infrared satellite imagery. Tropical Ocean-Atmosphere Newsletters, March 1983. Publ. by the University of Washington, Joint Institute for the Study of the Atmosphere and Oceans, USA.

Arpe, K. 1983: Diagnostic evaluation of analyses and forecasts: climate of the model. ECMWF Seminar/Workshop on Interpretation of Numerical Weather Prediction Products, 13-24 September 1982, ECMWF, Reading, UK, 99-140.

Arpe, K., and E. Klinker, 1984: Systematic errors of the ECMWF operational spectral model. Part I: midlatitudes. Paper presented to the Scientific Advisory Committee, 12-14 September, 1984, ECMWF, 53pp.

Barrett, E.C., 1970: The estimation of monthly rainfall from satellite data. Mon.Wea.Rev., 98, 322-327.

Barrett, E.C., and D.W. Martin, 1981: The use of satellite data in rainfall monitoring. Academic Press, London, 340pp.

Corona, T.J., 1978: The interannual variability of northern hemisphere precipitation. Environmental Research Paper No.16, Colorado State University, USA, 27pp.

Dorman, C.E., and R.H. Bourke, 1979: Precipitation over the Pacific Ocean, 30°S to 60°N. Mon.Wea.Rev., 107, 896-910.

Dorman, C.E. and R.H. Bourke, 1981: Precipitation of the Atlantic Ocean, 30°S to 70°N. Mon.Wea.Rev., 109, 554-563.

Geiger, R., 1965: World maps 1:30 M: The Earth's atmosphere No.5, mean annual precipitation. Justus Perthes, Darmstadt.

Heckley, W.A., 1981: Preliminary results of an investigation into the quality of ECMWF forecasts in the tropics. ECMWF Tech.Memo.No.43, 27pp.

Heckley, W.A., 1985: Systematic errors of the ECMWF operational forecasting model in tropical regions. Quart.J.R.Meteor.Soc., 111, 709-738.

Jaeger, L., 1976: Monatskarten des Niederschlags für die ganze Erde. Berichte Deutscher Wetterd., Vol. 18, No.139, 38pp.

Jaeger, L., 1983: Monthly and areal patterns of mean global precipitation. Variations in the Global Water Budget, A. Street-Perrott, M. Beran and R. Ratcliffe, eds., Reidel, Dordrecht, 129-140.

Johannessen, K.R., 1982: Verification of ECMWF quantitative precipitation forecasts over Europe, January 1980 to April 1981. ECMWF Tech.Memo.No.51, 71pp.

Kilonsky, B.J., and C.S. Ramage, 1976: A technique for estimating tropical open-ocean rainfall from satellite observations. J.Appl.Meteor., 15, 972-975.

Newell, R.E., J.W. Kidson, D.G. Vinant, and G.J. Boer, 1974: The general circulation of the tropical atmosphere and interactions with extratropical latitudes, Vol.2 Massachusetts Institute of Technology Press, Cambridge, Mass., 371pp.

NOAA, 1983: Climate Diagnostics Bulletin, January 1983. NOAA/National Weather Service, National Meteorological Centre, Climate Analysis Centre, Washington, USA.

Peixóto, J.P., and A.H. Oort, 1983: The atmospheric branch of the hydrological cycle and climate. Variations in the Global Water Budget, A.Street-Perrott, M. Beran and R. Ratcliffe, eds, Reidel, Dordrecht, 5-65.

Ramage, C.S., 1975: Preliminary discussion of the meteorology of the 1972-73 El Nino. Bull.Amer.Meteor.Soc., 56, 234-242.

Rao, M.S.V., and J.S. Theon, 1977: New features of global climatology revealed by satellite-derived oceanic rainfall maps. Bull.Amer.Meteor.Soc., 58, 1285-1288.

Richards, F., and P. Arkin, 1981: On the relationship between satellite-observed cloud cover and precipitation. Mon.Wea.Rev., 109, 1081-1093.

Street-Perrott, A., M. Beran and R. Ratcliffe, 1983: Variations in the global water budget. Reidel, Dordrecht, 518pp.

Tibaldi, S., 1982: The production of a high resolution global orography and associated climatological surface fields for operational use at ECMWF. Riv.Meteor.Aeronaut., 42, 285-308.

Tiedtke, M., 1984: The sensitivity of the time-mean large-scale flow to cumulus convection in the ECMWF model. ECMWF Workshop on Convection in Large-Scale Numerical Models, 28 November-1 December 1983, ECMWF, Reading, UK, 297-316.

Tucker, G.B., 1961: Precipitation over the North Atlantic Ocean. Quart.J.Roy.Meteor.Soc., 87, 147-158.

Wallace, J.M., S. Tibaldi and A.J. Simmons, 1983: Reduction of systematic forecast errors in the ECMWF model through the introduction of an envelope orography. Quart.J.Roy.Meteor.Soc., 109, 683-717.

Wilheit, T.T., A.T.C. Chang, M.S.V. Rao, E.B. Rodgers and J.S. Theon, 1977: A satellite technique for quantitatively mapping rainfall rates over the oceans. J.Appl.Meteor., 16, 551-560.

ECMWF PUBLISHED TECHNICAL REPORTS

No.1 A Case Study of a Ten Day Prediction

No.2 The Effect of Arithmetic Precisions on some Meteorological Integrations

No.3 Mixed-Radix Fast Fourier Transforms without Reordering

No.4 A Model for Medium-Range Weather Forecasting - Adiabatic Formulation

No.5 A Study of some Parameterizations of Sub-Grid Processes in a Baroclinic Wave in a Two-Dimensional Model

No.6 The ECMWF Analysis and Data Assimilation Scheme - Analysis of Mass and Wind Fields

No.7 A Ten Day High Resolution Non-Adiabatic Spectral Integration: A Comparative Study

No.8 On the Asymptotic Behaviour of Simple Stochastic-Dynamic Systems

No.9 On Balance Requirements as Initial Conditions

No.10 ECMWF Model - Parameterization of Sub-Grid Processes

No.11 Normal Mode Initialization for a Multi-Level Gridpoint Model

No.12 Data Assimilation Experiments

No.13 Comparisons of Medium Range Forecasts made with two Parameterization Schemes

No.14 On Initial Conditions for Non-Hydrostatic Models

No.15 Adiabatic Formulation and Organization of ECMWF's Spectral Model

No.16 Model Studies of a Developing Boundary Layer over the Ocean

No.17 The Response of a Global Barotropic Model to Forcing by Large-Scale Orography

No.18 Confidence Limits for Verification and Energetic Studies

No.19 A Low Order Barotropic Model on the Sphere with the Orographic and Newtonian Forcing

No.20 A Review of the Normal Mode Initialization Method

No.21 The Adjoint Equation Technique Applied to Meteorological Problems

No.22 The Use of Empirical Methods for Mesoscale Pressure Forecasts

No.23 Comparison of Medium Range Forecasts made with Models using Spectral or Finite Difference Techniques in the Horizontal

No.24 On the Average Errors of an Ensemble of Forecasts

ECMWF PUBLISHED TECHNICAL REPORTS

No.25 On the Atmospheric Factors Affecting the Levantine Sea

No.26 Tropical Influences on Stationary Wave Motion in Middle and High Latitudes

No.27 The Energy Budgets in North America, North Atlantic and Europe Based on ECMWF Analyses and Forecasts

No.28 An Energy and Angular-Momentum Conserving Vertical Finite-Difference Scheme, Hybrid Coordinates, and Medium-Range Weather Prediction

No.29 Orographic Influences on Mediterranean Lee Cyclogenesis and European Blocking in a Global Numerical Model

No.30 Review and Re-assessment of ECNET - a Private Network with Open Architecture

No.31 An Investigation of the Impact at Middle and High Latitudes of Tropical Forecast Errors

No.32 Short and Medium Range Forecast Differences between a Spectral and Grid Point Model. An Extensive Quasi-Operational Comparison

No.33 Numerical Simulations of a Case of Blocking: the Effects of Orography and Land-Sea Contrast

No.34 The Impact of Cloud Track Wind Data on Global Analyses and Medium Range Forecasts

No.35 Energy Budget Calculations at ECMWF: Part I: Analyses

No.36 Operational Verification of ECMWF Forecast Fields and Results for 1980-1981

No.37 High Resolution Experiments with the ECMWF Model: a Case Study

No.38 The Response of the ECMWF Global Model to the El-Nino Anomaly in Extended Range Prediction Experiments

No.39 On the Parameterization of Vertical Diffusion in Large-Scale Atmospheric Models

No.40 Spectral characteristics of the ECMWF Objective Analysis System

No.41 Systematic Errors in the Baroclinic Waves of the ECMWF Model

No.42 On Long Stationary and Transient Atmospheric Waves

No.43 A New Convective Adjustment Scheme

No.44 Numerical Experiments on the Simulation of the 1979 Asian Summer Monsoon

No.45 The Effect of Mechanical Forcing on the Formation of a Mesoscale Vortex

ECMWF PUBLISHED TECHNICAL REPORTS

No.46 Cloud Prediction in the ECMWF Model

No.47 Impact of Aircraft Wind Data on ECMWF Analyses and Forecasts during the FGGE Period, 8-19 November 1979 (not on WP, text provided by Baede)

No.48 A Numerical Case Study of East Asian Coastal Cyclogenesis

No.49 A Study of the Predictability of the ECMWF Operational Forecast Model in the Tropics

No.50 On the Development of Orographic Cyclones

No.51 Climatology and Systematic Error of Rainfall Forecasts at ECMWF